Degradation Analysis by Accelerated Ageing of Epoxy based Mortar

Durability Research on the Lantern of the Liverpool Metropolitan Cathedral

Lisette de Bie

Technische Universiteit Delft

TU Delft Delft University of Technology

Challenge the future

December 2, 2019

Degradation Analysis by Accelerated Ageing of Epoxy based Mortar

Durability Research on the Lantern of the Liverpool Metropolitan Cathedral

by

Lisette de Bie

in partial fulfilment of the requirements for the degree of

Master of Science
in Aerospace Engineering

at the Delft University of Technology
to be defended publicly on Thursday December 12, 2019 at 10:00 AM.

Supervisors: Dr. J.A. (Hans) Poulis
Prof. dr. N.H. (Norman) Tennent

TU Delft Delft University of Technology

Acknowledgements

I would like to express my special thanks Hans Poulis and Norman Tennent for giving me the opportunity to work with them on this wonderful project. Their insightful comments and help were invaluable during the course of my thesis.

Hans, as my daily supervisor, helped my greatly with his feedback. I appreciated the freedom I got to form this research in the direction I found the most interesting.

Norman's help on tracing back the history of the cathedral's construction and the help he offered me on understanding the workings behind chemistry and epoxies were much valued. I also enjoyed visiting Norman at the restoration atelier of the Rijksmuseum. Furthermore, the time he took to travel all the way to Delft (from all over the world) to our meetings was greatly appreciated.

I would also like to thank my thesis committee; Roger Groves and Johan Bijleveld, for taking the time to review my work and for their interest in my research.

My gratitude goes to Marlies, Yasmine and Laura for helping me on my experiments and reviewing my work.

Many thanks to the DASML laboratory team for enduring my endless questions. Without them my experiments would not have produced the results they did.

Thanks to the team of masters-room 'NB 1.07' for the well needed fun and distraction.

Furthermore, I would like to express my gratitude to my friends and family, above all my parents, for their moral support and warm encouragements. Last but not least, thanks to my boyfriend Gerard for all his love and endless support.

Abstract

The Liverpool Metropolitan Cathedral is the Roman Catholic Cathedral in Liverpool. It was constructed between 1962 and 1967, to the 1959 competition winning design of Sir Frederick Gibberd. The roof of the building is crowned by a tapering lantern formed from coloured glass adhered by means of an epoxy-based mortar. This construction method was experimental and at the forefront of the technology of the period. Soon after opening, the Cathedral began to exhibit flaws in detailing and construction. Leaks through the glazed lantern, between the epoxy and the glass, were observed. Therefore, the effects of outdoor exposure on the stability and strength of the used epoxy was assessed.

Accelerated ageing tests allow the prediction of the effects of weathering and the state of degradation of the mortar used in the LMC in an expedited manner. Since a limited amount of original material from the cathedral is available for testing, a replica mortar was made. After a performed material analysis, the original epoxy/sand/carbon black mortar formulation was replicated. This replica mortar as well as the original mortar core samples were used to undertake accelerated ageing tests (e.g. by moisture, UV exposure and elevated temperature). This was followed by mechanical tests on the replicated specimens, to observe changes in structural integrity and adhesion. The link between the original and the replicated material was made with various chemical analysis, such as FTIR, DSC, DMA and XPS.

The generated data showed evidence on that the likelihood of major structural loss is small, within the undertaken testing period. The loss of adhesion is attributed to high relative humidity. Changes in the chemical and physical properties of both materials is difficult to observe. The high filler content in the epoxy may hinder physical changes substantiality.

Contents

List of Tables

List of Figures

Nomenclature

List of abbreviations

ATR	Attenuated Total Reflectance
BL	Baseline (samples that are not aged or modified)
CB	Carbon Black
DEMO	Dienst Elektronische en Mechanische Ontwikkeling
DGEBE	Diglycidyl Ether of Bisphenol A
DGEBF	Diglycidyl Ether of Bisphenol F
DMA	Dynamic Mechanical Analysis
DSC	Differential Scanning Calorimetery
DSC	Differential Scanning Calorimetry
FTIR	Fourier Transfer Infrared (Spectroscopy)
LMC	Liverpool Metropolitan Cathedral
Mortar	A mixture of sand, a binder and water
mXDA	m-xylylenediamine
NW	North west
RH	Relative Humidity
SE	South east
SEM	Scanning Electron Microscope
TC	Temperature Cycling
Tg	Glass transition temperature
TGA	Thermogravimetric analysis
TMA	Thermomechanical analysis
UV	Outdoor light exposure
WS	Water Spray, in combination with outdoor light expousure
XPS	X-ray photoelectron spectroscopy

I

Background and Related work

1 Introduction

The Liverpool Metropolitan Cathedral is the Roman Catholic Cathedral in Liverpool. It was constructed between 1962 and 1967, to the 1959 design of Sir Frederick Gibberd. It is one of the most recent cathedrals in the UK, and of a striking modern design. The building is circular in plan and is constructed from of a concrete frame with walls clad in Portland stone and a conical roof covered in stainless steel. The roof is crowned by a tapering lantern formed from colored glass held together by an epoxy mortar and are build in concrete panels between narrow concrete columns.

Many of the details and construction methods used for the Cathedral were experimental and at the forefront of the technology of the period. Soon after opening, the Cathedral began to exhibit flaws in detailing and construction. Leaks through the aluminum roofs and the glazed lantern were observed.

External surveys of the glazing have shown that the glass itself is generally in good condition with only small areas where there appears to have been mechanical damage. However, the epoxy with fillers, used as the mortar, has deteriorated more significantly. Specifically, the adhesion to the glass blocks has failed.

A Conservation Management Plan [1] has been commissioned by the Metropolitan Cathedral of Christ the King (Liverpool Metropolitan Cathedral) to inform maintenance and repairs to the Cathedral. From this report several assessments have been made to determine the current state of the lantern, the weather exposure and analysis of the epoxy mortar. However, after this assessment there are still gaps in knowledge on the current state of the epoxy mortar. The main idea behind this research project is to get an idea of the life expectancy of the epoxy mortar used for building and construction of the glass- and concrete based lantern.

(a) (b)

Figure 1.1: (a) Front view of the Liverpool Metropolitan Cathedral [2]and (b) red-side of the lantern's stained glass [3]

2

The Liverpool Metropolitan Cathedral

In the following chapter, the relevant history of the Liverpool Metropolitan Cathedral is discussed. The construction method of the lantern's windows can be found in section 2.2. The deterioration found in the lantern is reviewed in section 2.3. Lastly, section 2.4 goes over the types of weather that could contribute to the degradation of the windows.

2.1. History

The lantern of the Liverpool Metropolian Cathedral (LMC) was designed around 1959 by Sir Frederick Gibberd. The cathedral was constructed between 1962 and 1967. The glass windows inside the lantern were designed and constructed by John Piper and Patrick Reyntiens. It made use of the 'Dalle de verre' technique, which is a glass art technique that uses pieces of coloured glass set in a matrix of concrete and epoxy resin. The 1950s was the time that the use of synthetic adhesives began an exponential increase in the use of industrial, domestic but also art and conservation applications. The use of this technique in the LMC was on the forefront of this technology [1]. The cathedral has suffered deterioration from immediately after its completion. De-bonding and moisture ingress were observed due in part to defects in designs or construction materials, as well as to the environmental conditions to which it is exposed. Repairs have been carried out throughout the life of the cathedral culminating in a major intervention in the 1990s [4].

Research has been performed by Norman Tennent [5] to investigate the lifetime of appliqué stained glass build around the 1960s. He found that in four important stained glass structures (the lantern glass of Blackburn and Sheffield Cathedrals, the baptistery glass of St John the Evangelist Church in Eastbourne and the Churchill Memorial Screen in Dudley), all showed degradation due to natural weathering. Degradation reactions caused, the loss of solubility of coatings, the failure of adhesives and the yellowing and crazing of structural polymers. Because the delamination of the glass ultimately became so extreme that conservation was not deemed feasible or proved unsatisfactory, all of these windows have been destroyed or removed to storage.

2.2. Construction

The construction of the lantern was recorded in a video made by the Shell film unit [6]. The construction process, consisted of the glass sections (dalles), being 1 inch thick (25 mm), cast into squires and then crudely cut into shape. The reinforced concrete frame (150 mm thick with 100 m sections of internal concrete tracery) was laid horizontally and plastic sheeting was applied over polystyrene supports in the openings, onto which the glass dalles were laid out to form a skin on top of the frame.

It was noted that the individual glass dalles were cleaned before being laid out, presumably to ensure that there was a clean surface for the adhesion of the resin. A resin mixture comprising (according to the Shell film) Epikote epoxy resin, hardener, carbon black pigment and sand was then applied in the thin gaps between the glass using a piping bag, figure 2.1. The resin between the glass dalles was applied in two layers and was reinforced with strands of fibre glass. While the thick section on the concrete appears to have been applied in a single layer without reinforcement. The resin was then cured at room temperature.

Pictures were obtained from David Kirby, who was working on the project along with architect Reyntiens at the time. They show buckets of epoxy used on the construction site, see figure 2.2. The used epoxy can be identified to be a Kollercast 332 epoxy. This epoxy was distributed by Synthetic Resins Ltd (a Unilever subsidiary at the address in Edwards Lane, Speke, Liverpool where James Beadel & Co Ltd were located). They were taken over in the 80s by Scott Bader and essential parts of the business transferred to their Northamptonshire operation. This contradicts with the information given in the Shell film [6] that an Epikote resin was used. Possibly multiple types of resin were used in the construction. Kirby also stated that the quartz flour (sand) which was used in the mix, is identified to be a grade M3

Figure 2.1: Construction of the cathedral, applying resin mix between the glass dalles [6].

quartz flour. A 'sand'/resin mixing ratio of 2/1 was used for the lantern mortar. The company supplying this type of sand, British Industrial Sand (Scotland) Ltd, was dissolved in 2014.

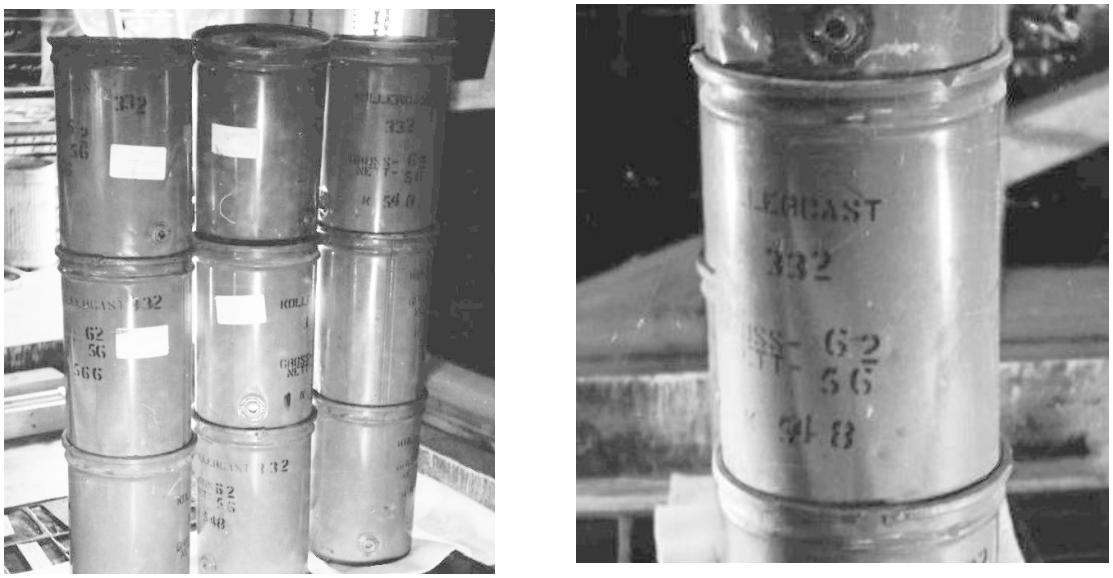

Figure 2.2: Images of the presumably used epoxy (Kollercast 332) during construction.

2.3. Deterioration of the epoxy mortar

There are distinct patterns of deterioration on the different aspects of the lantern. By far the worst deterioration is apparent on the SE (or blue) section and significantly less on the NW (red and yellow) sections. This deterioration manifests itself with more severe cracking and degradation of the external resin and the resulting water penetration and damage to the internal faces. There is also more extensive pooling and staining on the walkway below. External surveys of the glazing have shown that the glass itself is generally in good condition. However, the resin has deteriorated more significantly. In particular, there are areas of cracking both on the thin sections between the glass dalles, where cracks can be full depth, and at the junction between thick resin over the concrete members. the separation of the resin around the glass dalles, figure 2.3 (left). It was found in numerous locations that the adhesion at the interface between the glass and the resin has failed, so water has the chance to penetrate, figure 2.3 (right).

Figure 2.3: Visible cracks in the epoxy mortar and de-bonding of the glass-resin interface simultaneously with moisture ingress [4].

2.4. Location and climate

The Liverpool Metropolitan Cathedral is located on the west side of Liverpool, 2km from the from the Mersey estuary. The cathedral is situated approximately 67m above sea level and is flanked on the north and south sides by wide plazas. Because of the height of the cathedral and the comparatively low level of the surrounding architecture, the upper part of the cathedral, and in particular the lantern, is severely exposed to prevailing weather conditions. In combination with its proximity to the sea this means that the conditions to which the lantern is exposed can be characterized as aggressive, with the effects of differential solar gain, wind loading and marine aerosol likely to play a significant part in the deterioration processes [4].

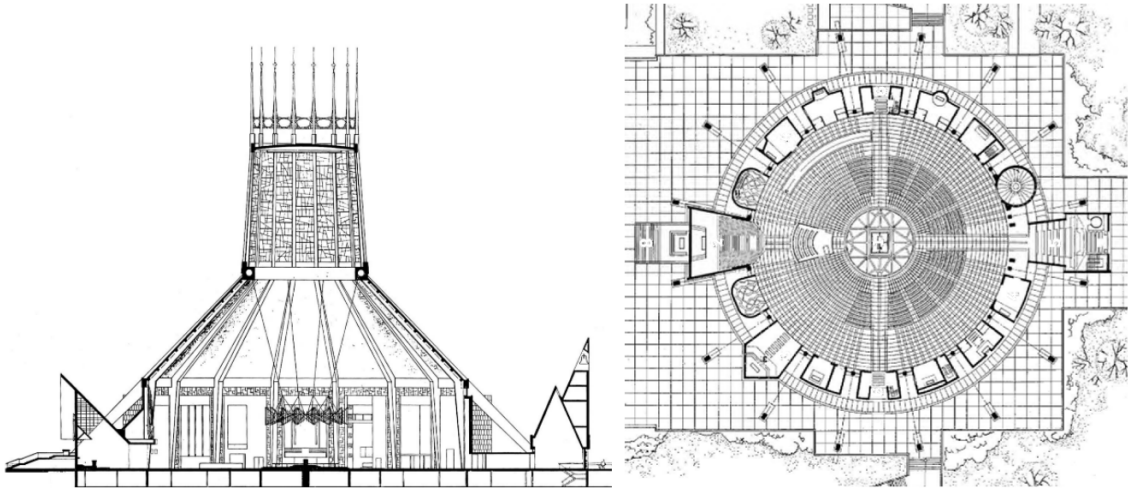

Figure 2.4: Drawing of the cathedral and lantern front view and top view.

The main part of the cathedral, which comprises a large circular room with a diameter of 59m with a shallow conical roof, figure 2.4. The lantern, which is approximately 21m in diameter and 22.5m in height, consists of 16 concrete framed panels, each approximately 3.6m in width, rising to a reinforced shallow domed concrete roof with a covering of a synthetic membrane. The glazing, is constructed of sections of colored glass framed by concrete tracery with individual panels between 1.2m and 2.4m in height. The glass sections, which are up to approximately 30mm in thickness, are resin bonded in place in a variation of the Dalle de verre technique. [4].

Purcell was commissioned [4] to investigate the occurring weather patterns at the cathedral. Research was done over a period of one year. It showed that external air-temperatures ranged from -2 °C to 32°C with maximum humidity of 100% RH with average values of 11°C AT and 74% RH. Fluctuations were greatest during the summer months where changes of >60% RH and 10°C were observed on many occasions. By contrast, in the winter, fluctuations of 40% RH and 5°C, were more common. The

south side experienced significant solar effects with high lux levels due to direct sunlight. The maximum temperature on the south glazing was approximately 51°C and the minimum 2°C with an average of 16°C. On the north glazing, maximum and minimum values were approximately 40°C and 3°C with an average of 14°C. Ambient conditions on the south side of the lantern were far more unstable than on the north side, with large fluctuations in air temperature due to solar heating resulting in variations in relative humidity.

Wind loading and associated pressures will also vary on the different elevations. In Liverpool, the prevailing directions are NW in the spring and summer and SE in the autumn and winter. Rain exposure is directly linked to wind activity. Therefore, it is likely that, depending on the time of year, the SE and NW elevations will suffer the most direct driven rain, while on the opposite sides, the rainfall might be more complex and less focused.

Condensation was seen to occur on all areas of resin and glazing throughout the year, but most significantly, between September and April. On the north side, periods of wetness were likely to be longer, while on the south side, drying occurred more swift as a result of the exposure to sunlight. This means that, on the south side, a greater number of wetting and drying cycles are likely to have taken place, generally in the region of 75% RH. Condensation also occurs on the external surface of the glazing. It is likely that the north side undergoes more regular and prolonged condensation with the surface remaining wetter for longer period of time. This is consistent with the far higher level of microbiological contamination observed on the resin on the north side. It also showed a smaller variation between the temperature of the glass and resin, with the resin generally remaining below the temperature of the glass. On occasions because of this marginal temperature difference, condensation occurred on the epoxy when it did not occur on the glass.

Table 2.1: Occurring weather patterns at the LMC [Purcell [4]].

	Min	Maximum	Average
External air temperature	-2 °C	32 °C	74 °C
Temperature on glazing (south-side)	2 °C	51 °C	16 °C
Temperature on glazing (north-side)	3 °C	40 °C	14 °C
External relative humidity	36 %	100 %	74 %

3
Literature

This chapter discusses the relevant literature that identifies the mechanisms that contribute to degradation of the material as used in the LMC lantern. The analysis of the material previously done by Purcell is discussed in section 3.1. The weathering factors are discussed in section 3.2, followed by the effects of the material composition (section 3.3) and the workings of accelerated ageing (section 3.4).

3.1. Material analysis

Since the knowledge on the exact material composition of the epoxy mortar is not known today, tests were performed on the state and composition of the epoxy mortar. This was done by dr. R. Merola from Purcell [7]. Several test specimens were taken from the epoxy mortar of the lantern. The specimens were taken from different locations, figure 3.1. Sixteen core samples were extracted from five panels of the Lantern. The composition of the polymer resin component of the mortar was then analysed. The type of epoxy was analysed using infrared spectroscopy analysis, Attenuated Total Reflectance (ATR) and Diffuse Reflectance Infrared Fourier Transform Spectroscopy (DRIFTS). This confirmed the mortar as an epoxy, based on either or both of the DGEBA (Diglycidyl Ether of Bisphenol A) and DGEBF (Diglycidyl Ether of Bisphenol F) variants. It is unsure what curing agent has been used. Purcell predicts it to be amine-based, probably m-xylylenediamine (mXDA). Glass fibres were also observed in some of the specimens.

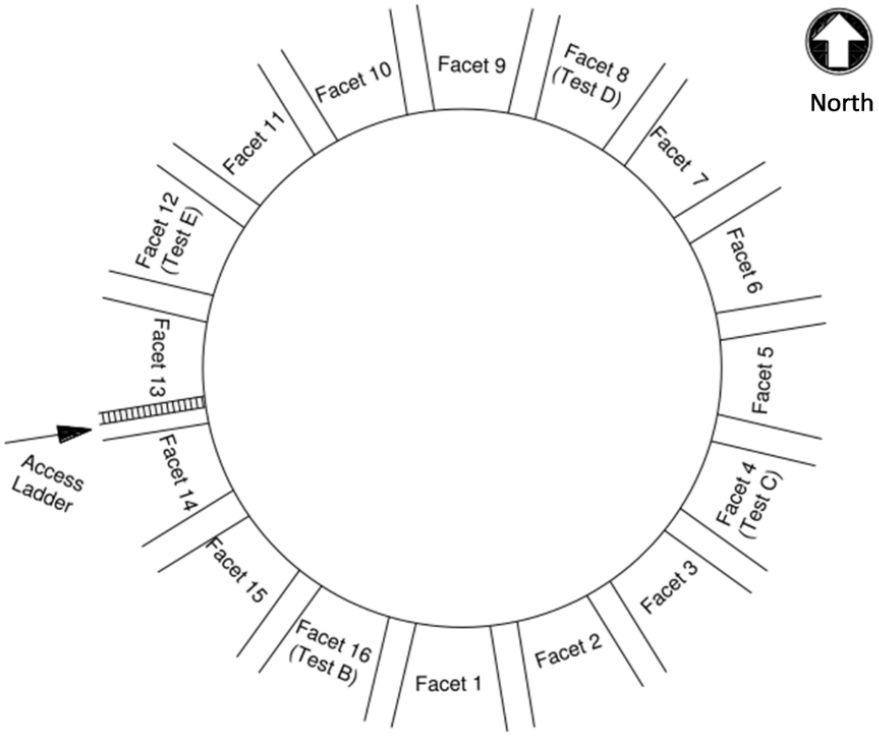

Figure 3.1: Locations in the lantern where test samples were taken [7].

Thermogravimetric Analysis (TGA) tests determined the composition of the material. Samples of approximately 10 mg were placed in alumina crucibles and heated from 35 to 600ºC at a heating rate of 20ºC/minute under a nitrogen gas flow of 50 ml/minute. The gas was then switched to air at the same flow rate of 50 ml/minute and the samples further heated to 1000ºC at 20ºC/minute. For this test, core 5, 9 and 12 were tested. Core 2 and 9 were analysed five times for different parts of the core (top, under

top, upper middle, lower middle, bottom). Core 12 was tested four times. This showed the composition of the fourteen tested samples to be:

- Epoxy Resin 22% to 32%
- Sand 60% to 75%
- Carbon black 1% to 3%
- Water 1.6% to 2.7%

The analysis of core 9 shows three distinctive decomposition steps; around 200°C, 300°C and 600°C. The first step can be assigned to volatile products in the mortar, such as moisture. The step around 300°C comes from the pyrolysis of epoxy present in the mortar, which generally starts between 250°C and 300°C. At 600°C the purge gas switches from nitrogen to air. This is a common technique to identify the percentage of carbon in a material, because carbon black starts to oxidize at a temperature of approximately 500°C. So, the third degradation step was identified to be the amount of carbon present in the material (3%). The left over residue (60% to 75%) is the percentage of incombustibles present in the mortar, this is stated to be the sand.

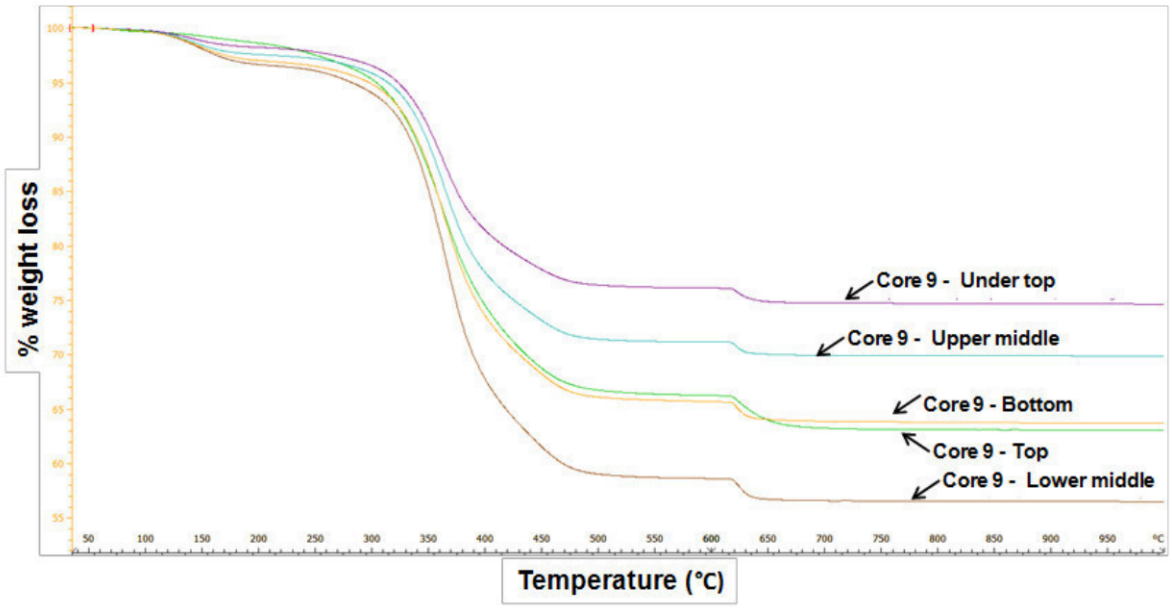

Figure 3.2: TGA analysis of core 9, as done by Purcell [7]

3.2. Weathering

To determine the factors affecting the ageing of the epoxy mortar, several environmental parameters were identified. The main environmental factors that attack and deteriorate adhesive joints are oxygen, UV, temperature, water and salt-spray. Furthermore mechanical stress is known to accelerate environmental degradation [8]. These factors, and their impact on the epoxy, are further discussed in this chapter.

3.2.1. Humidity

Water is the substance which gives the greatest problems in terms of the environmental stability of adhesive joints. The biggest problem with water is weakening of the glass-adhesive interface by hydrolysis. The rate of environmental attack by water is greater if the temperature is relatively high or the joint is subjected to stress. Chemically, water leads only to hydrolysis at high temperatures, see section 3.2.4. The physical interaction of the adhesive with ingressing water results in plasticization of the adhesive, by disrupting the hydrogen bonding between the molecular chains of the adhesive. On longer exposure times, water causes a decrease in molecular weight and Young's modulus because of this degradation and plasticization [8–10]. It is widely investigated that joints can be exposed to humidity levels lower than 50% for very long periods without weakening. Significant weakening due to attack by moisture

ingress only occurred in the adhesive system above roughly 75% RH. [8, 9, 11]. Above this critical value the adsorption or diffusion of water in the adhesive material can alter the mechanical properties by plasticization, hydrolysis, cracking or crazing [12].

At long exposure times the Tg of an epoxy decreases, mainly due to plasticization. At short exposure times, post-curing reactions (that raise the Tg) are often observed with water exposure [9, 11]. In experiments done by Lettieriand Frigione [11], measured Tg values were always lower on epoxy aged by water immersion than those measured on the untreated resin. This suggests that the plasticization prevailed over the post-curing reactions. In the research on 'Applications of FTIR on Epoxy Resins' by González [13], changes were observed in the amount of hydroxyl groups in an epoxy subjected to water. An increase of the bandwidth between 3200–3700 cm^{-1} was observed. Where the upper range of this bandwidth (≈3600 cm^{-1}) is related to changes in the highly mobile free water molecules. The lower part of the bandwidth (≈3300 cm^{-1}) is related to water bounded to specific sites through hydrogen bonding.

Mechanically, plasticization leads to a generalized decrease on the ultimate tensile stress and E-modulus [14]. In some cases the original properties of the adhesive could be restored by removing the water by drying [11]. However, this will not be the case if plasticization has progressed too much. Whether plasticization of epoxy by water ingress actually affects the strength of the joint is difficult to predict.

3.2.2. Temperature

Generally, prolonged heating at an excessive temperature will split polymer molecules (chain-scission). This causes lower molecular weight and degraded cohesive strength. It will also continue cross-linking and evaporation of plasticizer resulting in bond embrittlement and shrinkage. Lastly oxidation can occur (if oxygen or a metal oxide interface is present) resulting in lower cohesive strength and weak boundary layers [15].

The thermal degradation of a cured epoxy results in the increase in carbonyl (C=O) groups. In FTIR analysis changes in the amount of carbonyl groups can be detected in the bandwidth 1600–1800 cm^{-1}. In the absence of oxygen it also results in a decrease in hydroxyl (-OH) groups (3200–3700 cm^{-1}). However, thermal exposure in the presence of oxygen will lead to the oxidation of the surface first. Oxidation increases the polarity of the material, which results in the attraction of water, and thus an increase in hydroxyl groups. The difference between thermal and thermo-oxidative reactions is in the degradation rate. In the presence of oxygen, the radicals formed are oxidized to form peroxides. These form on dissociation two radicals from each hydroperoxide group which accelerates the degradation process [10].

The Tg is an important parameter when looking at the temperature behaviour of a polymer. When tested below this temperature, the adhesive will behave like a low-strain rigid material while above this temperature it will have a more rubber-like behaviour, thus a lower strength and stiffness. Reis et al. [16] tested the strength and stiffness of DGEBA samples in ambient temperatures ranging from 25 to 130°C. It is observed that, although the Tg of the epoxy tested in this research is higher than test conditions, both stiffness and ultimate tensile strength decreased with increasing temperature. It is uncertain in what extend long term temperature exposure effects mechanical strength. Silva et al. [14] observed that the ultimate tensile stress and E-modulus increased up to 33% and 15%, respectively for epoxy submitted to thermal cycles. The thermal cycles might have caused a post-curing phase that could explain the increase on the epoxy specimen strength and stiffness, due to increased cross-linking.

3.2.3. UV

Epoxy resins are susceptible to light (UV) damage. It can cause yellowing and cracking. From literature there is not a clear consensus on how the strength of epoxies is affected by UV exposure. Nguyen [17] mentions that this cracking behaviour for epoxies only occurs after sufficiently long exposure times, of more than 300 hours. It was shown that the change of colour of the surface layer of the epoxy adhesive to UV exposure has no effect on the mechanical performance of joints. Coutinho et al. [18] tested an epoxy (Araldite 2020) on UV ageing. They noticed that ultimate strength, Young's modulus and Tg go up with increasing UV exposure time. This material response to the mechanical tests can be explained as an increase in chain cross-linking due to the ageing effect of light in polymers. However, the observed Tg values remained the same (56.9°C) throughout the ageing period after the first 100 hours. It is possible that this increase of cross-linking may not be enough to alter the Tg within this period. A yellowing of the samples is observed with increasing UV ageing. Nikafshar et al. [19] showed that after 800 hours of UV radiation, mechanical test results revealed that the lack of the UV absorber can lead to a 30% reduction in tensile strength. On the other hand, Amorim et al. [20] tested single lap joints exposed to UV

radiation (at a constant temperature of 40-50 °C) for 6 months. They found that UV radiation contributed to increase the shear strength and did not degrade the tested single lap joints, most likely because of the influences on the post-curing process. In a study on photo-degradation from UV exposure in epoxy [19], a relative increase of the absorbance was observed in the FTIR spectra of the bandwidths related to carbonyl groups and hydroxyl groups.

3.2.4. Hygrothermal conditions

Kinloch [9] states that most thermosetting adhesives are hydrolytically stable in the presence of water and moderate strengths of acids and bases. However, at relatively high temperatures, e.g. 70 to 100 °C, many of these types of adhesives will be susceptible to hydrolysis and show appreciable loss of mechanical properties as their molecular weight is decreased. In normal usage such temperatures are not very often attained and so this mechanism of attack is not commonly observed.

3.2.5. Salt spray

Due to the close proximity of the LMC to the ocean, the effects of salt spray (chlorides in water) should be considered. Salt water is particularly damaging to metal-adhesive joints, because it causes corrosion at the adhesive-metal interface [8, 9]. In the LMC no metallic surfaces are present that come in contact with the epoxy mortar.

In concrete/epoxy systems osmotic blistering can occur. This is a chemical phenomenon where two substances attempt to reach equilibrium through a semi-permeable membrane, and is promoted by salts. Concrete is usually very porous and the epoxy is not very permeable so the water will stop at the polymer interface, which functions as a membrane. However, in the presence of salts the force of the water, due to the semi-permeable membrane, results in water to collect in-between the concrete and the layer of epoxy. Humidity above 85% at elevated temperature causes blistering [10]. Silva et al. [14] compared epoxy specimens subjected to pure water immersion, water with 3.5% chlorides and wet-dry cycles. The dynamic E-modulus of the pure water immersion samples were approximately 19%. Those subjected to chlorides were 13% and wet-dry cycles were 5%. They concluded that chlorides present in water de-accelerated the degradation (due to plasticization) since the molecules of salts work as a semipermeable membrane. So, the presence of salts is likely to de-accelerate moisture damage in pure epoxies, but can retain water in concrete-epoxy interfaces.

3.2.6. Biological attack

Biological growth was observed on the epoxy mortar, mainly on the north side [4]. Although the micro-biological growth is visually disruptive, it is unclear whether it is in itself an active deteriorating factor or simply a symptom of variations in moisture conditions. Certainly the presence of microbiological growth will retain water and hinder evaporation, and the by-products might be corrosive to sensitive materials. Bacteria are less effective in degrading epoxies than fungi. Many fungi are capable of utilizing chemicals in the epoxy as a carbon energy source [21]. The degradation is caused by increasing the leaching of additives and monomers out of the polymer matrix by microbial degradation. The attack by enzymes or radicals of biological origin, leads to to both embrittlement and loss of mechanical stability. Lastly, biological films causes an accumulation of water within the material [22]. These biological effects are especially severe on natural adhesives. Such environments effect the thermoplastic and elastomeric adhesives and have lesser effect on the thermosetting and hybrid adhesives [15]. Thorp et al. [21] tempted to determine mechanical changes in composite coupons after exposure to a fungal culture. No significant mechanical changes could be measured after 120 days of exposure. So, other than the retention of moisture, microbiological growth is not expected to have great effects on epoxy adhesives.

3.2.7. Mechanical stress

The effect of simultaneous exposure to both mechanical stress and a chemical environment is often more severe than the sum of each factor taken separately. Mechanical stress, elevated temperatures, and high relative humidity can be a fatal combination for certain adhesives and sealants if all occur at the same time. In high humidity, stressed joints weaken more rapidly than unstressed ones. The mechanical applied stress contributes to chemical bond-scission, this leads to the more rapid rate of reaction. Exposure to cyclic temperature changes can induce thermal stresses. This has a similar effect on the material as applied mechanical fatigue stress. [8, 15, 23, 24].

3.3. Effects of material composition

From the analysis on the epoxy mortar as discussed in section 3.1, it was noted that presumably two additives were added to the epoxy, quartz flour(sand) and carbon black. The changes that occur, by addition of these materials, on the (mechanical and chemical) properties of the mortar are discussed below. Furthermore, the effects of weathering on the glass-adhesive bond is discussed.

3.3.1. Sand

Young and Lowell [25] state that an increase in toughness can be achieved in polymers trough the addition of a rigid filler such as silica particles. The filler impedes the propagation of cracks, resulting in higher toughness values. However it can reduce the fracture strength and elongation till failure. Other studies report an embrittlement of polymers and a significant loss of toughness compared to the neat polymer [26]. In the study of Dubnikova et al. [27] it was found that the tensile strength and toughness, increases or decreases compared to the neat polymer, depending on the particle size of the rigid filler. Sand, and other hard fillers, are also known to raise the glass transition temperature of the host polymer [28]. Sangermano et al. [29] employed silica nanoparticles to obtain hybrid coatings. The influence of the presence of silica on the rate of polymerization was investigated by real time FT-IR. The silica nanofiller induced both a bulk and surface modification of the coatings with an increase on Tg, modulus and surface hardness. A strong decrease on water uptake in the presence of silica was observed.

Research done by Reis and Ferreira [30] deals with the evaluation of the fracture properties of epoxy polymer concrete under marine exposure. Polymer concrete is the composite material made by fully replacing the cement hydrate binders of conventional cement concrete with resin. This material can be compared to the mortar used in the LMC, due to the high sand percentages in the thermoset resin. The research showed that Spring–Summer exposure period is the most aggressive for epoxy concretes, due mainly to elevated temperature and UV radiation. Silva and Silva [31] researched the effects of ageing on both epoxy and polyester mortars. Prism shaped specimens were made from a DGEBA resin (2/3) mixed with an aliphatic amine hardener (1/3) and subjected to: dry-wet, thermal, radiation and salt fogging cycles. Compressive and flexural tests were performed, that showed that the salt fog spraying cycles caused the most severe effects on strength reduction, especially on the epoxy mortar. A substantial decrease of ultimate strength of epoxy mortar was observed after humidity cycles reaching 30% at 10,000 hours, and its average ultimate deflection almost doubled. Similar values of a 30% decease of ultimate strength and 40% decrease in bending strength after 10,000 hours of thermal cycling were observed. The effects of solar radiation on strength were minor, however simultaneous ultraviolet action and moisture cycles are likely to be harmful to the strength of the mortars. Also a significant change of colour of the mortar was observed due to the UV exposure. Changes of physical texture, as detected by microscopic observations, do not seem explanatory of the modification of mechanical properties. However, observations indicate that thermal cycles affect the texture and cause coalescence of pores in the epoxy mortar.

3.3.2. Carbon black

Carbon black has been used as a (UV) light stabilizing additive in polymers for many years. Ghasemi-Kahrizsangi et al. [32] showed that degradation with many microcracks happened after 1000 h UV exposure to epoxy coatings without fillers. Microcracks were not observed on surface of coating with 2.5 wt% CB nanoparticles. In this research, a reduction of three times the amount of formed carbonyl bonds under UV, compared to aged epoxy without filler, was observed. However, lower amounts of carbon black (0.25 and 0.75 wt%) did not delay the degradation. Nikafshar et al. [19] tested the Tg values for samples after 0 up to 800 h of UV irradiation, with and without an organic UV absorber. It was observed that with increasing UV irradiation time, the Tg increased. After 800 h UV radiation, mechanical test results revealed that the lack of the UV absorber can lead to a 30% reduction in tensile strength. However, in the presence of the UV absorber, the tensile strength was reduced only by 11%. Accorsi [33] investigated the effects of particle size (15-60 nm) and percentage (0.5-3.5%) on UV protection. They concluded that a higher CB percentage provided better protection and smaller particles disperse better and contribute to better UV protection.

3.3.3. Glass-epoxy systems

Ageing tests on glass-adhesive connections are not widely studied in literature. Van Lancker et al. [12] developed an experimental setup to test glass-metal adhesive connections subjected to moisture, temperature and UV-radiation. It showed that exposure to moisture (vapour and liquid) led to significant damage of the adhesive layer of the point connections resulting in a decrease in stiffness and strength.

Water can permeate the adhesive or sealant and migrates to the glass-epoxy interface, displacing the bulk adhesive material at the interface, figure 3.3 [10, 34]. Thermal ageing did not, other than a small decrease of stiffness, decrease the strength of the epoxy glass connection. Glass for any type and thickness, blocks UV-B- and UV-C-radiation, thus the effects on the mechanical behaviour of the adhesive are less pronounced. The tests showed UV-radiation did not significantly change the strength and stiffness of the epoxy. However, the additional exposure to UV-radiation after exposure to humidity and thermal cycling further decreased the stiffness and strength of the adhesive layer significantly. So, UV-radiation was only of importance when initial damage, in this case due to moisture, or locations of impurities were already present.

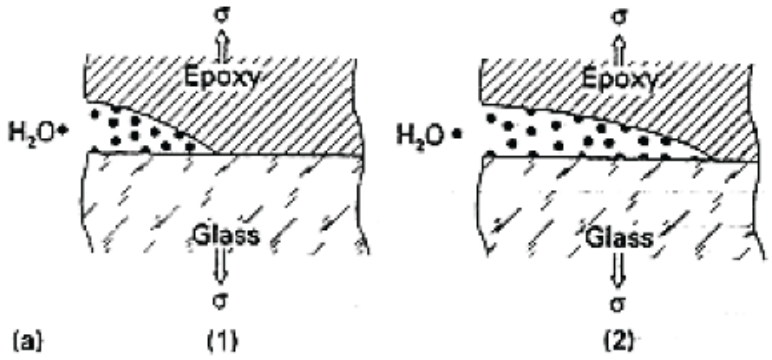

Figure 3.3: Water ingress on the epoxy-glass interface [10]

3.4. Accelerated ageing

To more accurately predict the effects of weathering and the state of degradation of the mortar used in the LMC, accelerated ageing tests will be used. Accelerated tests are widely used for testing environmental effects and the lifetime prediction of a material or system. ASTM standard C1850−17 [35] states that the goal of laboratory accelerated testing is to provide a relatively rapid means of measuring the rate of property changes typical of those that occur in long-term in-service use. However, the intensity of degradation factors used in these accelerated tests should be considered, so degradation by mechanisms that do not occur in-service are avoided. The potential of synergism should always be borne in mind in the development of accelerated tests. For example, the combined effects of weathering factors, such as solar radiation, temperature, applied strain and moisture, may be greater than the sum of the effects of the individual factors. ”Long-term in-service tests are necessary to validate the degradation factors of importance for the sealant.” In case of the LMC the test samples obtained from the lantern can be used as long-term in service reference. If it is established that the type of degradation induced by the accelerated tests are the same as those observed in-service, the rates of change of the properties can be calculated. However, the relationship between the accelerated tests and the in-service tests are seldom linear. From findings, it is often observed that the applied artificial ageing procedures completely exaggerate the long-term behaviour under accelerated outdoor conditions, making the correlation difficult [12].

3.4.1. UV

Feller [24] states that an acceleration factor of five to ten times would represent an acceptable level and that the ultraviolet intensity should not exceed more than three times the standard solar intensity in a given climatic zone. An irradiance between 300 and 800 nm of vertically impinging direct sunlight would produce an acceleration factor seven and a half times compared to outdoors in central Europe. Tweedie et al. [24] employed a hypothetical equivalence of five hours in xenon-arc machines to one day of summer sunlight. Using the first method, with an average of 1300 hours of sunlight yearly in Liverpool [36], 1500 hours of UV irradiation would be approximately equal to 8.6 years in real life.

3.4.2. Moisture

The action of moisture in deterioration, difficult to predict, must be verified in each specific situation. For the moisture content used in ageing tests, the relation between strength and RH is not linear but often S-curved, similar to the isotherm for the absorption of water. The present consensus is that a moderate level of moisture (20-80% RH) is advisable in accelerated photochemical or thermal ageing tests [24]. In

the ASTM standard D1151−00 [37], humidity levels of 50%, 88%, immersed and uncontrolled humidity are used. While in ASTM D1183-03 [38] levels of 85 to 90% RH are alternated with <25% RH for multiple cycles, up to 72 hours.

3.4.3. Thermal

Thermal degradation can be accelerated by exposure to temperatures higher than those expected in-service. However caution should be taken that applying extreme levels of stress to accelerate the rate of degradation may activate mechanisms and induce changes that are not predictive of in-service degradation [35]. Especially temperatures above the Tg can cause chemical changes, and should not be considered if they do not occur in-service.

3.4.4. Hygrothermal

A common method to test hygrothermal ageing is the immersion of the joint in water at, 70 to 100 °C, at long times of immersion this will lead to hydrolysis and loss of bulk strength. However, such exposure temperatures are not reached during normal outdoor ageing. Therefore, too extreme temperatures in laboratory ageing trials should not be used in order to accelerate the rate of attack by moisture upon the joint, since the mechanism of joint failure may prevail via a mechanism which will never be observed during the service life of the bonded structure [9].

II

Research definition and Experimental setup

4

Research definition

4.1. Scientific gap

The objective of the proposed research is to gain insight into the effects that environmental ageing might have on the epoxy mortar as used in the Liverpool Metropolitan Cathedral. Specifically, the extent of mechanical and chemical degradation of the epoxy mortar and the strength of the adhesive connection to the glass is of interest. Only a very limited amount of original epoxy-mortar material from the lantern is available for testing. A link of the change in properties due to environmental degradation, with a similar reproduced material will be made.

4.2. Research question

What is the mechanical and chemical stability of the (fifty years) environmentally exposed epoxy-mortar, as used in the Dalle de verre (stained glass windows) of the Liverpool Metropolitan Cathedral?

- Can the type of material as used in the epoxy-mortar from the LMC be determined and reproduced?
- Does (accelerated) ageing, by outdoor light exposure, moisture and temperature, degrade the mechanical performance of reproduced epoxy-mortar and glass-mortar samples?
- Does (accelerated) ageing alter the chemical properties of the epoxy mortar, observed using FTIR spectroscopy and Tg analysis?
- Does accelerated ageing cause the same interface adhesion failure in glass-mortar samples, as observed in the Liverpool Metropolitan Cathedral?
- Do the samples obtained from the Liverpool Metropolitan Cathedral degrade further under accelerated ageing (UV, moisture, temperature)?
- Can the amount of degradation, as used in the Liverpool Metropolitan Cathedral, be quantified for the epoxy mortar based on the above outcome?

4.3. Hypothesis

This thesis will be based on the possible correlation between the changes in the mechanical and chemical properties of a epoxy mortar, due to accelerated ageing. Based on findings from studied literature (section 3), it was found that environmental degradation causes both changes in mechanical strength as well in the chemical properties. By linking these two properties, it is hypothesized that a correlation can be found in the changes of the reproduced specimens with the original specimens from the cathedral. The main hypotheses proposed are presented below:

1. **The adhesive failure observed in the LMC between the glass and the epoxy mortar is most likely caused by moisture** In the LMC, the interface between the glass and epoxy-mortar has failed. This can be linked to literature, where the de-bonding of epoxies from glass is caused by moisture ingress.

2. **The combination of moisture with solar exposure will most likely be the biggest mechanical degradation factor of the epoxy-mortar. Whereas temperature or outdoor light exposure alone will not degrade the strength much.** he mechanical tests will most likely give the most tangible results on the extent of degradation of the mortar. It is predicted that outdoor light exposure has little effect on the strength of the epoxy mortar, mainly because the carbon black acts as a UV absorber. From literature, it showed that UV does not degrade the mechanical properties greatly, in some cases it even increases strength due to post-curing. Most effects from UV are likely to come from the simultaneous occurring raised temperature. Hygrothermal exposure showed to be the biggest degradation factor in previous research on epoxies. Although the climate of Liverpool is not a tropical one, high levels of humidity are present due to the proximity of the LMC to the sea.

3. **Changes in the glass transition temperature and functional groups will likely be visible from chemical/physical analysis performed. However, this will not yield a direct correlation with degradation.** Chemical analysis (FTIR) will most likely show an increase in bandwidths around 1600–1800 cm^{-1} related to the formation of carbonyl groups and between 3200–3700 $cm^{-1}$to hydroxyl groups. The formation of these groups is an indication of degradation due to oxidation and increased cross-linking of aged samples. However, FTIR samples can most likely not directly be compared to the LMC test samples. The chemical properties are dependent on the initial material composition (material, mixing ratio, curing etc.). These initial properties are not exactly known, so only an approximation of degradation types can be made. The glass transition temperature can also be a good indicator of the chemical degradation, but similarly to the FTIR analysis, the initial Tg of the LMC test samples are not known. So, degradation in each ageing cycle can be predicted individually, but it will be difficult to compare degradation with the LMC samples directly.

4.4. Research

The research consists of three main parts. First, performing material analysis on the LMC mortar. This is done to determine the material properties, so the material can be replicated. The second part consists of accelerated ageing of the reproduced specimens and the original specimens from the LCM. This is done by performing different weathering cycles. Thirdly, results of the changes induced by the accelerated ageing on both chemical and mechanical properties are assessed. The steps undertaken to be able to answer the research questions are presented below:

1. Determine the material composition of the epoxy mortar;
2. Reproduce epoxy-mortar samples, with a as similar as possible material composition, suitable for mechanical and chemical testing;
3. Perform accelerated ageing procedures on both reproduced samples and original samples from the cathedral;
4. Perform mechanical tests on artificially aged reproduced samples;
5. Perform physical/chemical tests on artificially aged reproduced samples and aged original samples from the LMC;
6. Analysis of obtained data from mechanical and physical/chemical tests;
7. Find a link between the changes due to ageing of reproduced samples and the original LMC samples.

5
Methodology

This chapter will outline the experimental procedure and set-up used to acquire the data and results used in this thesis. First a material analysis was performed to determine the composition of the epoxy mortar as used in the LMC. This helps to determine the material that is used for the reproduced samples, as used in the experimental part of the thesis. The specimen design and experimental setup for the accelerated ageing, mechanical, physical and chemical tests are described.

5.1. Design of experiments

An overview of all tests that have been performed is shown in table 5.1. Only a very limited amount of original material from the cathedral was available for this research. Sixteen cylindrical core samples (figure 5.1), all with dimensions around 2 cm in height and diameter of 1 cm, were obtained from Purcell. Some samples where already modified or cut for their research. Therefore, limitations in the choice of experiments that can be performed on the LMC samples is present. Due to the destructive nature of mechanical testing and the need for multiple tests samples to minimize scatter, the amount of available LMC samples is not sufficient for standard mechanical tests. Therefore, the choice was made to make a model material (with a similar composition as the LMC mortar) to perform ageing experiments on. Mechanical tests are only performed on the reproduced mortar. Changes in physical/chemical properties of reproduced material with the aged LMC samples are compared. These physical tests form the link between the mechanical stability of the reproduced and the original specimens.

Figure 5.1: LMC core sample [7]

Mechanical test were done to measure the mechanical stability of the reproduced mortar under the selected ageing cycles. To measure the (physical) changes within the material FTIR and DSC tests were selected. These test can serve as a link between the LMC and reproduced (RP) samples. To get a more in depth understanding of the changes in the LMC material, Dynamic mechanical analysis (DMA) tests were performed on the LMC samples. The geometry of the LMC cores is suitable to produce DMA specimens, the samples were cut in rectangles of 2cm long and 2mm thick. DMA is a good way to obtain more physical properties. Material analysis is performed by using Thermographic analysis (TGA) and (SEM) microscopy. Weight changes are measured to compare the amount of water absorbance in the samples. X-ray photoelectron spectroscopy (XPS) was selected after all the performed tests, because FTIR did not give conclusive results. It is used to analyse surface changes and bonds. For this research it is used to measure the amount of oxidation of the epoxy.

5.2. Material analysis

Material analysis is performed to determine the composition of the epoxy-mortar of the reproduced samples. The results of this material analysis is discussed in chapter 6. To determine the composition of the reproduced epoxy mortar, the following considerations are made to make a material as similar as possible to the LMC epoxy mortar. The type of epoxy used in the cathedral is unknown, it is either based on an Epikote resin (as mentioned in the Shell film) or the Kollercast 332 resin. Neither of these original

Table 5.1: Overview of all performed tests (where ✓is performed, ✗is not performed and ✓*only on limited amount of samples)

Part	Test	LMC samples	Reproduced samples
Material analysis	TGA	✓	✓
	SEM	✓	✓
Mechanical testing	Compression test	✗	✓
	Tensile test	✗	✓
	Lap-shear test	✗	✓
Chemical and physical analysis	FTIR spectroscopy	✓	✓
	DSC	✓	✓
	DMA	✓	✓*
	Weight change	✓	✓
	XPS	✓*	✓*

epoxies, or technical datasheets, are available anymore. These resins are most likely based on a DGBA + amine resin.

A commercially available epoxy with similar properties, Araldite 2020, is selected. Carbon black powder is obtained from 'Verfmolen de Kat' [39]. The epoxy mortar from the lantern was investigated using a scanning electron microscope (SEM) to determine the grain size of the sand used. TGA tests were performed to verify the results obtained in the tests done by Purcell, see section 3.1. From this the ratios of the epoxy, sand and carbon black were determined as will be used in the reproduced epoxy-mortar.

5.2.1. Thermographic analysis (TGA)

To verify the Thermographic analysis (TGA) results obtained from Purcell [7], TGA analyses were performed using a PerkinElmer TGA 4000. The samples were heated at a constant heating rate of 20°C/min from 20°C to 900°C. From 20 to 600°C the test was performed under a nitrogen atmosphere. When the temperature set point reached 600 °C the purge gas was switched to air and further heated up to 900°C. To compare the influence of the carbon black percentage on the TGA results, samples were reproduced that consist of a similar composition as the LMC samples. The reproduced samples were made from a Araldite 2020 resin combined with quartz sand in a ratio of 1:2. Each sample has a different carbon black content of respectively, 0%, 0.05% and 3%. Hypothesized is that pyrolysis of the epoxy happens before 600°C under the inert nitrogen atmosphere. After this temperature the two left over components are the (incombustible) sand and the carbon black. Likely, is that the degradation step around 600°C is due to the combustion of carbon black present in the mortar. The left over material after 900°C is due to the sand. The results of the TGA of the reproduced specimens, with known properties, were compared to the LMC samples.

5.2.2. Scanning Electron Microscopy (SEM)

To determine the grain size of the sand present in the mortar Scanning Electron Microscopy (SEM) images were made. A Jeol JSM-7500F field emission scanning electron microscope was used [40]. Using this microscope a magnification of 25 to 1,000,000 times is possible.

5.3. Accelerated ageing

Four types of ageing cycles were performed on the specimens, table 5.2. Each ageing procedure was performed for the total duration of 1050 hours. Where tests were done at 350, 700 and 1050 hours.

For the relative humidity cycle (RH) and temperature cycle (TC) tests the WEISS WK111-340 climate test chamber was used [41], figure 5.2a. This chamber can control temperature and relative humidity. The humidity cycle will follow the practices of ASTM test D7444−18a [42]. The relative humidity is set to an constant RH of 80% on room temperature (20 °C). This value is chosen to be above the critical humidity of 75% observed in literature, while still being close to the most occurring average humidity in Liverpool of 75% RH (see section 2.4).

Solar expose (UV) and solar exposure in combination with water spray (WS), was simulated in the Q-SUN® Xe-1 chamber [43], according to ASTM D904−99 [44]. A outdoor daylight (Q) filter (nominal cut-on 295 nm) is placed in front of the UV lamps. Hygrothermal cycling will be simulated by means of solar exposure cycled with a distilled water spay (WS), according to ASTM D2565−16 [45]. This is a

Table 5.2: Ageing cycles and parameters (RH= relative humidity, TC= temperature cycling, UV=ultraviolet light, WS= ultraviolet light + water spray))

Test	Cycle description	Set point	Temperature
RH	High relative humidity	80% RH	21°C
UV	18 hours UV light, 6 hours dark + no water	Light: 41.5 W/m2 from 300 to 400 nm	Light: 63°C, Dark: 38 °C (uninsulated black panel temperature)
TC	18 hours high temperature 6 hours low temperature	20 % RH 40% RH	42 °C, 25°C
WS	18 hours UV + water spray, 6 hours dark	Light: 41.5 W/m2 from 300 to 400 nm	Light: 63°C, Dark: 38 °C (uninsulated black panel temperature)

standard practice for xenon-arc exposure of plastics intended for outdoor applications. Test method 2H for standard plastics was selected. In this test 18 hours light (irradiance of 42 $\mathrm{W/m^2}$ with a insulated black panel temperature of 63 °C) with water spray is followed by 6 hours dark (irradiance of 0 with a insulated black panel temperature of 42 °C). In the light cycle 102 minutes of light is alternated by 18 minutes of light and front water spray. Pulse rate of the water spray is 5 seconds with 25 seconds no spray.

To test the effects of outdoor light exposure (UV) this standard test is adjusted to by removing the water spray: alternating 18 hours of light (42 $\mathrm{W/m^2}$, insulated black panel temperature of 63 °C) with 6 hours of dark (insulated black panel temperature of 42 °C). From the UV chamber it was given that 1050 hours of light cycles is equal to approximately 121000 $\mathrm{kJ/m^2}$ of solar irradiance.

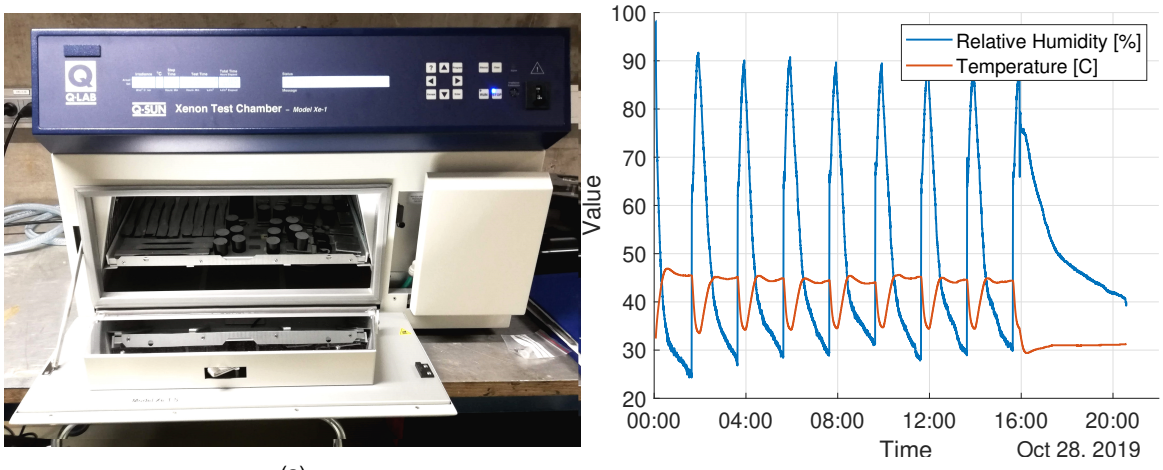

(a) (b)

Figure 5.2: (a) Weiss climate chamber with samples. (b) Measured temperature and relative humidity during WS cycle in the Q-sun climate chamber.

In the temperature cycling tests (TC), the air temperature and humidity are set to be the same as the UV cycle, 18 hours of high temperature is alternated by 6 hours of low temperature. It was noted that the set point temperature of the UV ageing chamber does not match the actual air temperature. So, to match the temperature of TC cycle with the temperature used in the UV ageing the ambient temperature and relative humidity were recorded for 24 hours during the UV cycles. This was done by means of a 'RS pro 1365' temperature and relative humidity meter. This recorded that during the light cycle, a set point of 63 °C (insulated black panel temperature) is equal to an air temperature of 45°C. The relative humidity at this temperature is around 20%. Similarly, in the dark cycle, an insulated black panel temperature of 42 °C is equal to 30 °C with a relative humidity of 30%. So, for the temperature cycle (TC) 18 hours of 45°C and 20% RH is alternated with 6 hours of 30 °C and 30% RH.

The temperature and humidity levels of the WS cycle were measured as well. During the 18 minutes light with water spray, the temperature and relative humidity reached 35.5 °C and 82 %, respectively.

In the following 1:42h of only light (without water spray) temperature and humidity go to a maximum of 47.1 °C and 33%. After repeating this 9 times, the dark cycle starts. Here the temperature slowly drops to 31.5°C and with a humidity around 40%, figure 5.2b.

5.4. Mechanical testing

Mechanical tests were performed on the reproduced specimens. The methods of performing compression, tensile and glass-bonded lap-shear tests are described in this section.

5.4.1. Compression testing

To obtain the compressive strength of the reproduced specimens, cylindrical epoxy-mortar specimens are prepared according to the ASTM standard ASTM C579−01 [46]. This test describes a standard of testing the compressive strength of polymeric concretes and mortars. Compressive tests are performed on a Zwick 250kN universal test machine. The displacement is measured in the cross-head. An uniform compressive cross-head speed of 3mm/min is applied until after reaching the maximum force, the applied force reduces with 50% of this maximum value.

The cylindrical samples for the compression tests will be have a diameter of 25 mm with a height of 25mm, figure 5.3b. A total of 5 specimens, for each duration of each ageing cycle, will be made (15 per cycle type). The specimens will be prepared in a mould made out of a Teflon plate of 25 mm thickness with holes of 25 mm diameter(≈1 inch), figure 5.4b. Teflon as a moulding material is selected so the mortar does not adhere to the mould, since it has a low surface energy. The mortar will be cast into the mould and cured in laboratory conditions (21 °C, 50% RH). The uneven top surface of the specimens are sanded into a flat and smooth surface to a total specimen height of 25 mm $\pm$ 1 mm.

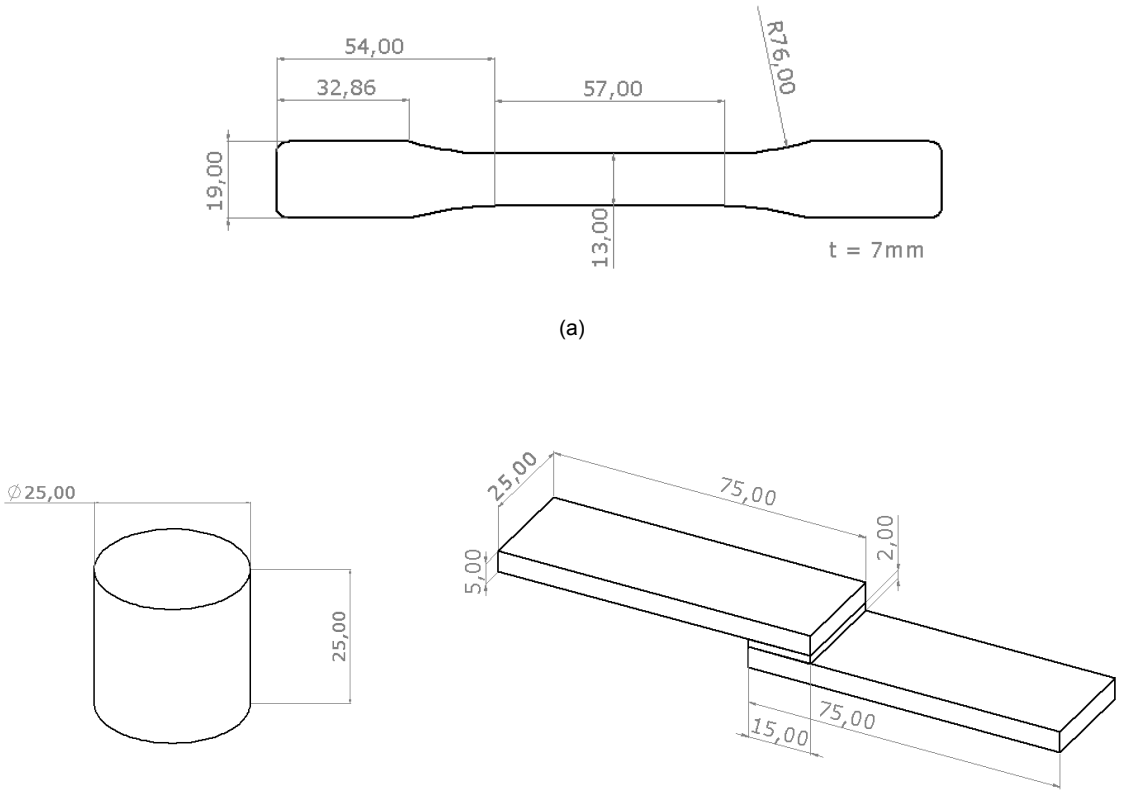

Figure 5.3: Design of tensile (a), compression (b) & lap shear (c) specimens in mm. Drawing size not on real scale

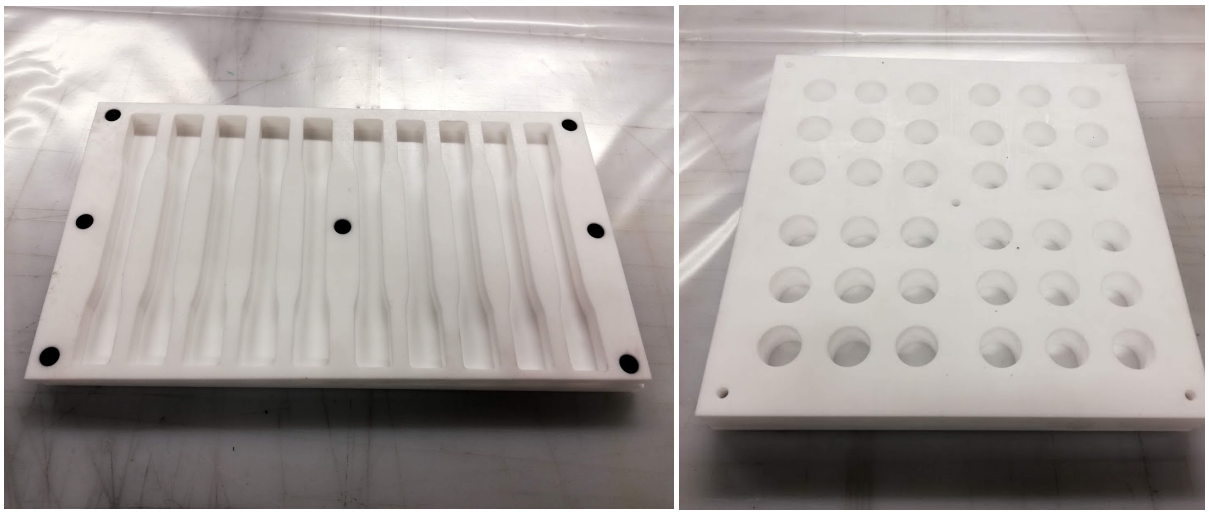

(a) (b)

Figure 5.4: Teflon moulds for dogbone and compression samples

5.4.2. Tensile testing

Tensile tests were conducted on the Zwick 250kN test machine, which is equipped with an extensometer with a gauge length of 40mm. An uniform cross-head speed of 1 mm/min is applied until failure of the specimen. Five dogbone samples for each duration of the RH and TC cycles are tested. Due to limited capacity of the q-sun chamber 4 samples for the WS and UV cycles are used.

The dogbone samples were manufactured as defined by the standard ASTM D638-03, type III (Standard test method for tensile properties of plastics). A Teflon mould was manufactured to make the dogbone samples, figure 5.4a. The epoxy mortar was cast into the mould and cured during 48 hours at 21 °C and 50% RH. After curing the bottom plate can be detached to release the samples. The top part of the samples are open to the air, this irregular surface is milled into a final specimen thickness of 7mm. All the samples were conditioned at 23°C for 1 week at a relative humidity of 50% before undergoing accelerated ageing tests.

Initially the top of the dogbone specimens were milled by DEMO to 7mm thickness, however due to limited capacity they were only able to mill the RH cycle specimens. To overcome this problem, a mould was made out of a 7mm thick wood plate with the specimen outline cut out. By placing the specimens inside, the excess thickness of the specimen was could be removed by the use of a router. Then top was sanded to a smooth surface. However, this is a very time consuming process, so for future specimen creation, the use of a milling machine would be recommended. The final thickness of the specimens is measured to be 7 ± 0.1 mm.

5.4.3. Lap-shear testing

To see if the adhesive failure occurs between glass and adhesive, lap shear specimens were created. Lap shear tests were performed based on the 'Standard test method for lap shear strength of sealants' ASTM C961-15 [47]. For each sample two glass plates of 75x25 mm are adhered to each other with an overlap length of 15 mm and adhesive thickness of 2 mm, as can be seen in figure 5.3c.

Testing of the lap shear specimens is performed on a Zwick 10 kN testing machine. The specimens are eccentric clamped using hydraulic grips, with a clamping pressure of 8 bar. The specimens are loaded in tension with a cross-head speed of 1 mm/min, displacement controlled.

The used glass is a float glass. Before adhesion it was ensured that the tin side of the glass is not on the side of the epoxy-mortar, to prevent unwanted effects from the metallic surface. This side was identified using a UV lamp. Specimens were created in two steps. First, glass was bonded by the mortar by means of a template to distance the two glass plates, as can be seen in the ASTM standard [47]. The template is placed on a 700 x 700 mm aluminium plate covered with a plastic layer. The wood sticks were used to prevent outflow of the mortar from the sides of the overlap. This can be seen in figure 5.5a. A vacuum bag is put over the specimens to ensure a constant pressure difference of 200 mbar. The second step is the adhesion of four 60 x 25 mm aluminium tabs to all sides of the specimen. The aluminium tabs protect the glass from the clamping force during testing. This is done in the same manner as the bonding of the glass. The specimens are placed on the template. Using the Araldite

2020 the tabs are adhered to all sides and cured under 200 mbar under atmospheric pressure. The final test specimens are displayed in figure 5.5b.

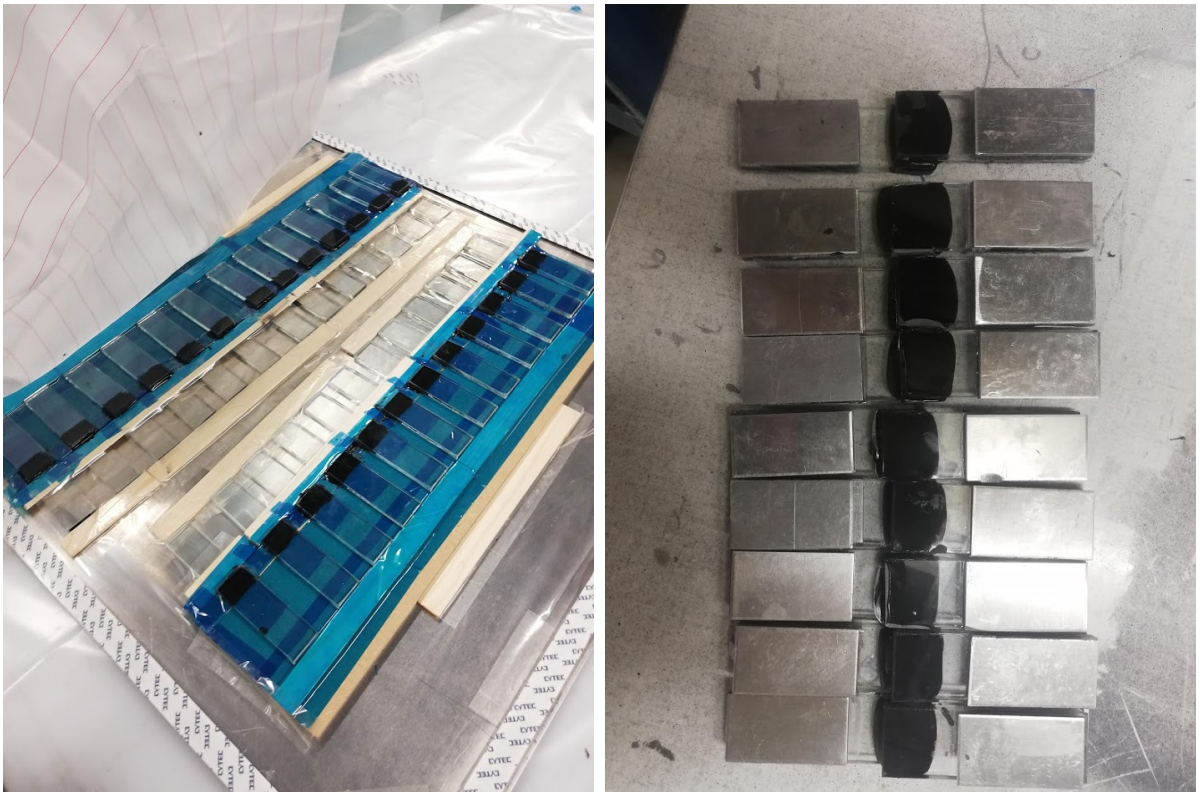

(a) (b)

Figure 5.5: Preparation of lap shear specimens (a) and finished product with aluminium tabs (b)

5.5. Physical and chemical tests

Chemical composition is greatly influenced by the used materials and the production process (mixing ratio, type of epoxy and hardener, additives). Since the exact composition of the original epoxy mortar is not known, physical and chemical analysis of the reproduced samples in comparison with the LMC test specimens, will not yield direct quantitative results. However, some test can be done to determine the effects of accelerated ageing on the material. On the specimens of all ageing cycles Fourier Transfer Infrared spectroscopy (FTIR), Differential scanning calorimetry and X-ray photoelectron spectroscopy (XPS), will be performed. Dynamic mechanical analysis (DMA) will be carried out on the aged LMC samples.

5.5.1. Fourier Transfer Infrared spectroscopy (FTIR)

Fourier transfer infrared spectroscopy (FTIR) is a common method for evaluating chemical changes during the degradation process in epoxy systems. FTIR spectroscopy test were carried out on the PerkinElmer Spectrum 100 spectrometer. A background scan was performed before every test. The outer surface of the specimen was placed onto the machine and scanned from 550 to 2000 cm-1. For every sample 8 scans were made and combined into the final absorbance spectrum. Changes of functional groups in the scans of the different samples will be compared. An overview of frequency ranges of different functional groups commonly present in DGEBA epoxies is used [48] for the analysis of the spectra.

5.5.2. Differential scanning calorimetry (DSC)

Differential scanning calorimetry (DSC) tests were conducted to measure the glass transition temperature (Tg). Tests are done on the reproduced mortar and the original LMC samples, before and after the ageing procedures. Each measurement sequence comprised a temperature ramp of 3°C/min from 0°C to 150°C. All DSC measurements were conducted on the TA Instruments Modulated DSC, and have a approximate sample weight of 10 µg. The total heat flow is normalised for the weight of the tested

sample. The DSC tests were done using a modulated heating profile. This method is chosen since modulated DSC can record both the non-reversing and the reversing heat flow signals. The heat capacity obtained from the reversing signal could give a better indication of the location of the Tg.

5.5.3. Dynamic mechanical analysis (DMA)

Dynamic mechanical analysis (DMA) can be performed to obtain the tensile, flexural or compressive moduli by applying a oscillating frequency. Figure 5.6a shows the DMA samples in the UV ageing chamber. The standard ASTM D7028-07 [49] is used to analyse the glass transition temperature (Tg) and maximum loss factor temperature (Tt) from the DMA tests. The Tg determined by this test method (referred to as 'DMA Tg') is not the same as the Tg obtained from DSC measurements. The difference in the Tg measured by DSC or DMA can be as much as 20°C [50]. Tests were performed on a TA instruments RSA-G2 solids analyser. The program starts at room temperature (25 °C) and runs up to 120 °C with a constant heating rate of 2 degree/min. A test frequency of 1 Hz was used. The instrument is operated in constant strain mode, with a maximum strain amplitude of 0.02% and sampling interval of 1 s/pt.

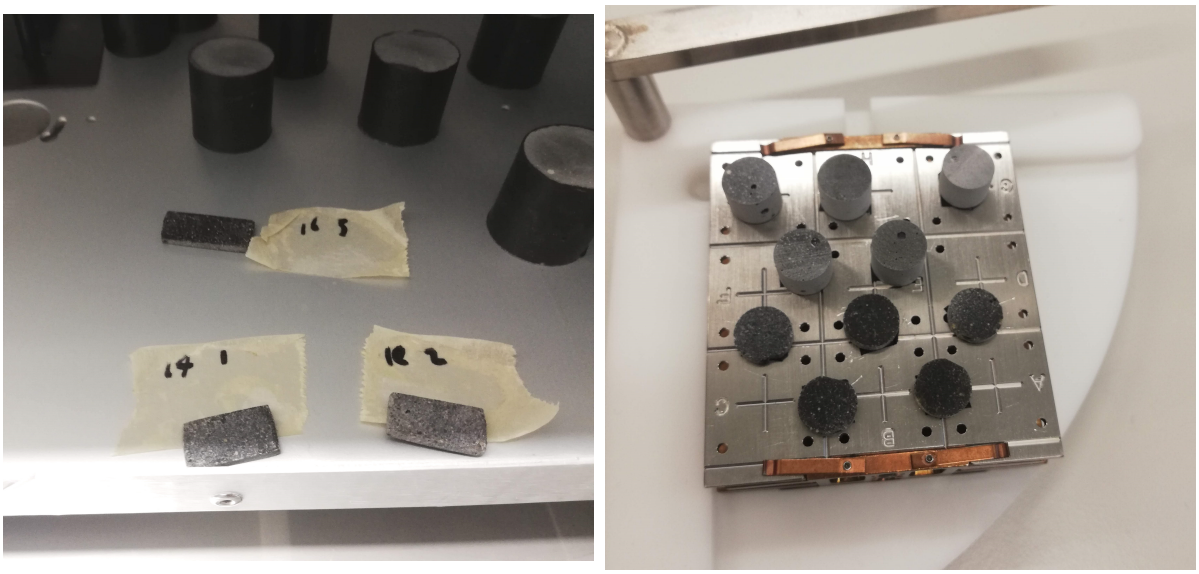

(a) (b)

Figure 5.6: LMC DMA samples in ageing chamber (a) and XPS samples (b)

5.5.4. X-ray photoelectron spectroscopy (XPS)

X-ray photoelectron spectroscopy (XPS) was used to show what elements are present on the surface and to what other elements they are bonded to. The average depth of analysis for an XPS measurement is approximately 5 nm. XPS measurements were performed externally, in the Faculty of Applied Sciences of the Delft University of Technology. Tests were performed on one sample for each ageing cycle, after 1050 hours of ageing, as well as one unaged sample. So, a total of This was done for both the LMC as the reproduced samples. Figure 5.6b displays the ten tested samples. Spectral analysis was conducted using CasaXPS software. The samples were not measured both before and after ageing, since initially this test was not selected. This would be preferable in further research.

5.5.5. Weight change

Change in weight due to water absorbance in the moisture exposed (RH) cycle was recorded. Mass is measured before and directly after each ageing time (350, 700 and 1050 hours) on a Mettler Toledo AV204-S scale with an accuracy of 0.1 mg. Furthermore, water absorbance is tracked over the course of one week on one LMC sample and one reproduced sample. The amount of absorption and recovery due to drying are measured.

III

Results and Discussion

6

Material analysis

Since no data-sheets are available to indicate the chemical composition of the resin that was used in the LMC mortar, its specific features remain unclear. Material analysis by means of TGA (section 6.1) and SEM microscopy (section 6.2) were performed to get a better understanding of the material as used in the epoxy-mortar of the LMC. Lastly, the material is selected to manufacture the reproduced epoxy-mortar as used in the experimental part of this research.

6.1. Thermogravimetric analysis (TGA)

Three reproduced epoxy-mortar samples, each with a different carbon black (CB) percentage (3%,0.05% and 0%), and two samples from the cathedral (core 9, retrieved from Panel C on the east side) were tested.

6.1.1. Results

TGA analysis from the samples obtained from the cathedral and the reproduced samples are plotted in figure 6.1. The samples from core 9 of the cathedral show similar weight loss curves as the previous tests done by Purcell, see figure 3.2 in section 3.1.

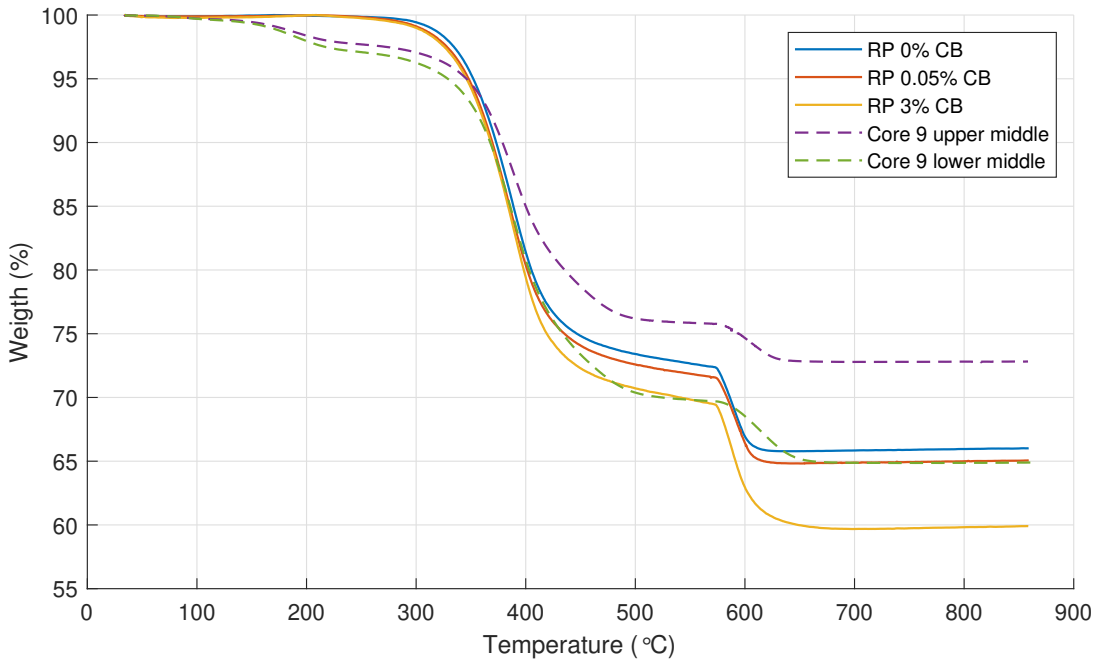

Figure 6.1: TGA analysis of replicated samples with different CB percentages (RP) and core 9 from cathedral

The tested LMC samples show a first weight loss step around 200 °C. This could indicate volatile products in the material. The reproduced epoxy samples do not show this step around 200°C. The onset of the second step in all samples is around 300 °C. This step is linked to the degradation of the epoxy present in the material. Both samples from core 9 show a third weight loss step around 580 °C of approximately 3%, similarly to the previously done tests by Purcell. The amount of material left over at the highest temperatures in the two LMC samples is 60 and 73%, linked to the sand.

All reproduced samples show a distinct step around 580 °C as well, regardless of the CB content. The weight loss percentages around this temperature of the 0%, 0.05% and 3% CB samples are respectively, 6%, 6.5% and 8%.

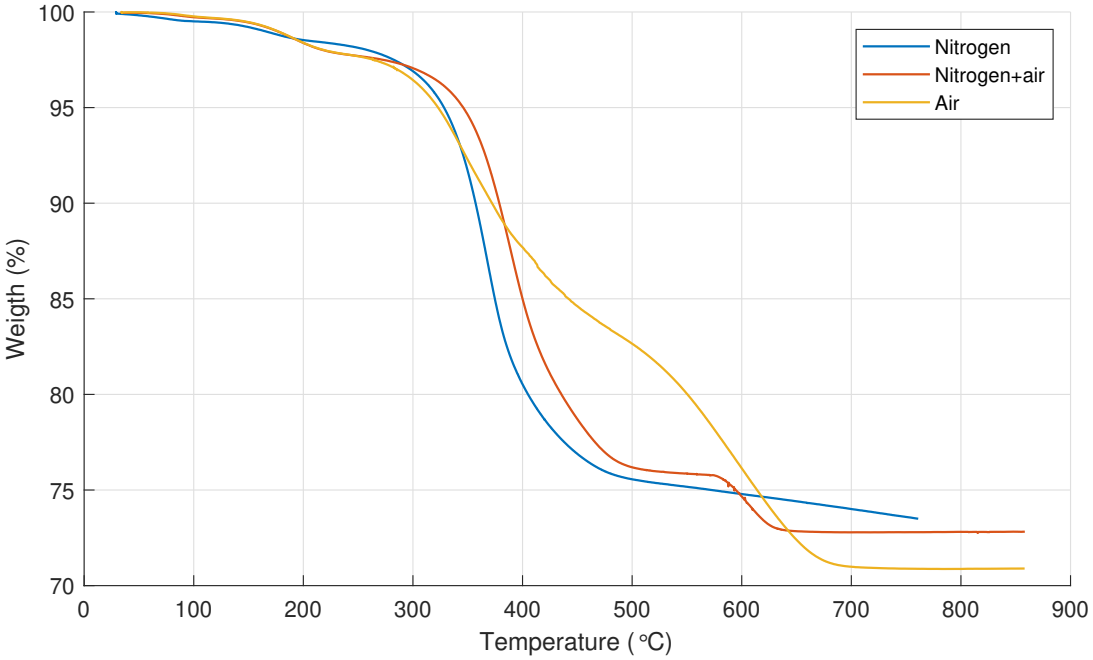

Figure 6.2: TGA analysis core 9 (upper middle) under nitrogen, nitrogen+air and air

The onset of the degradation temperature of the last step is lower than 600°C as compared to the test done by Purcell. This is because of the settings of the TGA machine used that switches from nitrogen to air at the set point rather than the actual temperature. This difference does not alter the height of the step greatly compared to the previous test.

When comparing the different atmospheric gasses, it is verified that under a pure nitrogen atmosphere, the weight loss step around 580°C is not present, figure 6.2. When using laboratory air only as a purge gas, the oxidation happens around 500°C, simultaneously with the pyrolysis of the epoxy. The test where the purge gas is switched from nitrogen to air gives the clearest differentiation of the epoxy and the combustible products.

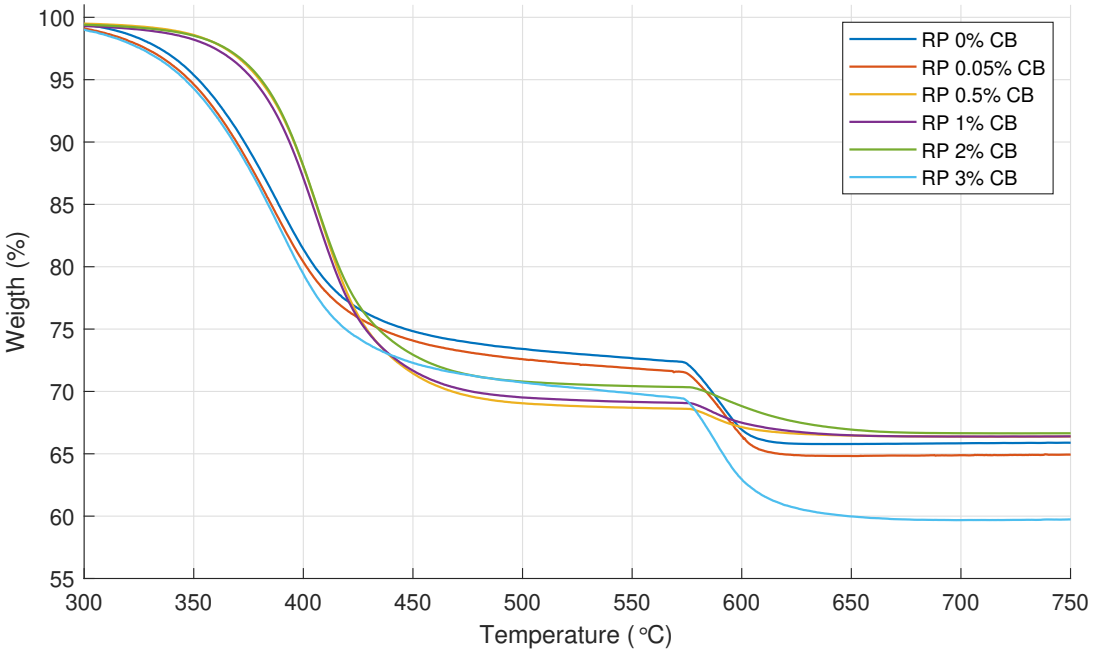

Figure 6.3: TGA analysis of replicated samples with different CB percentages (RP) from cathedral

To compare if the height of the last weight loss step from the is due to the carbon black scales in height accordingly with increased carbon black percentages, more samples were made. In figure 6.3 the previous samples of 0, 0.05 and 3% are plotted. Additionally, the TGA results of the extra manufactured

samples of 0.5, 1 and 2% are shown. It is observed that the step height of the 0, 0.05 and 3% samples is much greater than the step of the extra made samples.

6.2. Microscopy (SEM)

To determine the grain size of the sand, Scanning Electron Microscopy (SEM) was used. From the information obtained from David Kirby, see section 3.1, a M3 sand flour was most likely used in the mortar. This is very fine sand with a grain size of 62.5–125 µm. SEM images are taken from the powdered epoxy mortar of the LMC material, figure 6.4a. The sand particle size is estimated to be between 30 and 70 µm. This would be the same particle size as the M3 sand flour. 'Sand, white quartz' >230 mesh [51] was selected to make te reproduced samples. In this sand 90% of the particles can fit trough a 63 µm sieve.

SEM images were made of the reproduced epoxy-mortar with this selected 230 mesh sand. From the powdered samples it is noticed that the sand particles are difficult to detect, see figure 6.4b. It could be that the epoxy in the reproduced samples is more bound to the sand than in the LMC samples.

SEM images were also taken from the solid reproduced samples, figure 6.5b. These are compared to SEM images made by Purcell, figure 6.5a [7] of the LMC mortar. It can be noted that the variation of particle size in the LMC samples is much greater, up to 1000 µm. Whereas the reproduced sand goes up to 100 µm in size.

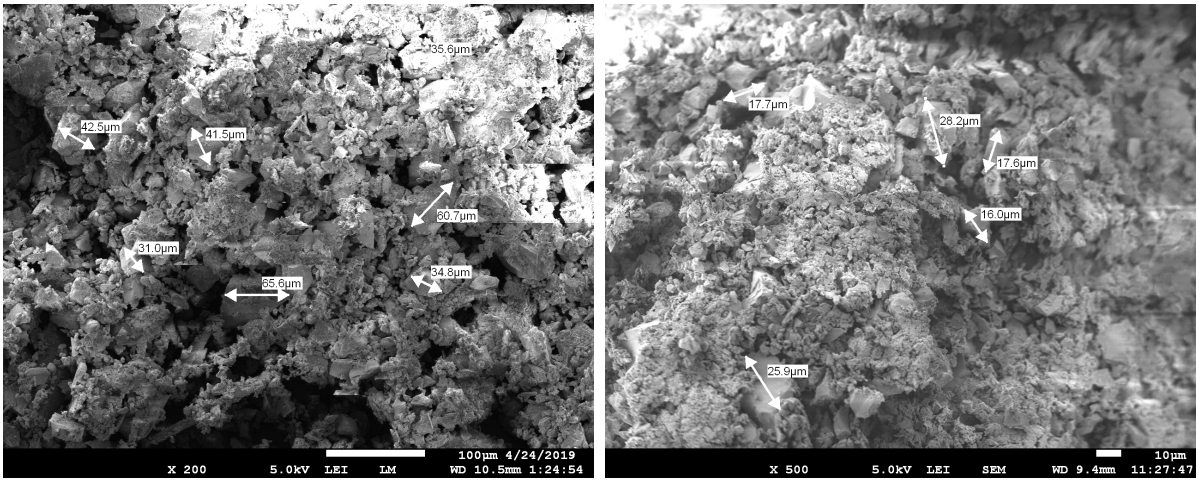

(a) (b)

Figure 6.4: SEM images of powdered epoxy-mortars from the LMC (a) and reproduced specimen (b)

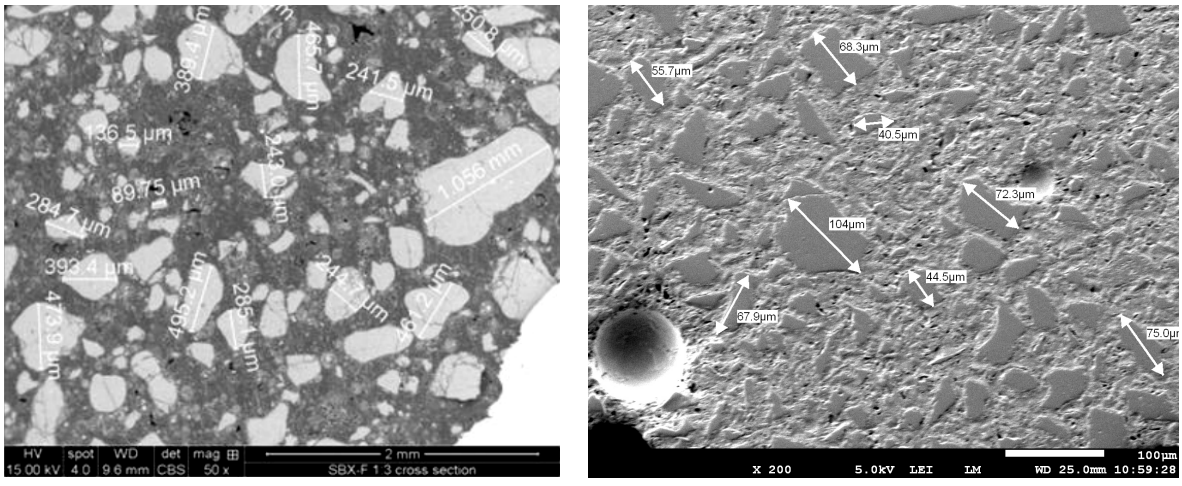

(a) (b)

Figure 6.5: SEM images of solid epoxy-mortars from the LMC (a) [7] and reproduced specimen (b)

6.3. Discussion

6.3.1. TGA

From the TGA tests done by Purcell as discussed in section 3.1, it showed that a 60 to 75 wt% sand is present in the epoxy mortar. Two samples with the most (core 9 upper middle) and least (core 9 lower middle) weight fraction of sand were tested. The sand is left over at the highest temperature when the epoxy has burnt away, this can be observed in figure 6.1. The amount of sand present in the two samples are verified to be 60 and 73 wt%. The large variations in the amount of sand present in the LMC epoxy mortar are likely due to variations in the mixing process when the lantern was constructed. The reproduced samples are manufactured to have a 66 wt% of sand. These all display in the TGA analysis a sand content of 66 +- 1%. This concludes that TGA is an accurate method of analysing sand present in a epoxy mortar.

The reproduced samples do not show a step around 200°C, from volatile products. This could indicate that degradation or moisture uptake has taken place in the cathedral, compared to newly made mortar samples. However this is not guaranteed as unknown solvents or other materials could be added to the mortar from the cathedral.

Hypothesized was that the weight loss step, as seen around 600 °C is due to the carbon black present in the mortar. The left over material from 900°C onwards is likely due to the incombustible sand. However, from the TGA tests done with reproduced samples containing different percentages of carbon black (3%,0.05%, 0%), the degradation step as seen around 600°C can not with certainty be assigned to the amount of carbon black in the mortar. The percentage of carbon black does influence the height of this step.

In an additional test done on more samples with different weight fraction, figure 6.3, it is observed that the step height of the 0, 0.05 and 3% samples is much greater than the additionally made samples with carbon black percentages of 0.5, 1 and 2%. It is likely that because both sets of samples were made in a different batch, the exact same mixing ratios are difficult to obtain by hand measurements. The step size of the last step is determined by the amount of carbon black plus the combustible residues from the epoxy. So, if not exactly the same mixing ratio of resin, harder and carbon black are used every time, the step height will differ. Thus, although the step size is influenced by the amount of CB in the material, it can not be linearly be linked to the amount of CB present in the mortar.

6.3.2. SEM

From David Kirby it was obtained that a M3 sand flour was most likely used in the mortar. This is very fine sand with a grain size of 62.5–125 µm. From SEM images taken from the epoxy mortar, figure 6.4, the sand particle size is estimated to be 30-70 µm. This would be compatible to a commercially available 'Sand, white quartz' >230 mesh [51], this type of sand has a size of 63 micrometer. The sand content as obtained from the performed TGA tests is around 66%.

In SEM images made from reproduced mortar made with the chosen quartz sand, the grain size is observed to be between 17-106 µm. In the the powdered specimen the sand is harder to detect, due to the epoxy. In the powdered specimen the average particle size seems to be smaller (25 µm). From the SEM image from the solid reproduced sample, the sand is clearly visible and also smaller in size as the LMC sample. Visually the sand in the LMC has larger particles compared to the (smoother) reproduced sample. It can be concluded that the chosen sand for the reproduced samples is slightly finer than the LMC sand. Most likely, the sand as used in the LMC has a greater variation in size than the selected quartz sand. Whether this influences the experiments conducted greatly is not certain.

6.3.3. Material selection

For the experiments in the next chapter the epoxy mortar will be reproduced to undergo accelerated ageing test. To approach the composition of the epoxy mortar, the following considerations are made to reach a composition as similar as possible to the real LMC epoxy-mortar.

The type of epoxy used is unknown, it is either based on an Epikote resin (as mentioned in the Shell film [6] or a Kollercast 332 resin. Neither of these original epoxies, or technical data-sheets, are available any more. The used resin is most likely based on a DGBA + amine resin. This is comparable to a Araldite 2020 [52], clear glass bonding two component epoxy adhesive. This epoxy is widely used and used in research glass adhesive bonds [5, 18, 53]. It is based on a DGEBA + cycloaliphatic amine resin 6.7. Optimal mixing ratio obtained from the data sheet is 100:30 by weight and will be used [52]. It takes 25 hours to reach a lap shear strength > 10N/mm2.

From the results of the SEM analysis, 'Sand, white quartz' >230 mesh [51], is selected for the reproduced specimen. The sand is mixed into the epoxy resin in a ratio of 2:1 sand/epoxy.

Asthe carbon black percentage can not with certainty be determined, this weight percentage is chosen by comparing the colour of the LMC samples to reproduced samples with different weight fractions. The samples from the LMC show a black/gray colour. Since the effect of low carbon black weight percentages make the mortar turn deep black, the carbon fraction that has the greatest similarity to the real colour was chosen to be 0.05% by weight. The reproduced specimen compared to the LMC core can be seen in figure 6.6. This amount of carbon black is used in the reproduced specimens in all further experiments.

Figure 6.6: LMC core sample and reproduced sample

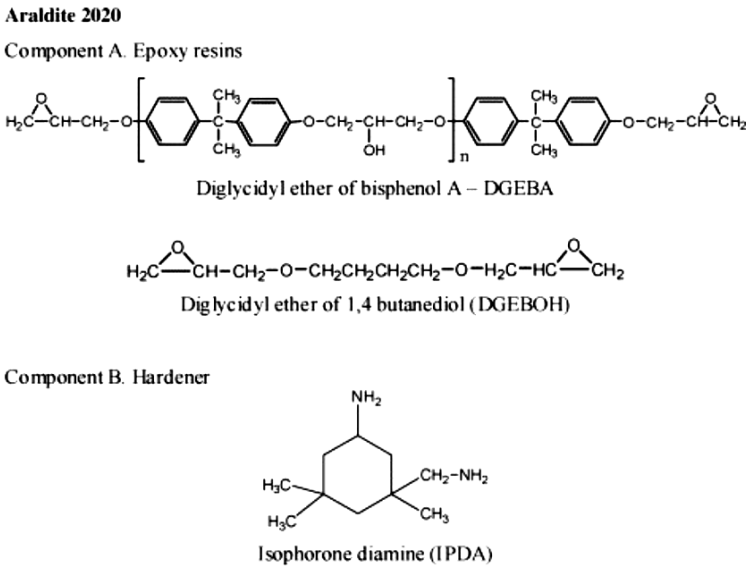

Figure 6.7: Chemical composition of Araldite 2020 [54]

7

Mechanical testing

The results of the tests for the different ageing durations (0, 350, 700 and 1050 hours) are discussed in this section. The aged reproduced specimen are tested in compression, tension and lap-shear. The results of these tests can be found in section 7.1, 7.2 and 7.3, respectively. In the appendix the A.2

7.1. Compression testing

Figure 7.1a shows a typical stress-strain curve of the reproduced cylindrical epoxy mortar specimens. The ultimate compressive strength and the strain at that point can be directly obtained as the maximum of the curve (red dot). The elastic modulus is approximated by taking a regression line between zero and the ultimate strength, this is visualized as the red line. On average this method slightly underestimates the true elastic modulus of the material. However, since it is used to compare the relative change in elastic properties between the samples after ageing, this estimation will be used. Curves that show a large 'step' in the first part, figure 7.1b, are discarded for the elastic modulus analysis. As, in these cases the compressive modulus becomes unrealistic low. The results for each duration, for every ageing cycle, are obtained from tests on five samples.

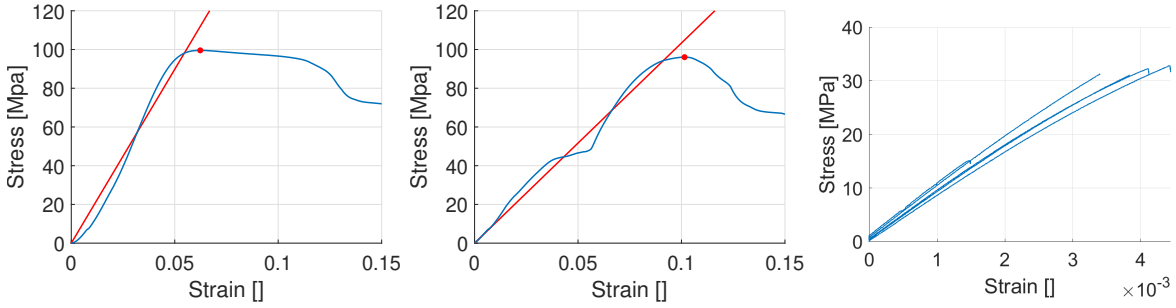

(a) (b) (c)

Figure 7.1: Stress-strain curves of compression tests (a&b) with ultimate strength (red dot) and approximation of compressive modulus (red line) and tensile tests (c)

The change of the ultimate strength, strain and compressive modulus of the aged samples after 350, 700 and 1050 hours can be seen in figure 7.2. The mean of the ultimate strength of each test and the corresponding standard deviation is plotted. The un-aged baseline strength of the reproduced specimens lies around 95 MPa and is indicated as the black dashed line. The dashed blue line represents the range of the standard deviation of the baseline test.

After 1050 hours of humidity (RH) ageing, the ultimate strength stays approximately the same as the baseline strength. The outdoor light exposed specimens (UV) show an increase of ultimate strength after 350 hours of ageing. This strength stays approximately the same for the rest of the ageing duration. The thermal (TC) and outdoor light plus water spray ageing (WS) also show a slight increase of strength after 350 hours, that stays constant for the 1050 hours of ageing. However, this increase in strength is of a lesser magnitude than the UV cycle.

No clear trend can be observed in the compressive moduli of the tested specimen. The baseline modulus has a large standard deviation. The compressive modulus of all aged specimen variate within the same range. The measured strain at the ultimate strength displays a large variation too. The deviation of the strain of the un-aged sample lies between 0.06 and 0.09. The RH and WS aged samples display strains within this range, whereas the UV and TC aged specimen are in the upper end, or slightly above of this range.

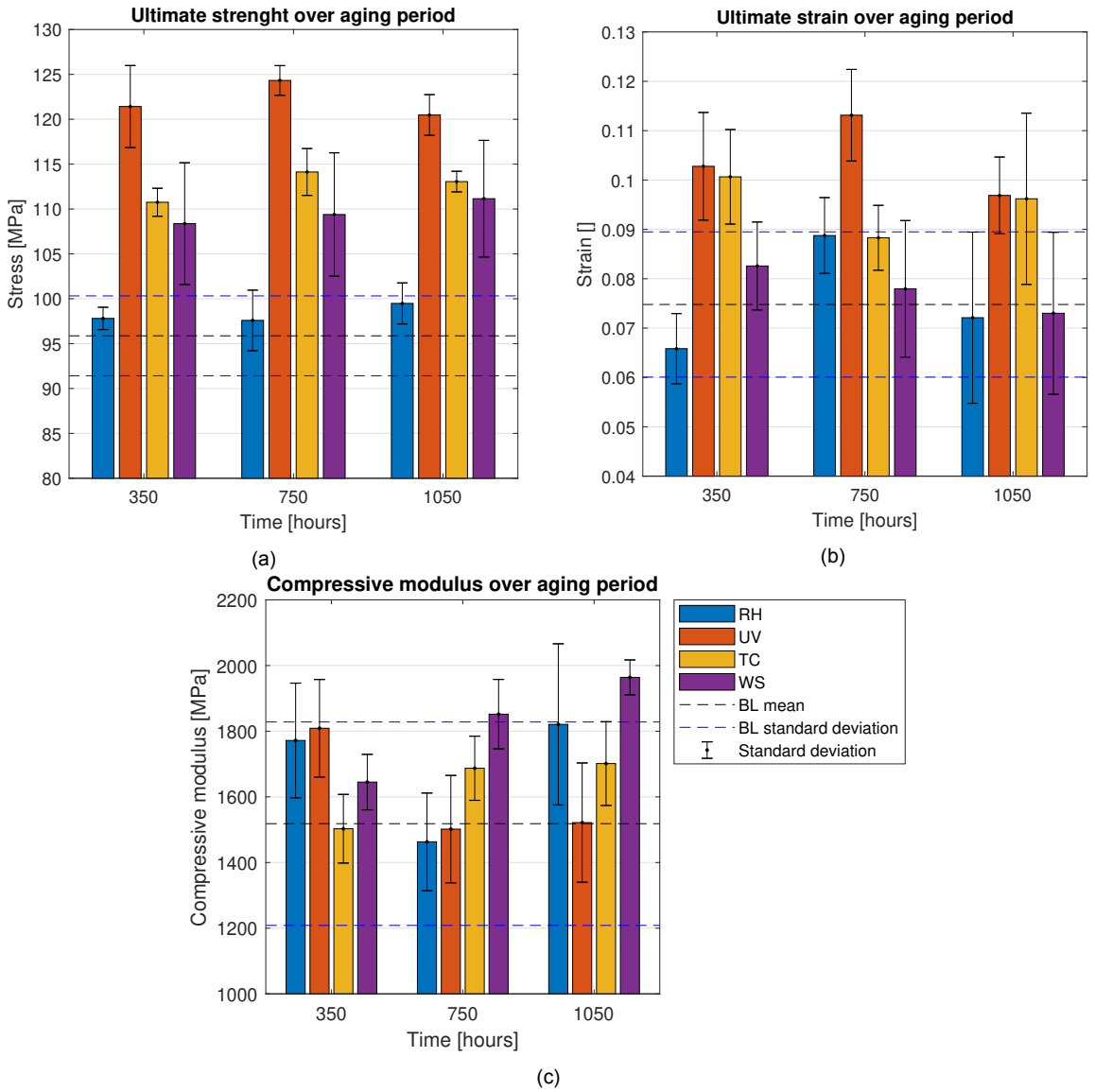

Figure 7.2: Compressive strength (a), strain (b) and modulus (c) change over aging period

7.2. Tension testing

Typical plots obtained from the tensile tests performed are shown in figure 7.1c. The stress-strain curve of the material shows a linear course before failure, this it typical for brittle materials. These materials do not have a well-defined yield point. Therefore, the ultimate strength and breaking strength are the same. Since the stress-strain curves are approximately linear before failure, the elastic modulus is calculated by dividing the ultimate strength over the strain at that point. The following properties are calculated from the raw stress-strain data: Ultimate strength [MPa], strain at ultimate strength [], Young's modulus [MPa]. Plot 7.3 shows the development of the ultimate strength of the aged samples after 350, 700 and 1050 hours. The black dotted line indicate the mean baseline strength(at t=0) and the error of this value is indicated in blue.

A large scatter is observed in the results of the tensile tests. This is likely due to the brittleness of the material. The majority of the samples did not break at the (preferred) centre of the dog-bone specimen, the majority broke at one of the clamping locations. Pictures of the tensile specimens after testing can be seen in appendix A.2.

The tensile strength is significantly lower than the compressive strength. At first glance the ultimate tensile strength shows a opposite trend with respect to the compression tests. The ultimate strength of the RH-cycles is the highest, while the UV followed by the WS cycle show the lowest tensile strength. However, when looking at the scatter present in each test, all values are close to the deviation of the baseline strength (indicated by the region between the blue dotted lines). Similar as the compression

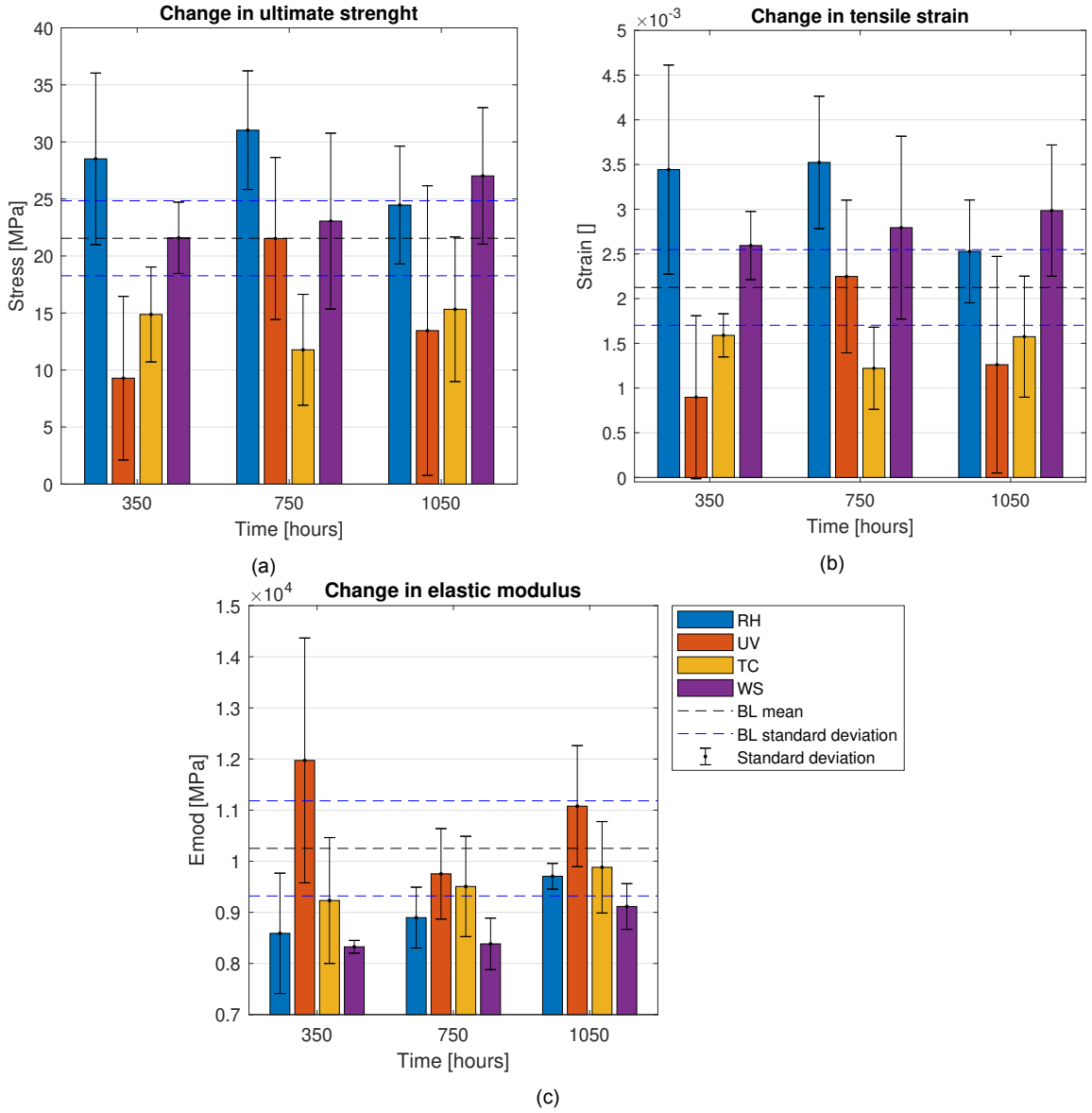

Figure 7.3: Tensile strength (a), strain (b) and modulus (c) change over ageing period

tests, the values that show the highest ultimate strength, also show the highest strain at this ultimate strength. The elastic modulus values also show a large scatter. However, the elastic modulus of UV and TC cycles show to be a little higher relatively to the RH and WS aged samples.

7.3. Glass-bonded lap shear testing

The glass-bonded lap shear specimens should give an indication of the adhesive strength of the mortar to glass. The mechanical strength and corresponding failure mode (adhesive de-bonding or glass failure) from the lap-shear tests can be found in table A.1 in appendix A.1. Pictures of the samples after testing are found in appendix A.2. Similar to the tensile tests, the glass samples display brittle failure, so the ultimate strength and breaking strength are the same. Samples that have corrupted values are indicated by NA. This mainly includes samples that broke before testing. Either by out-of-plane bending when gripping the specimens or by glass failure due to the clamping force of the hydraulic grips. It was found that this way of testing is difficult due to the weakness of the glass.

The results show that the UV, TC and WS cycles never display adhesive failure, all specimens break in the glass part of the sample, figure 7.4. Therefore, the ultimate strength values are only the tensile strength of the glass.

After 700 hours of RH, one out of the three specimens failed in adhesion, figure 7.5a (left specimen). After 1050 hours all RH specimens show adhesive or partial adhesive failure, figure 7.5b. The second

specimen has no recorded ultimate strength, because of out-of-plane bending failure. However, this test is still considered as adhesive failure because the broken specimen shows de-bonding of the glass.

(a) (b)

Figure 7.4: Glass failure in UV cycle after 350 hours (a) and TC cycle after 700 hours (b)

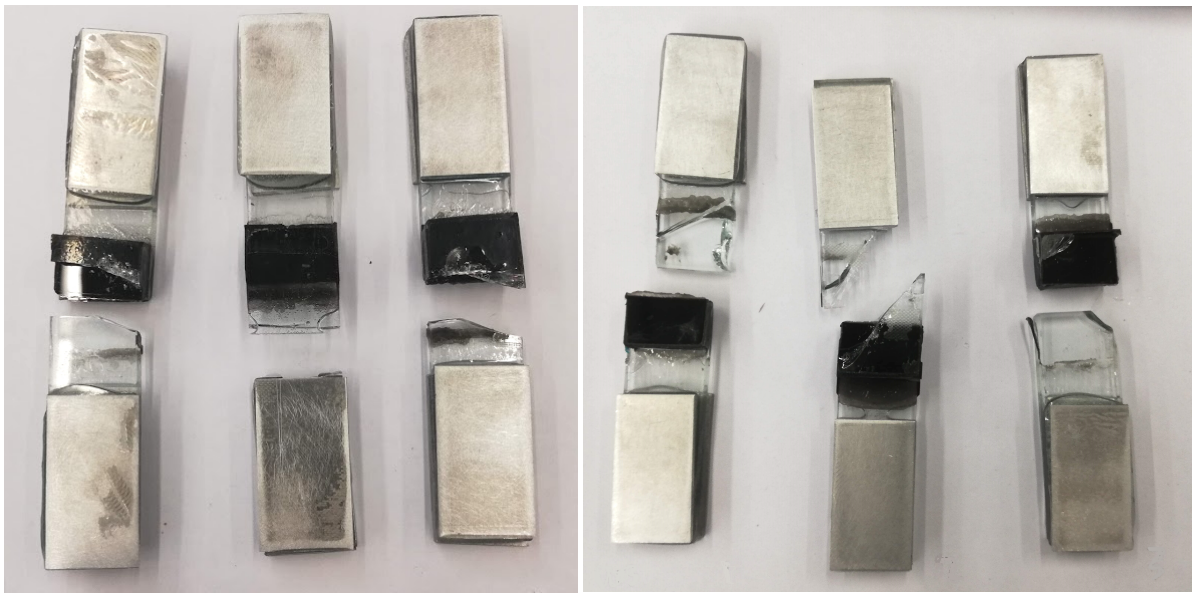

(a) (b)

Figure 7.5: Adhesive failure in RH cycle after 700 hours (a) and 1050 hours (b)

7.4. Discussion

Tensile tests displayed a large scatter, therefore these strength values were not considered representative. This scatter could be caused by the brittleness of the sand filled epoxy-mortar. It is observed that the fracture location often goes trough a defect such as where a void is present, see figure 7.6a. The results from the compressive tests display much lower deviations. Therefore, the ultimate compressive strength is used to compare changes in strength.

In the results from the compressive tests the specimen aged in UV show the highest overall compressive strength, followed by TC and WS whose values are slightly above the baseline strength. The strength of the RH samples maintain around the same value as the baseline strength. The increase in compressive strength of the UV, TC and WS cycles could be caused by post-curing reactions. Post-

curing reactions occur with exposure to high temperatures. This would increase the amount of cross-linking in epoxy, thus result in a higher ultimate strength.

The ultimate strength of the RH specimens is significantly lower than those subjected to raised temperatures. The WS cycles show a lower strength than the TC and UV samples. It is likely that the effect from moisture, induces a weakening to the material. However, the strength is in none of the samples lower than the initial baseline strength. Likely, no degradation has occurred, only a softening effect from plasticization is present in the mortar.

The data shows that all strength values from the compressive and tensile tests, with respect to ageing time (350, 700 and 1050 hours), stay roughly the same. This can indicate that over time, no degradation of strength is observed. From literature on a tested an epoxy-mortar, composed of 1/3 sand and 2/3 epoxy [31], it was reported that after 1000 of hours of wet/dry cycles, no substantial reduction of strength was observed. Only after 10.000 hours of exposure the strength of the mortar reduced from 84 MPa to 61 Mpa. This could suggest that the tested exposure period in this research is not long enough to induce significant degradation mechanisms. How the amount of hours of ageing in this research is linked to the amount of exposure in the real world is difficult to determine. Thus, the amount of ageing hours from this source can not be compared directly with the tests performed in this research.

With increased cross-linking in samples subjected to temperature ageing, a higher elastic modulus would also be expected. The scatter in the calculated compressive modulus obtained from the compression tests, is too large to draw conclusions. The elastic modulus of the the tensile tests are linear and independent of the strength. From these values it can be concluded that the UV and TC cycles show a slightly higher stiffness than the RH and WS cycles. However, this is not a substantial change.

The de-bonding of the glass and the epoxy mortar as observed in the LMC is likely caused by moisture ingress on the interface. In the glass-bonded lap-shear tests, specimens show adhesive failure after 700 hours of relative humidity ageing. None of the other specimens show adhesive failure. The surface of the adhesively failed specimens are smooth, with no left over adhesively bonded epoxy left, see figure 7.6c. So, moisture causes complete de-bonding between the glass and epoxy-mortar.

Adhesive failure by moisture ingress is also observed in literature 3.3.3. Unlike the RH ageing, none of the WS samples (subjected to water spray and UV) show adhesive failure. Possibly due to the UV exposure the absorbed water evaporates from the mortar. From literature it can be shown that original properties of the adhesives after humidity ageing could be restored by drying [11]. This could explain the delay in adhesive failure in the WS cycle, likely after longer exposure times adhesive failure will also occur in the WS aged samples. This result would be in line with the mechanical tests performed, where a slightly higher compressive strength of the WS cycle compared to the RH cycle is observed. Thermal stress cycling could contribute to de-bonding, however the stresses induced by temperature cycling alone is likely not enough to de-bond the material. Similarly, mechanical stress could contribute to the de-bonding, but the effects of mechanical loading and fatigue are not reviewed in this research.

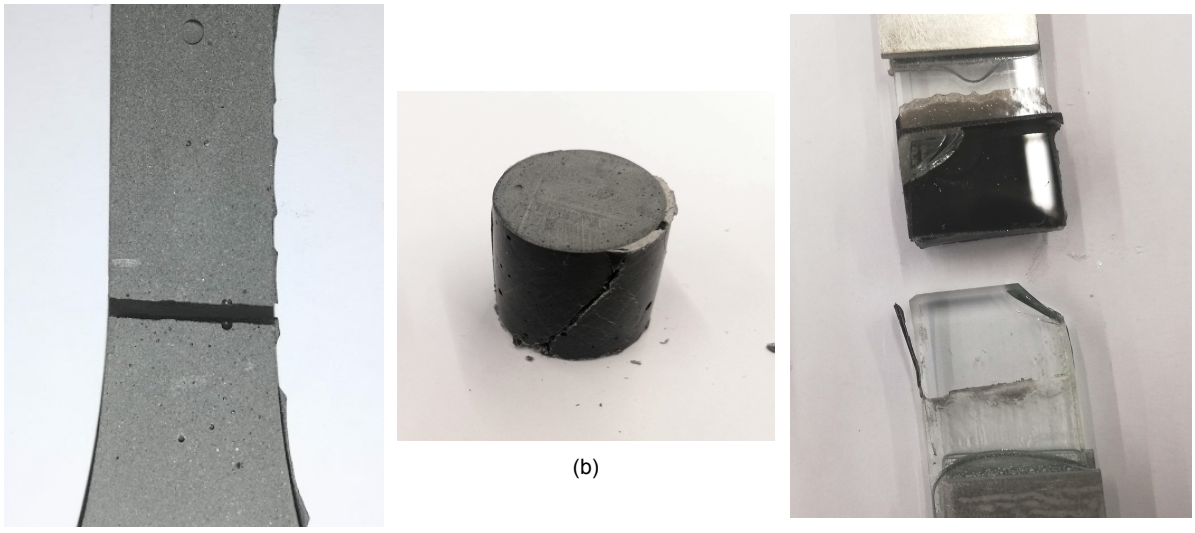

(a) (b) (c)

Figure 7.6: Failed tensile (a), compression (b) and adhesive (c) specimens.

8

Physical and chemical testing

8.1. Fourier Infrared Transfer Spectroscopy (FTIR)

To compare chemical changes in both the aged epoxy mortar and aged LMC samples, Fourier Infrared Transfer (FTIR) spectroscopy analysis is done to see changes in functional groups. Changes in the bandwidths 1600–1800 cm^{-1} (carbonyl) and 3200–3700 cm^{-1} (hydroxyl) are most commonly observed in ageing of epoxies as noted in literature (section 3.2).

8.1.1. Peak analysis

A number of clear peaks can be observed in the FTIR analysis. The interpretation of the peaks of different functional groups present in the material is done by looking at characteristic IR absorption frequencies of organic functional groups [48]. Figure 8.1 shows the FTIR spectra of un-aged reproduced samples, pure epoxy and pure sand. The two most prominent peaks in the reproduced material, between 700-800 cm^{-1} and 850-1200 cm^{-1}, are related to the sand present in the mortar.

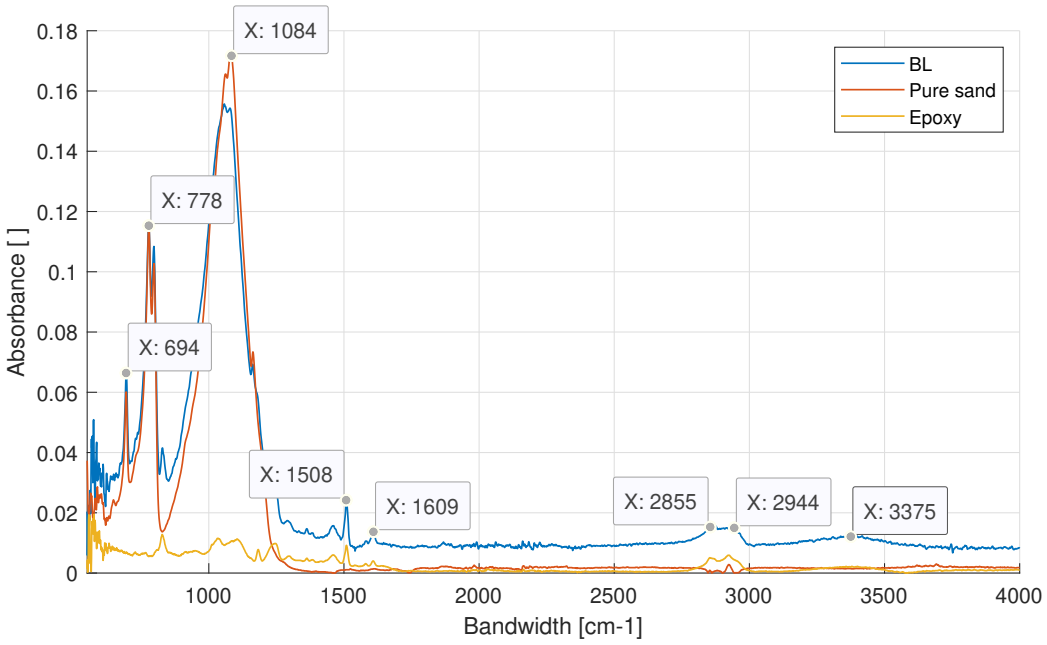

Figure 8.1: FTIR Reproduced sample, Sand only and Epoxy only

Multiple medium-weak bands are visible in the bandwidth 1400-1600 cm^{-1} that are most likely related to the stretch of aromatic groups (C=C). Around 1610 cm^{-1} a small sharp peak is visible that belongs to the stretching of carbonyl groups (C=O). Between 3200-3600 cm^{-1} a broad peak related to the stretch of hydroxyl (O-H) is observed. This peak is of interest to compare the effects of water absorbance during ageing. An absorption band in the range 2400–3400 cm^{-1} attributed to carboxylic acid groups can appear. This is a strong peak that ranges over this whole bandwidth. This peak would overrule the visibility of the hydroxyl groups. However in all graphs, the peak related to water uptake (OH-stretch) is clearly visible so it can be concluded that no peak from carboxylic acid groups is present.

In the range of 2760-3000 cm^{-1} a strong merged peak of two peaks is visible. This peak can most likely be related to C-H stretch or =C-H stretch. No changes from =C-H stretch are expected during ageing. This is also observed in research on Araldite 2020 [53] after UV ageing, where the peak related to =C-H does not change during ageing. An effect of N-H stretch could theoretically be visible in this area. However, the amount of C-H bonds in the Araldite 2020 is significantly higher than the number of

N-H bonds (figure 6.7), so the effect of N-H groups should be low. Therefore, the peak between 2760-3000 cm^{-1} is used as a reference to compare the growth of the carbonyl and hydroxyl groups. The ratio between the peak of interest and this reference peak is calculated, to normalize the absorbance values:

$$R = A_{peak}/A_{reference} * 100 \tag{8.1}$$

$$A_{peak} = A_{trap} - [\frac{1}{2} * (y(1) - y(2)) * \delta x + y(2) * \delta x] \tag{8.2}$$

(when $y(1) > y(2)$)

A typical FTIR spectrum is shown in figure 8.2. In this graph the highlighted areas represent the analysed carbonyl (1550–1700 cm^{-1}) indicated by A_1; hydroxyl (3200-3600 cm^{-1}) indicated by A_2 and reference area (2760-3000 cm^{-1}) indicated by A_{ref}. The ratio R is calculated for all aged specimen, equation 8.1. The areas for the hydroxyl and carbonyl groups (A_{peak}) and the reference peak ($A_{reference}$) are calculated in the same manner. The total area under the curve (A_{trap}) is approximated with trapezoidal numerical integration in MATLAB. This integration takes the area over the bandwidth selected (δx) between the the curve and the x-axis. The area between the lower bounds of the curve has to be subtracted from (A_{trap}) to obtain the actual area under the curve (A_{peak}). A linear line is drawn between the two lowest points of the graphs ($y(1)$ and $y(2)$). The area underneath this line is then subtracted from the trapezoid integration area, as can be see in equation 8.2. The trapezoid method slightly underestimates the area because the peaks are concave down. However, when comparing between the different areas, this error is neglected.

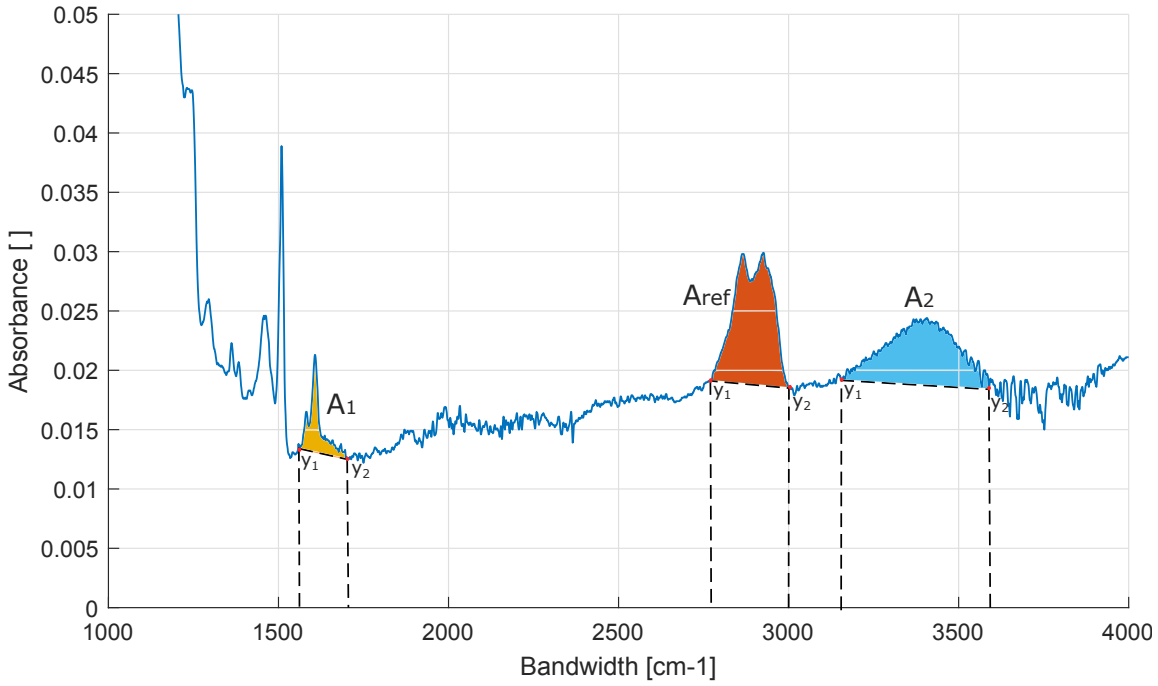

Figure 8.2: Typical FTIR spectrum with analysed areas indicated

8.1.2. Results

All results obtained from the FTIR tests for the different ageing cycles can be found in appendix C. To compare the change in hydroxyl and carbonyl peaks over time, these peaks are normalized in relation to a reference peak (2760-3000 cm^{-1}) that does not change during ageing. The changes in the hydroxyl and carbonyl bands relative to the reference peak (see equation 8.1 and 8.2) are given in table 8.1 and 8.2. The value BL is the peak area of the hydroxyl and carbonyl groups before ageing. Due to unexpected break down of the FTIR spectroscope, tests indicated in the graphs with an astrix (*) were performed on a 'PerkinElmer Spotlight 400' FTIR microscope. These spectra show great differences with tests performed on the PerkinElmer spectrometer. Therefore, for the calculations of the peak-ratio these values are neglected. This is indicated in with NA in both tables.

When looking at the spectra of the reproduced samples, figure 8.3, no big changes of the carbonyl or hydroxyl peaks are visible after 1050 hours of ageing. This can also be related to the changes in the

Table 8.1: Peak ratio of carbonyl groups (top) and hydroxyl groups (bottom) of aged reproduced samples for different ageing durations

Ageing type	0 hours	350 hours	700 hours	1050 hours
BL	21.7			
RH		20.9	28.5	27.1
UV		18.9	52.1	31.8
TC		32.6	22.6	NA
WS		NA	35.7	35.7
BL	53.6			
RH		64.7	89.5	63.6
UV		56.9	102.1	67.8
TC		102.7	71.9	NA
WS		NA	70.3	62.9

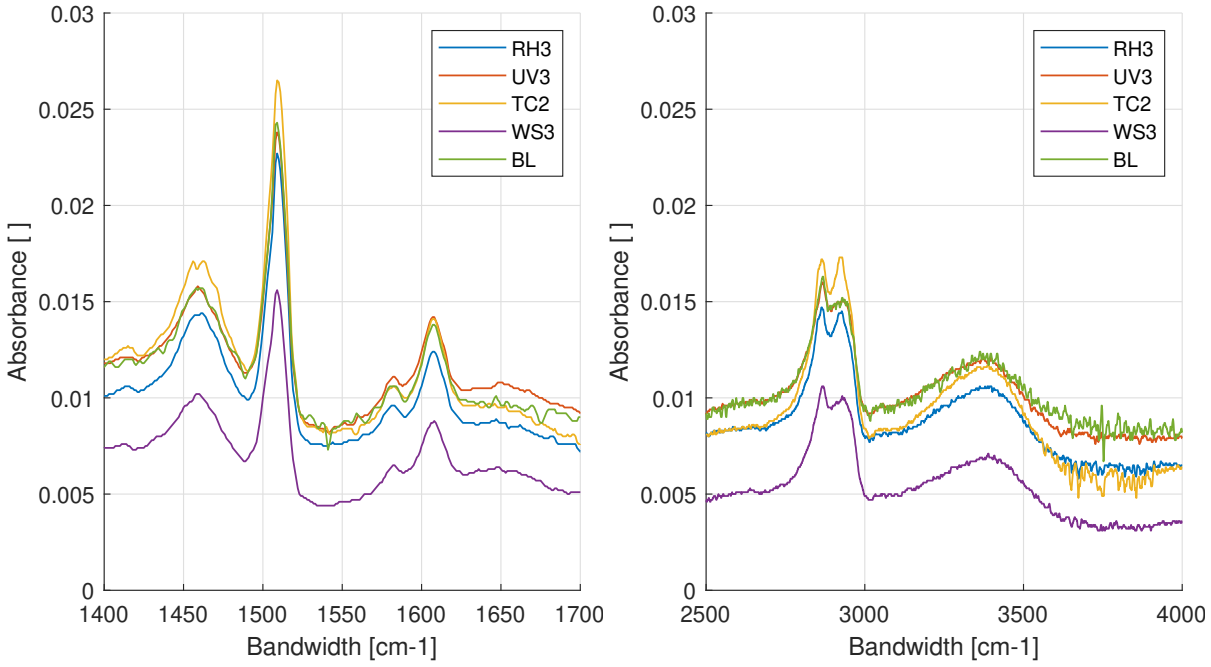

(a) Carbonyl peak (1610 cm^{-1})

(b) Hydroxyl (3400 cm^{-1}) and reference (2900 cm^{-1}) peaks

Figure 8.3: FTIR graphs of reproduced samples after 1050 hours of ageing and baseline (BL)

peak areas, table 8.1. The biggest change is observed at 350 hours of TC and 1050 hours of UV ageing, where the area of the hydroxyl group is twice that of the baseline.

The spectra of the carbonyl and hydroxyl groups of the aged LMC samples shown in figure 8.4, it shows that most of the peaks do not visually change relatively in size. Only a slight increase of the hydroxyl peak after 750 and 1050 hours of RH ageing an after 750 hours of UV ageing are visible, see appendix D.2. When comparing the peak area ratios, table 8.2, a bigger increase of the peaks can be observed in the LMC samples. Most noticeable is the increase of the hydroxyl groups for the LMC RH and UV ageing. The area for both ageing procedures show an increase of 2 to 7.5 times that of the baseline value.

An additional test was performed to test the influence of ozone on the carbonyl groups. This was done by putting a powdered reproduced sample in an ozone chamber for ten hours. The area of the carbonyl peak did not visually change.

Table 8.2: Peak ratio of carbonyl groups (top) and hydroxyl groups (bottom) of aged LMC samples

Ageing type	0 hours	350 hours	700 hours	1050 hours
BL	91.5			
RH		14.4	84.7	68.7
UV		75.4	124.3	72.8
TC		NA	52.3	NA
WS		NA	89.2	75.9
BL	40.4			
RH		180.3	311.0	86.1
UV		197.6	210.9	95.3
TC		NA	47.2	NA
WS		NA	42.2	30.1

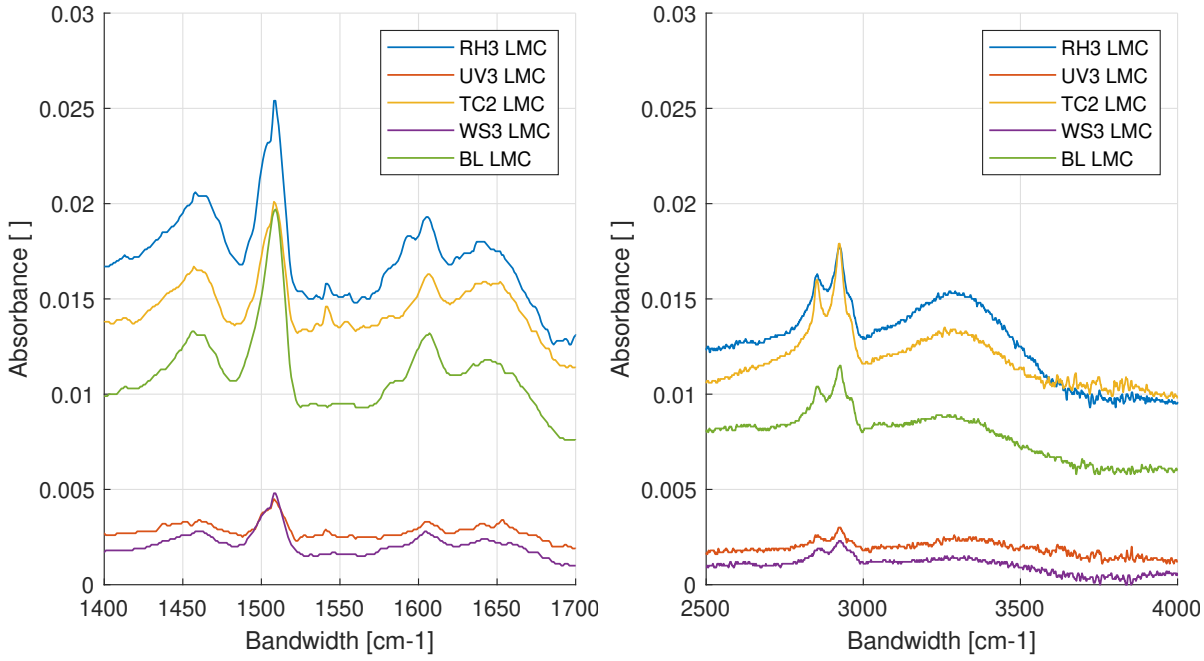

(a) Carbonyl peak (1610 cm^{-1}) (b) Hydroxyl (3400 cm^{-1}) and reference (2900 cm^{-1}) peaks

Figure 8.4: FTIR graphs of LMC samples after 1050 hours of ageing and baseline (BL)

8.1.3. Discussion

From the performed FTIR analysis, the most noticeable result is the increase of the peak area of hydroxyl groups for the LMC samples aged with high relative humidity and outdoor light exposure (RH and UV). An increase of hydroxyl groups of the RH and UV cycle is in line with literature studied. The UV ageing and temperature cycling do not introduce an significant increase in carbonyl groups, as would be expected from previous studies on ultraviolet and thermal degradation. In the same way contrary to expectancy, the LMC samples subjected to UV+water spray (WS) and the reproduced samples aged with moisture exposure (RH and WS) do not have a noticeable increase in hydroxyl groups. None of the reproduced samples show considerable visual changes or variations in peak area ratio of both the hydroxyl or carbonyl groups for all ageing procedures.

In general, UV exposure only causes a chemical alteration of carbonyl groups on the surface. The effects on carbonyl groups from UV exposure most likely only show on the surface of the specimen. The penetration depth of FTIR is approximately 2-3 µm. When performing the FTIR tests, material was scraped off the specimens with a blade before putting it in the machine. In this manner material deeper within the specimen is also tested. This could result in the changes in the carbonyl groups to not be visible in FTIR. In an additional test done on a powdered sample exposed to ozone, no visual change was visible on the carbonyl groups. This sample was powdered before testing, so the tested sample were sufficiently exposed. However, no changes were visible. This can indicate that changes in carbonyl groups do not occur or are hard to detect.

FTIR spectroscopy might possibly not be sensitive enough to observe changes in the chemical properties of the material. One aspect that contributes to the low sensitivity, is the sand present in the material. Sand absorbs IR light much stronger then polymers. This contributes to the low visibility of the epoxy in the FTIR scans. The weak signal could also be caused by bad surface contact when scanning. The rough surface induced by the sand can contribute to this. On the other hand, normalization of the compared peaks also induces an error in the values of the ratio. Graphs that show a low overall absorbance give less accurate results after normalization. This has to do with the sensitivity of the FTIR spectroscope at low absorbances.

The studied literature [53] showed a significant increase in hydroxyl and carbonyl groups on a Araldite 2020 epoxy (without additives). In this test the height of these bands increase visually greatly, in the order of four times that of the un-aged material. It can be argued that because the samples in this research do not change visually in size greatly, the amount of modifications in functional groups is limited in the tested epoxy-mortar. Tests on pure epoxy samples can be performed in a further study to detect if physical changes can be detected in a pure-epoxy due to ageing. It is highly possible that the sand and carbon black filler protect the epoxy from degradation. Literature reports low carbon black weight percentages to have a little effect on the weather resistance of epoxy. In research on epoxy with carbon black nano fillers [32], it was observed that low amounts of carbon black (0.25 and 0.75 wt%) did not delay the formation of carbonyl groups, measured by FTIR analysis. So, potentially sand is the biggest inhibitor of environmental degradation of the epoxy.

8.2. Calorimetric analyses (DSC)

In literature it showed that the Tg is a good detector of changes in epoxies, such as post-curing, water uptake and physical degradation. DSC tests were performed on the aged samples to detect the glass transition temperature.

8.2.1. Results

The obtained results from the differential scanning calorimetry analysis (DSC) for all samples can be found in Appendix D. The DSC results from the reproduced and LMC samples after 1050 hours of ageing are shown in figure 8.5 and 8.6, respectively (exo up). The specimens were tested immediately after removal from the ageing chamber. All DSC measurements show an inflection from 0°C downwards in the endothermic direction. This deflection goes into an endothermic peak around 50 degrees. In some samples an smaller exothermic peak is observed around 70 degrees. After this peak the heat flow graph flattens. Both the endothermic and the exothermic peak interfere with the observation of the glass transition temperature.

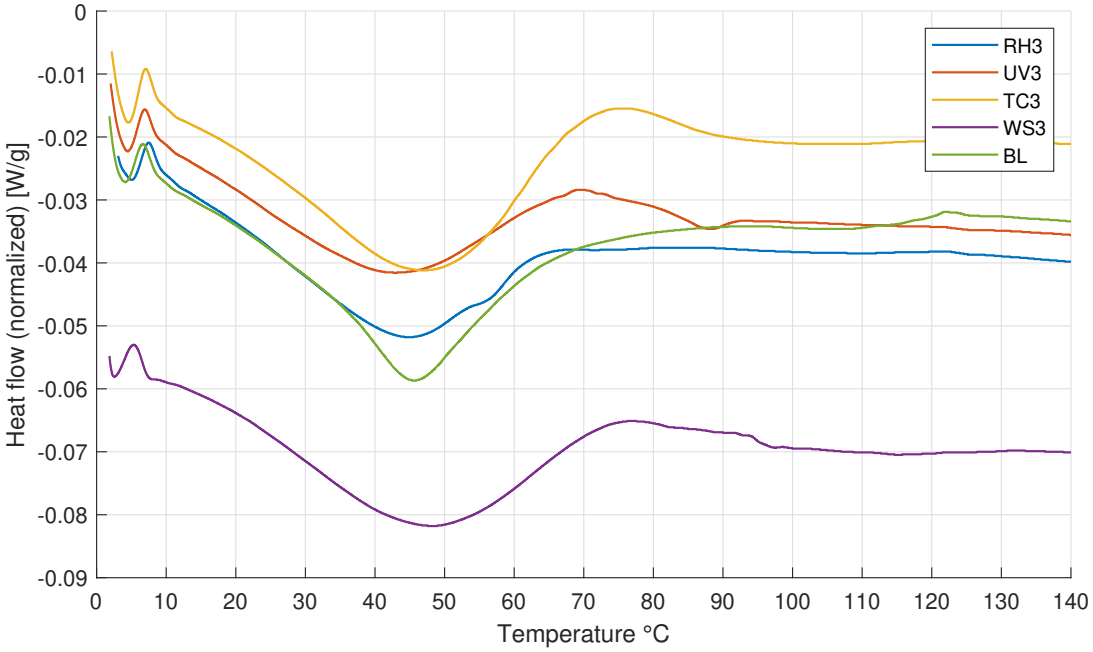

Figure 8.5: DSC of reproduced samples after 1050 hours of ageing

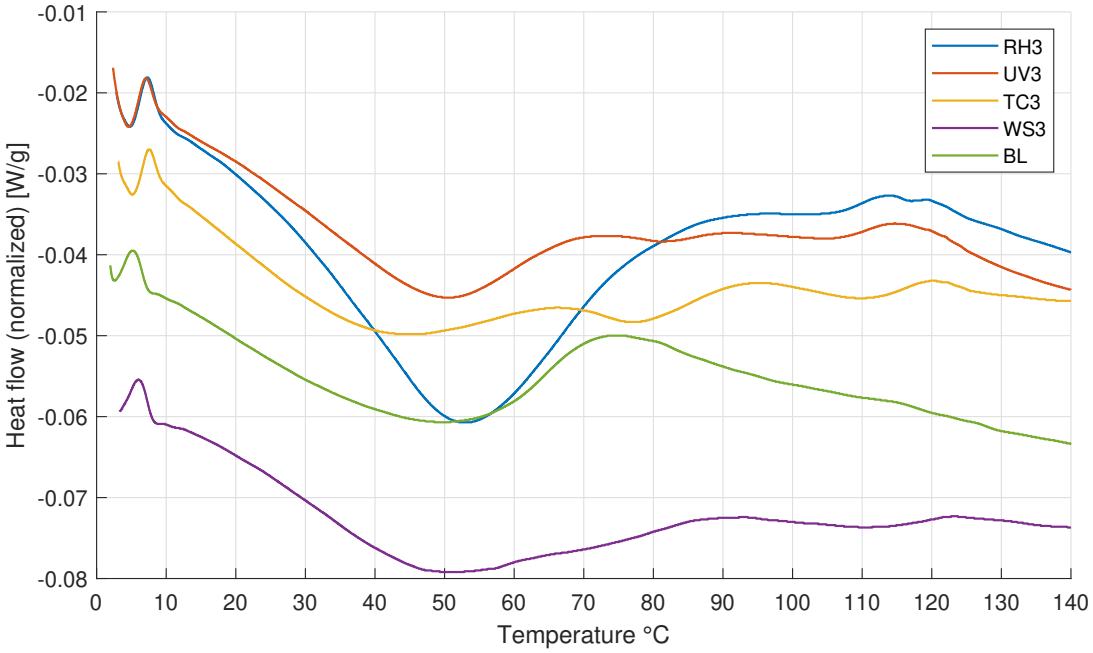

Figure 8.6: DSC graph of LMC samples after 1050 hours of ageing

To find out if the endothermic and exothermic transitions are reversible, an additional test with multiple heating and cooling cycles was performed. It is stated that heating above the glass transition relieves the endo- and exothermic stresses. The thermally aged sample (After 1050 h TC ageing) is heated and cooled multiple times. The heat loss profiles of this test can be seen in figure 8.7. In the first heating cycle the graph has the same behaviour as the regular test done (figure 8.5). When cooling the sample, the endothermic and exothermic peaks disappear. This is also observed in the following heating and cooling cycle, indicating that a heating cycle relieves the stresses or removes residual solvents. In these three heating and cooling curves, the glass transition temperature can clearly be observed around 70 degree.

An other solution of finding the glass transition temperature is by analysing the modulated signals. The overlapping peak from the endothermal stresses with the Tg could be disentangled by modulated DSC. The sinusoidal heating rate used in modulated tests permits the simultaneous measurement of the reversing and non-reversing heat flow signals. The enthalpy relaxation (or hysteresis) peaks separate into the non-reversing heat flow signal. This leaves only a heat capacity jump from the Tg in the reversing signal. In all the samples tested a modulated heating rate was used. Figure 8.8 displays this signal for four different samples. Here can be observed that in some cases (RH3) the Tg can be observed around 70 °C. However, no clear transition could be observed in the majority of the heat capacity signals.

8.2.2. Discussion

From the DSC analysis done on all the samples, it is observed that the LMC and RP samples show similar curves. In both an endothermic peak around 50 °C is present. The exothermic peak (around 70°C) is not visible in all samples. Some LMC samples show varying signals, this could be due to the fact that limited material was available for testing. With a lower tested sample weight, generally a weaker signal is obtained.

The endothermic peak can either be identified as an enthalpy relaxation peak or indicate the presence of residual solvents in the material [55]. The size of an enthalpy relaxation peak can indicate the amount of physical ageing (also known as thermal ageing) that has occurred in the material. The presence of residual solvents in the material could also cause this endothermic peak. Since, the epoxy is cross-linked under ambient conditions, this locks in both residual solvents and thermal stresses [56]. However, as seen in the TGA results in section 6.1, no weight loss step is observed around 50 °C, that could indicate the presence of solvents within the reproduced epoxy. Since signal from the glass transition temperature overlaps with the endo- and exothermic peaks, the peak size is not representable for quantifying the amount of physical ageing.

The UV, TC and WS cycles show an exothermic peak, while the RH and BL cycles do not display this peak. Exothermic behaviour could result during curing of a thermosetting resin [57]. A bigger exothermic

peak indicates a lower degree of curing. The un-aged baseline sample does not show this exothermic peak. From this it can be concluded that the samples are fully cured before ageing. The reason the UV, TC and WS cycles show an exothermic peak in contrast to the RH and BL cycles is unknown.

Heating multiple times relieves the exo- and endothermic peaks. The Tg of the epoxy-mortar is expected to be around 50 degrees Celsius, about the same temperature as that of Araldite 2020 [52]. In the test with multiple heating cycles the the glass transition temperature can clearly be observed around 70 degree. However, having multiple heating cycles will change the thermal history of the samples. This could result in the erasure of the properties from the accelerated ageing. So this method of detecting the glass transition temperature is not useful for the purpose of this research.

This concludes that the method, as used in this research to find the glass transition temperature is unsuitable. Further research could find a method of detecting the glass transition temperature without altering the material properties from accelerated ageing.

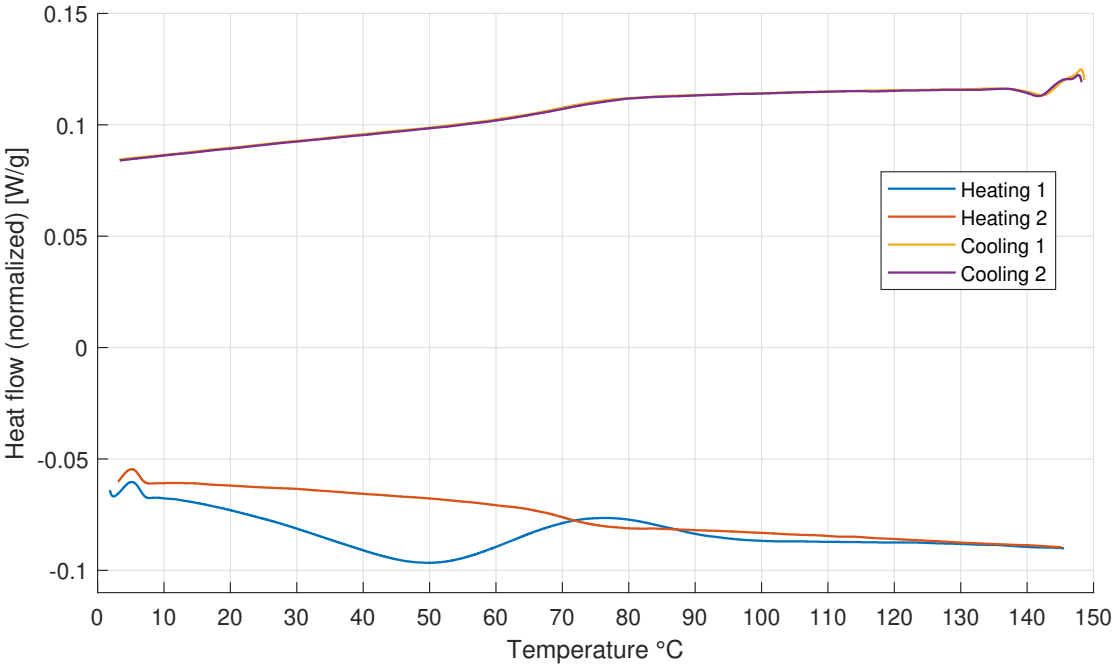

Figure 8.7: Repeated DSC test of sample TC 3

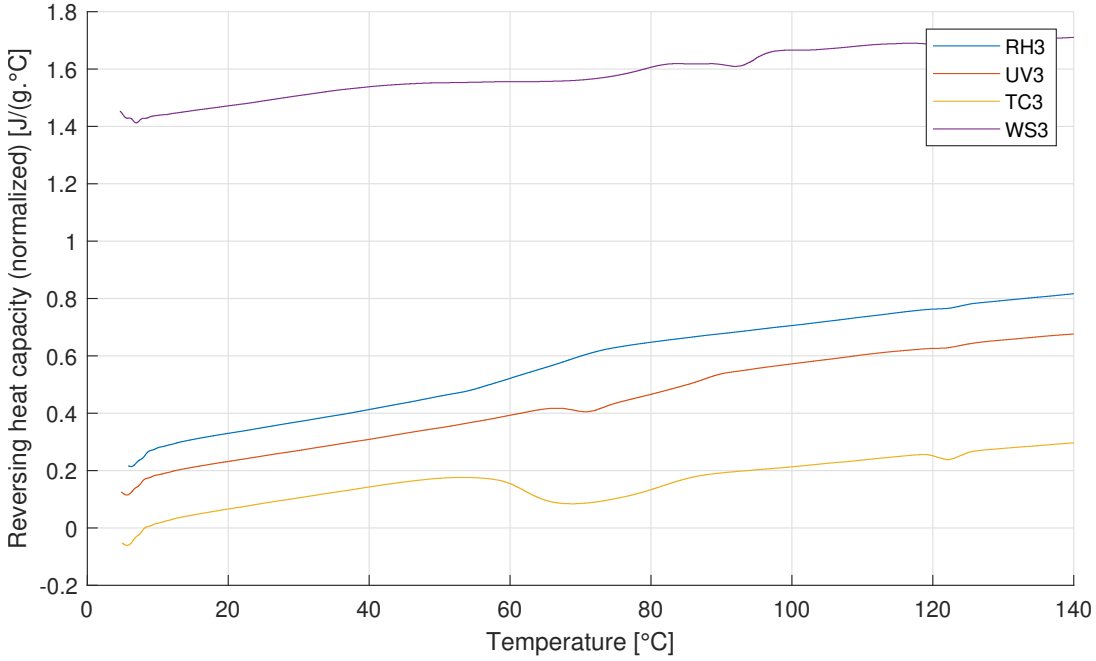

Figure 8.8: Reversing heat capacity from modulated DSC

8.3. Dynamic Mechanical Analysis (DMA)

This section discusses the results from the performed DMA tests on the aged LMC samples. One reproduced sample was tested to compare the original material with the reproduced epoxy-mortar.

8.3.1. Glass transition and peak temperature analysis

Figure 8.9 shows a typical plot obtained from the DMA tests performed. The storage modulus (E'), loss modulus (E") and loss factor (tan δ) are plotted. The ASTM standard 'Test method for glass transition temperature polymer matrix composites by Dynamic Mechanical Analysis' [49] is used to analyse the change in Tg during ageing on the LMC samples. The DMA Tg is determined to be the intersection of two tangent lines from the storage modulus by this test method. The first tangent line is selected at a temperature before the transition. The second tangent line is constructed at the inflection point to approximately the midpoint of the storage modulus drop. The maximum value of the loss factor curve, the peak temperature (Tt), is identified. This value indicates the temperature on what the material has the highest viscose response.

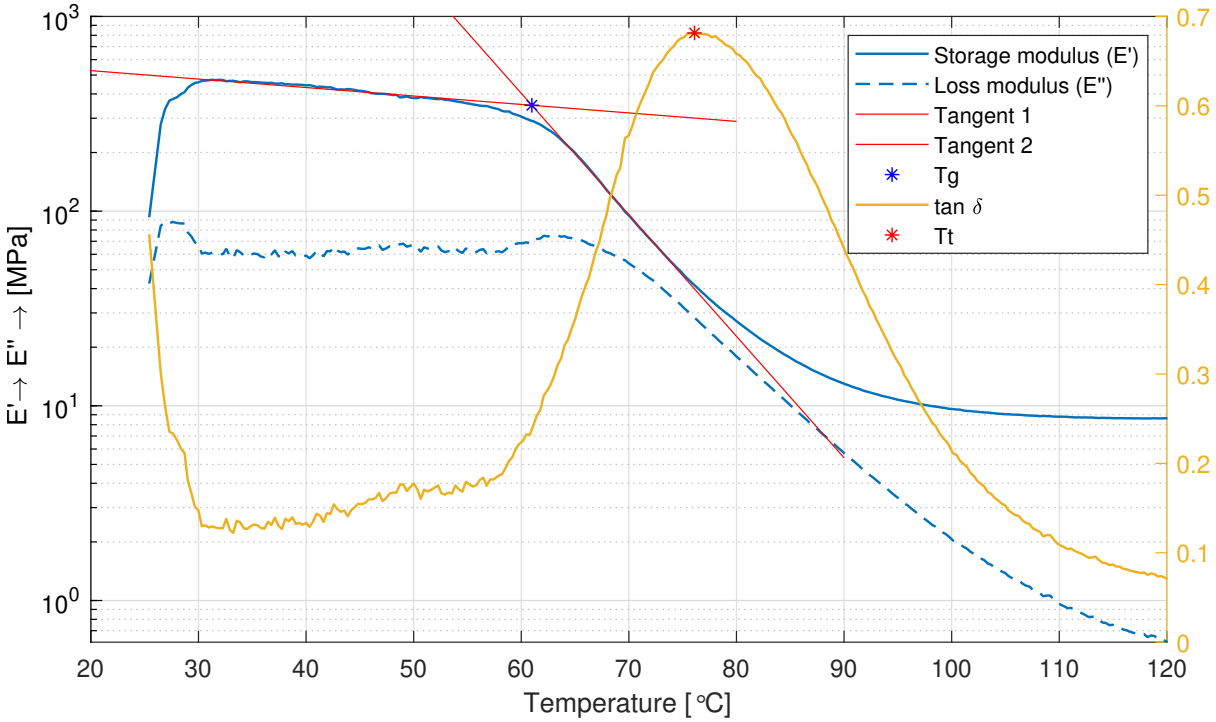

Figure 8.9: Typical DMA plot with the glass transition temperature (Tg) and peak temperature (Tt) indicated

8.3.2. Results

The values of the Tg and the Tt are given in table 8.3 and 8.4, respectively. The calculated temperature values are rounded to whole numbers. Two samples were tested before ageing one from the cathedral (BL LMC) and one reproduced sample (BL RP). For each ageing procedure, the samples were tested right after the indicated hours of ageing. Values expressed as NA are failed DMA tests, mostly as a result of the loss of clamping (in the grips) during testing. These samples were not tested again due to possible effects that the heating cycle may introduce on the polymer.

The baseline samples, from both the LMC and the reproduced mortar display a DMA glass transition temperature of around 50 °C. The Tg of the samples aged on relative humidity (RH) is between 40 and 45 °C over the whole ageing period, which is lower than the baseline Tg. The samples exposed to the combination of light and water spray (WS) shows a slightly higher glass transition temperature than the baseline. The UV and TC samples display the highest Tg, between 59 and 71 °C. The peak temperatures from the tangent delta curve show a similar relation as the Tg, where the RH aged samples have a lower Tt temperature then the samples exposed to temperature cycling (TC) or ultraviolet light (UV). However, the samples aged in WS (despite one failed test) display the highest Tt temperature.

Table 8.3: DMA glass transition temperature (°C) of aged LMC samples

Ageing type	0 hours	350 hours	700 hours	1050 hours
BL RP	47			
BL LMC	53			
RH LMC		42	45	40
UV LMC		68	59	71
TC LMC		61	63	NA
WS LMC		NA	53	60

Table 8.4: DMA peak temperature (°C) from tangent delta curve of the aged LMC samples

Ageing type	0 hours	350 hours	700 hours	1050 hours
BL RP	62			
BL LMC	72			
RH LMC		60	43	78
UV LMC		87	82	90
TC LMC		76	82	NA
WS LMC		NA	90	97

8.3.3. Discussion

In the DMA tests on the baseline samples, of both the LMC and the reproduced samples, the DMA Tg measured to be around 50 °C. This could imply that both samples have roughly the same properties, such as amount of crosslinking. This value is comparable to the Tg found in the data-sheet of the Araldite 2020 [52]. DMA test were only performed on the LMC samples, since it was expected that DSC would give more conclusive results on the change of the Tg. DSC tests were meant to be the link the LMC samples with the reproduced mortar. However, DMA tests have shown to give better results to identify the glass transition temperature and it can also identify the peak temperature.

The peak temperature from the tangent delta curve shows a similar relation as the Tg, where the RH aged samples have a lower Tt temperature then the samples exposed to temperature cycling (TC) or ultraviolet light (UV). However, the samples aged in WS (despite one failed test) display the highest Tt temperature. A higher Tt indicates a larger viscose response. This point might even be more relevant in indicating the amount of degradation since the Tg measures the transition at what the material starts to transition into a viscous state. The Tt indicates the point at what the material is the most viscous. This point takes into account the loss modulus, which is the energy dissipated as heat, representing the viscous portion. This means that at the top of the peak, the material performs the lowest on absorbing energy.

The Tg of the LMC samples aged on relative humidity (RH) is lower (between 40 and 45 °C) than the baseline over the whole ageing period. This is also observed in most of the Tt values from moisture ageing. The reduction of Tg and Tt can indicate softening or plasticization in the RH samples, as mentioned in literature [9]. This would also link to the mechanical tests where the ultimate strength of the reproduced RH samples is lower than those aged on higher temperatures (WS, TC and UV).

The same relation holds between the raise of the Tg and Tt of the UV and TC cycles and the raise in ultimate strength from the mechanical tests. Both phenomena would indicate post-curing reactions within the material due to thermal ageing.

The WS cycle displays the highest Tt values. It is possible that post-curing reactions have contributed to the raised Tg and Tt of the WS cycles due to the outdoor light exposure and temperature cycling. The fact that the Tt an Tg of the WS cycle has increased could indicate that the plasticization from moisture is reversible. As degradation would lower the Tg and Tt. This is in line with the mechanical tests performed. The WS samples showed to have the single lowest mechanical strength, likely due to plasticization from moisture. However, this ultimate compression strength is still higher than the un-aged baseline. So, likely post-curing reactions from thermal effects undo plasticization from moisture in some extend.

8.4. Gravimetric measurements

The weight variations measured of the samples exposed to moisture (80% RH) was used to assess the amount of water absorbed by the epoxy-mortar.

8.4.1. Results

The samples exposed to moisture as used in the tensile and compression tests were measured on weight change before each test (350, 700 and 1050 hours). On average a 0.1% weight increase from the absorption of water was observed. The maximum measured weight change is a 0.2% increase in weight. The results of all measurements are given in Appendix B.

The weight of one LMC sample (20mm x 10mm x 2mm) was tracked for water uptake over a duration of two weeks. This sample and a reproduced reference sample were dried and exposed in 80% RH. The results show that after 140 hours the maximum water absorbance is reached. The reproduced sample's weight has increased 0.23%, similar to the large bulk samples. The LMC sample has increased 0.68% in weight after 186 hours of exposure. This indicates that the water absorbance in the LMC material is approximately three times larger than in the reproduced material.

After three days of drying, the weight of both samples showed to restore to the original weight before moisture exposure.

8.4.2. Discussion

The LMC sample displayed to increase 0.68% of it's original weight, due to water uptake. This could be due to lower moisture stability of the epoxy. Another explanation would be that the LMC samples have a greater surface area between the sand and the epoxy. Sand does not greatly bond to epoxy (just like glass). In literature it is discussed that in Epoxy with mineral fillers, it has been seen that water destroys the bond at the interface between the filler and polymer. This creates additional cavities along the sand that can be filled with water [58]. The adhesion between sand and epoxy in the LMC may have decreased over the previous sixty years, what could explain the higher water absorbance measured in the LMC sample.

Literature on water absorption of an epoxy resin [59] reported that an absorption of water leads to a decrease in the glass transition temperature. A 1% absorption led to approximately a 8°C reduction in Tg This indicates plasticization of the polymer. This is in line with the DMA tests done, where the Tg of the humidity aged samples decreased by 8-13 °C. Whether these reactions are reversible is not touched upon in this research.

8.5. X-ray photoelectron spectroscopy

X-ray photoelectron spectroscopy (XPS) is performed to get an understanding of the change in the amount of oxidation on the surface of the aged specimen. This was done after the performed ageing procedures since the FTIR tests did not give conclusive results about changes in molecular bonds. Specimens of all ageing cycles are tested once (after 1050 hours) and compared to one un-aged sample. Two types of scans are made, a survey scan to obtain all the elements present in the material and detailed scans of oxygen, carbon, silicon and nitrogen peaks.

8.5.1. Results

From the survey scan of the samples the total percentage of oxygen on the surface is obtained. Oxygen bonds are present in both the epoxy as well as in the sand, so an increase of the total amount of oxygen on the surfaced does not necessarily indicate oxidation. To get a better understanding if the epoxy is oxidized, the detailed scans are further analysed.

Detailed spectra are performed on the carbon (C1s) and oxygen (O1s) peaks. The survey scans as well as the detailed scans of the C1s and 01s scans can be found in appendix E. In the detailed O1s scan, the peaks with BE around 531.5, 532, 533.3eV are the characteristic of O-H, C=O and C-O groups, respectively [60]. Silicon (SiO_2) is present at 532.9eV [61]. The silicon peak is found to overlap with the C=O peak. Therefore, a good fitting was not obtained in the oxygen scan.

In the C1s scan, the peaks with binding energy (BE) near 284.7, 285.9, 287.5, 288.7eV are the characteristic of C-C, C-O in alcohol or C-N in amine, C=O in amide, C=O in aldehyde, respectively. An additional bond (named C1s in the graph) was used to obtain good fitting, however the corresponding bond type is unknown or a contribution of C-C bonds. Carbon bonds are only present in the epoxy, so a increase of oxygen bonded to carbon indicates oxidation of the epoxy. It is observed in most samples that with an increase of C-O and C=O bonds, the number of C-C bonds decrease. The results of the

carbon detailed scan are found in table 8.5. The values represents what amount (%) of the specific bond (C-C, C=O or C-O) is present of the total amount of carbon in the material.

Table 8.5: Carbon bonds from XPS in percentage of total area (%)

Ageing type	C=O (amide)	C=O (aldehyde)	C-O	C-C	C1s	C-O + C=O	C-C + C1s
BL	1.65	1.37	21.46	73.89	1.63	24.48	75.52
UV	2.3	2.35	26.23	68.24	0.87	30.88	69.11
RH	1.79	1.64	35.81	60.22	0.53	39.24	60.75
TC	1.71	1.49	20.01	75.39	1.42	23.21	76.81
WS	2.41	2.11	25.08	69.04	1.37	29.6	70.41
BL	1.77	1.14	22.57	72.89	1.64	25.48	74.53
UV	1.98	2.22	16.42	77.89	1.49	20.62	79.38
RH	2.34	1.9	26.17	68.75	0.85	30.41	69.6
TC	2.5	1.66	25.65	69.05	1.15	29.81	70.2
WS	1.55	2.39	20.11	74.74	1.2	24.05	75.94

All reproduced samples show the relation of a decrease in the number of C-C bonds and a increase in the number of C=O and C-O bonds, compared to the baseline sample. Except the TC sample which shows a increase of C-C and C=O bonds and and a decrease in C-O bonds. For the LMC samples, the relation holds for the RH and TC samples. However, for the UV sample an increase of C-C and C=O and decrease of C-O is observed. In the WS cycle an increase in C-C and C-O with an decrease of C=O (amide).

When adding all groups of carbon bonded to oxygen together and comparing it to the amount of C-C bonds, the UV, RH and WS cycles of the reproduced samples show an increase in oxygen bonds. In the Liverpool samples the RH and TC show an increase of oxygen compared to the un-aged baseline sample.

8.5.2. Discussion

Since the results from FTIR analysis displayed little physical changes, XPS tests were carried out on the aged specimens. The XPS can detect C-O, C=O and C-C bonds, observed in the carbon scan. The bonds observed in the XPS analysis are compared to the FTIR results. Literature reports with increasing UV exposure, a decrease in the bands at 1508 cm^{-1} (benzene ring) and at 1245 cm^{-1} (C–O). While new bands appeared in the 1620–1740 cm^{-1} region due to the formation of and various carbonyl groups (C=O) such as aldehydes, amides and ketones. The results from the XPS displays a relationship between an increase in C–O and C=O bonds, with a decrease of C-C bonds.

In none of the FTIR plots a peak was observed at 1245 cm^{-1} (C–O), due to overlapping signals from the sand present in the mortar. Newly-formed band at 1726 cm^{-1} (attributed to aldehyde C=O stretching) are linked to UV-exposure in literature, however this bond is not found in any of the FTIR analysis. The XPS does observe this bond with values between 1.37-2.39% of the total amount of carbon bonds present. It is possible that FTIR is not sensitive enough to observe this bond.

The changes observed by XPS do not show links between the reproduced samples and the LMC samples. The UV, RH and WS cycles in the reproduced samples show an increase in oxidation based on this XPS. While in the LMC samples the RH and TC cycles show oxidation. So, in the one case TC does show oxidation while it does not in the other. The results are also not in line with literature, where the oxidation of outdoor light and temperature exposed specimen is expected.

It is preferred to test the same sample twice, once before ageing and once after ageing to limit changes due to differing composition in the material. It might be possible that since no XPS scan was performed before ageing, changes in the composition of the surface can not be quantified. Therefore, no conclusions about the amount of oxidation of the samples can be drawn from this test.

IV

Conclusion and Recommendations

9

Conclusion

This thesis sets out to investigate the question: *What is the mechanical and chemical stability of the over fifty years environmentally exposed epoxy-mortar, as used in the dalle de verre of the Liverpool Metropolitan Cathedral?* In answering this question, the stability and strength were assessed by mechanical and physical tests. Environmental degradation was simulated using accelerated ageing tests (by means of outdoor light exposure, moisture and temperature cycling) on both a model epoxy as well as the original epoxy-mortar from the cathedral.

Since only a very limited amount original material from the cathedral was available to assess, the composition of the mortar was analysed and reproduced. Mechanical tests were performed on the reproduced mortar, whereas chemical test could make the link between the reproduced and original mortar. The exact composition and manufacturing method of the original epoxy mortar could not be traced back. Thermogravimetric analysis displayed to be able to accurately determine the amount of sand and epoxy present in the original epoxy mortar, but it could not determine the percentage of carbon black using a widely used testing method.

From this research, it is evident that moisture is associated with the loss of adhesion between the glass and the mortar, but it provides no indication whether the epoxy-mortar is significantly degraded. The material exposed to moisture showed to have a overall lower strength than the un-aged material. The combination of moisture and thermal cycling displayed a higher strength than the samples aged on moisture alone. It is more plausible that this contributed to the softening of the polymeric chains by plasticization, rather then due to degradation by hydrolysis. Further research might reveal if the softening effects of water are reversible.

Both outdoor light exposure and temperature cycling displayed to raise the strength and (DMA) glass transition temperature. Likely because of post-curing reactions. None of the performed ageing cycles displayed a downward trend that indicated (compression strength) degradation over the 1050 hours. It could be possible that the tested exposure period is not long enough to induce permanent degradation mechanisms.

In this thesis a better understanding was gained on what factors could contribute to degradation of the epoxy-mortar as used in the glass lantern of the Liverpool Metropolitan Cathedral. Physical analysis by means of FTIR did not display substantial changes on functional groups. I argue that the great amount of filler material present in the mortar protect the epoxy from the effects of outdoor exposure. Given the unavailing results from most of the performed physical analysis, it can be concluded that degradation mechanisms from weathering are complex and can not be measured directly. The link between mechanical strength and physical changes is difficult to find. This does not conclusively prove that the epoxy-mortar of the Liverpool Metropolitan Cathedral has dramatically changed or that it's mechanical stability has decreased.

10

Recommendations

This thesis has identified the effects of different environmental factors on the mechanical and chemical stability of the epoxy-mortar as used in the lantern of the Liverpool Metropolitan Cathedral. Although the cause of the observed adhesive failure has been found, it was observed that linking mechanical and physical properties is difficult. There are two main fields that require attention in future studies. Specific for this study are the methods of examining and repairing of the cathedral's lantern. The other field is the more general study on environmental degradation of polymeric materials, similar to the one used in this research. Therefore, the following main recommendations for future research are proposed:

1. Find a way to stop water ingress in the lantern of the Liverpool Metropolitan Cathedral.

   The observed adhesive failure in the lantern is found to be caused by moisture. A method is needed to stop water ingress into the cathedral. This could be in the form of an adhesive that seals the mortar, to stop water ingress. This is also effective in preventing further deterioration of the epoxy-mortar. Requirements for the adhesive system are the ability to make a stable bond with both the glass and the mortar and the option to be removable.

2. Research the effects of moisture ingress on the used type of epoxy-mortar further.

   Are the effects of water, apart from the de-bonding of the glass and mortar, permanent or reversible? In this research it is observed that water lowers the glass transition temperature. The mechanical strength compared to the thermally exposed epoxy-mortar is also lower. However, a combination of both moisture and thermal cycles seemed to partially raise the strength. So, do the observed changes, such as a lower glass transition temperature alter the mechanical stability of the material permanently? Or can the properties be (partly) restored?

3. Examine how the lantern structure, and more specific the epoxy-mortar, is affected by mechanical loading (fatigue).

   This research has not touched upon the effects of mechanical loading on the stability of the structure. It could be useful to assess what stresses occur on the windows of the Liverpool Metropolitan Cathedral from wind loading. How these stresses are transferred trough the structure, and if these stresses load the epoxy-mortar structurally are unknown.

4. Assess how changes in physical properties can be linked with the stability of thermosetting polymers.

   It has been found that making the link between test methods, such as the used physical tests, and making a lifetime prediction of the epoxy-mortar is very difficult. A lot of research has been done on how polymers are affected by environmental ageing. Changes such as changes in Tg and molecular bonds are observed. Whether these changes induce permanent changes or reduction in mechanical stability, or in what extend they are reversible, is unknown. So, more knowledge is needed on the practical implications of these changes, on the stability and lifetime of these materials.

5. Examine the effects of a silica (sand) filler on environmental degradation.

   Hypothesised is that the silica as used as a filler in the epoxy adhesive greatly inhibits physical changes and degradation. The effects that sand has on possibly blocking UV light and moisture should be assessed. Tests can be performed by comparing changes due to accelerated ageing in an epoxy-mortar with a pure epoxy.

6. Find a method of performing better DSC tests for the purpose of accelerated ageing.

   The performed DSC tests, by using one heating cycle, has been found unsuitable. A method of measuring the glass transition temperature, without changing the physical properties before testing (by heating etc.) needs to be found.

Bibliography

[1] Purcell, “Research and Conservation Planning for Sir Frederick Gibbert’s Liverpool Metropolitan Cathedral in Liverpool, England”, no. ORG-201631354, 2018.

[2] *Curious About*. [Online]. Available: https://www.curiousabout.co.uk/liverpool2.html (visited on 05/10/2019).

[3] W. Starkey, *Stained glass at Liverpool Metropolitan Cathedral*, 2013. [Online]. Available: https://www.geograph.org.uk/photo/3328178 (visited on 10/30/2019).

[4] Tobit Curteis Associates LLP, “Survey and Monitioring of the Enviromental Factors Associated with The Conservation of the Glazed Lantern - Year 1 report”, Tech. Rep., 2017.

[5] N. H. Tennent, “Appliqué Stained Glass: The conflict between conservation and context”, *Studies in Conservation*, vol. 51, no. sup2, pp. 273–278, 2006.

[6] Shell, *Crown of glass*. [Online]. Available: https://www.youtube.com/watch?v=M-B-8uwf1-M (visited on 04/18/2019).

[7] R. Merola, “Liverpool Metropolitan Cathedral: Epoxy Mortar Analysis & Testing”, Purcell, Tech. Rep. April, 2016.

[8] J. Comyn, “Adhesive joints and the environment”, in *Adhesion science*, J. Comyn, Ed., 1999, ch. Chapter 10, pp. 126–143.

[9] A. J. Kinloch, R. Parker, P. Taylor, *et al.*, *Adhesion and Adhesives*. Chapman & Hall, 1987.

[10] G. Wypych, *Handbook of Material Weathering*, Fifth Edit, 620. ChemTec Publishing, 2013, vol. 741.

[11] M. Lettieri and M. Frigione, “Effects of humid environment on thermal and mechanical properties of a cold-curing structural epoxy adhesive”, *Construction and Building Materials*, vol. 30, pp. 753–760, 2012.

[12] B. Van Lancker, J. Dispersyn, W. De Corte, *et al.*, “Durability of adhesive glass-metal connections for structural applications”, *Engineering Structures*, vol. 126, pp. 237–251, 2016.

[13] M. G. González, J. C. Cabanelas, and J. Baselga, “Applications of FTIR on Epoxy Resins - Identification, Monitoring the Curing Process, Phase Separation and Water Uptake”, in *Infrared Spectroscopy - Materials Science, Engineering and Technology*, vol. 2, 2012.

[14] P. Silva, J. Sena-Cruz, D. Soares, *et al.*, “Effects of different environmental conditions on the mechanical characteristics of a structural epoxy”, *Composites Part B: Engineering*, vol. 88, pp. 55–63, 2015.

[15] E. M. Petrie, *Handbook of adhesives and sealants*, 585. 2008, vol. 2008, pp. 142–153.

[16] J. M. Reis, F. C. Amorim, A. H. Da Silva, *et al.*, “Influence of temperature on the behavior of DGEBA (bisphenol A diglycidyl ether) epoxy adhesive”, *International Journal of Adhesion and Adhesives*, vol. 58, pp. 88–92, 2015.

[17] T. C. Nguyen, Y. Bai, X. L. Zhao, *et al.*, “Effects of ultraviolet radiation and associated elevated temperature on mechanical performance of steel/CFRP double strap joints”, *Composite Structures*, vol. 94, no. 12, pp. 3563–3573, 2012.

[18] I. Coutinho, F. Fernandes, A. Ramos, *et al.*, “Studies on degradation of epoxy resins used for conservation of glass”, *Holding it all together*, no. February, pp. 127–133, 2008.

[19] S. Nikafshar, O. Zabihi, M. Ahmadi, *et al.*, “The effects of UV light on the chemical and mechanical properties of a transparent epoxy-diamine system in the presence of an organic UV absorber”, *Materials*, vol. 10, no. 2, pp. 1–18, 2017.

[20] F. C. Amorim, J. M. Reis, J. F. Souza, *et al.*, “Investigation of UV exposure in adhesively bonded single lap joints”, *Applied Adhesion Science*, vol. 6, no. 1, 2018.

[21] M. Kutz, *Handbook of environmental degradation of materials*. William Andrew Publishing, 2005.

[22] H.-C. Flemming, “Relevance of biofilms for the biodeterioration of surfaces of polymeric materials”, *Polymer Degradation and Stability*, vol. 59, no. 1-3, pp. 309–315, 1998.

[23] K. Mittal and A. Pizzi, *Handbook of sealant technology*. CRC Press, 2009, pp. 650–650.

[24] R. L. Feller, *Accelerated aging, Photochemical and Thermal Aspects*. 1994.

[25] R. j. Young, *Introduction to polymers*, Third edit. CRC Press, Inc, 2011.

[26] J. J. Liang, “Applied Polymer Science”, *Applied Polymer Science*, vol. 83, p. 1547, 2002.

[27] I. L. Dubnikova, S. M. Berezina, and A. V. Antonov, “Effect of rigid particle size on the toughness of filled polypropylene”, *Journal of Applied Polymer Science*, vol. 94, no. 5, pp. 1917–1926, 2004.

[28] A. V. Shenoy, *Rheology of Filled Polymer Systems*. Springer Science Business Media Dordrecht, 1999.

[29] M. Sangermano, G. Malucelli, E. Amerio, *et al.*, “Photopolymerization of epoxy coatings containing silica nanoparticles”, *Progress in Organic Coatings*, vol. 54, no. 2, pp. 134–138, 2005.

[30] J. M. L. Reis and A. J. M. Ferreira, “Effect of marine exposure on fracture properties of epoxy concretes”, *Polymer Testing*, vol. 24, no. 1, pp. 121–125, 2005.

[31] M. A. Silva and Z. C. Silva, “Degradation of mechanical characteristics of some polymeric mortars due to aging”, *ACI Materials Journal*, vol. 104, no. 4, pp. 337–343, 2007.

[32] A. Ghasemi-Kahrizsangi, J. Neshati, H. Shariatpanahi, *et al.*, “Improving the UV degradation resistance of epoxy coatings using modified carbon black nanoparticles”, *Progress in Organic Coatings*, vol. 85, pp. 199–207, 2015.

[33] J. V. Accorsi, “The impact of carbon black morphology and dispersion on the weatherability of polyethylene”, *KGK-Kautschuk und Gummi Kunststoffe*, vol. 54, no. 6, pp. 321–326, 2001.

[34] E. M. Petrie, “How moisture affects adhesives, sealants, and coatings”, *Metal Finishing*, vol. 109, no. 7, pp. 1–3, 2011.

[35] American Standards for Testing and Materials, “Standard Guide for Improved Laboratory Accelerated Tests to Predict the Weathering and for Use in Developing Protocols to Predict the Design Life of Building Sealant Systems. ASTM C1850-17”, pp. 1–5, 2017.

[36] H. Weather, *Avarage yearly weather in Liverpool*. [Online]. Available: https://www.holiday-weather.com/liverpool/averages/ (visited on 04/30/2019).

[37] W. Conshohocken, “Standard Test Method Practice for Effect of Moisture and Temperature on Adhesive Bonds 1”, *Test*, vol. 90, no. Reapproved, pp. 1–3, 1995.

[38] American Standards for Testing and Materials, “Standard Test Methods for Resistance of Adhesives to Cyclic Laboratory Aging Conditions. ASTM D1183 - 03”, Tech. Rep. Reapproved 2011, 2011, pp. 11–13.

[39] Verfmolen de Kat, *Carbon Black*. [Online]. Available: https://www.verfmolendekat.com/nl/carbon-black.html (visited on 10/28/2019).

[40] Jeol, *JSM-7500F Field Emission Scanning Electron Microscope*. [Online]. Available: https://www.jeol.co.jp/en/products/detail/JSM-7500F.html (visited on 10/28/2019).

[41] Alphatech Instrumentation, “Climate Test Chamber System Weiss Type WK3-340/70”, pp. 1–28, 2015.

[42] American Standards for Testing and Materials, “Standard Practice for Heat and Humidity Aging of Oxidatively Degradable. ASTM D7444-18a”, no. Reapproved 2018, pp. 1–6, 2011.

[43] Q-Lab Corporation, “Q-SUN Xenon Test Chambers, Specicifation Bulletin LX-5046”, 2018.

[44] American Standards for Testing and Materials, “Standard Practice for Exposure of Adhesive Specimens to High-Energy Radiation 1. ASTM D904−99”, *Current*, no. Reapproved 2013, pp. 5–7, 1999.

[45] American Standards for Testing and Materials, “Standard Practice for Xenon-Arc Exposure of Plastics Intended for Indoor Applications. ASTM D-2565-16”, vol. 14, no. Reapproved 2008, pp. 1–4, 2000.

[46] American Standards for Testing and Materials, “Standard test methods for chemical resistance of mortars, grouts, monolithic surfacings, and polymer concretes. ASTM C579−01”, Tech. Rep. Reapproved 2006, 2001, pp. 1–4.

[47] American Standards for Testing and Materials, “Standard Test Method for Lap Shear Strength of Sealants. ASTM C961-15”, no. Reapproved 2015, 1981.

[48] J. Hanson, *Characteristic IR Absorption Frequencies of Organic Functional Groups*. [Online]. Available: http://www2.ups.edu/faculty/hanson/Spectroscopy/IR/IRfrequencies.html (visited on 10/23/2019).

[49] American Standards for Testing and Materials, “Standard Test Method for Glass Transition Temperature (DMA Tg) of Polymer Matrix Composites by Dynamic Mechanical Analysis (DMA) ASTM D7028 − 07”, no. Reapproved 2015, 2012.

[50] G. Sime, *A Closer Look: Techniques for Obtaining Glass Transition Temperature of Polymeric Materials*, 2013. [Online]. Available: http://www.intertek.com/blog/2013-04-15-glass-transition-temperature/ (visited on 05/01/2019).

[51] Sigma Aaldrich, *Sand, white quartz*. [Online]. Available: https://www.sigmaaldrich.com/catalog/product/sigald/83340?lang=en%7B%5C&%7Dregion=NL (visited on 05/02/2019).

[52] Huntsman, “Araldite® 2020: Description Sheet”, vol. 100, no. October 2012, pp. 1–5, 2020.

[53] E. López-Ballester, M. T. Doménech-Carbó, J. V. Gimeno-Adelantado, *et al.*, “Study by FT-IR spectroscopy of ageing of adhesives used in restoration of archaeological glass objects”, *Journal of Molecular Structure*, vol. 482-483, pp. 525–531, 1999.

[54] E. G. Karayannidou, D. S. Achilias, and I. D. Sideridou, “Cure kinetics of epoxy-amine resins used in the restoration of works of art from glass or ceramic”, *European Polymer Journal*, vol. 42, no. 12, pp. 3311–3323, 2006.

[55] L. C. Thomas, “Interpreting Unexpected Events and Transitions in DSC Results”, *TA instruments*,

[56] J. D. Menczel and R. B. Prime, *Thermal Analysis of Polymers: Fundementals and Applications*. 2009.

[57] Hitachi High-Tech, “DSC Measurements of Thermosetting Resins”, *Application Brief*, pp. 1–3, 1981.

[58] S. Swapan Dutta, “Master of Science in Energy and Environment Water absorption and dielectric properties of Epoxy insulation”, no. June, pp. 1–51, 2008.

[59] B. De’Nève and M. E. Shanahan, “Water absorption by an epoxy resin and its effect on the mechanical properties and infra-red spectra”, 1993.

[60] K. Li, K. Wang, M.-s. Zhan, *et al.*, “The change of thermal e mechanical properties and chemical structure of ambient cured DGEBA / TEPA under accelerated thermo-oxidative aging”, *Polymer Degradation and Stability*, vol. 98, pp. 2340–2346, 2013.

[61] M. Biesinger, *X-ray Photoelectron Spectroscopy (XPS) Reference Pages*, 2018. [Online]. Available: http://www.xpsfitting.com/search/label/Oxygen (visited on 11/12/2019).

V
Appendix

A

Mechanical tests

A.1. Glass-bonded lap-shear results

Table A.1: Results glass-bonded lap shear tests *(NA = No value available)

Cycle	Hours	Specimen	Ultimate strength [MPa]	Adhesive failure (yes/no)
RH	350	1	NA	NA
		2	350	No
		3	1095	No
	700	1	1075	Yes, partial
		2	892	No
		3	1168	No
	1050	1	170	Yes
		2	NA	Yes, partial
		3	320	Yes
TC	350	1	494	No
		2	604	No
		3	1541	No
	700	1	495	No
		2	604	No
		3	1541	No
	1050	1	NA	NA
		2	NA	NA
		3	NA	NA
UV	350	1	NA	NA
		2	760	No
		3	NA	NA
	700	1	986	No
		2	581	No
		3	1030	No
	1050	1	672	No
		2	543	No
		3	205	No
WS	350	1	NA	NA
		2	NA	NA
		3	NA	NA
	700	1	705	No
		2	NA	NA
		3	1548	NA
	1050	1	NA	NA
		2	597	No
		3	73	No

A.2. Test specimens

A.2.1. Tensile specimens

(a) Tensile test specimens RH 1

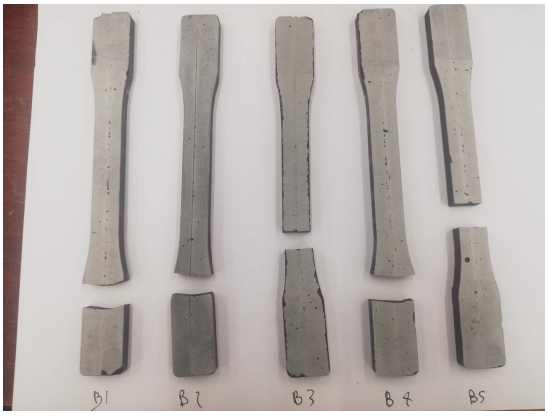

(b) Tensile test specimens RH 2

Figure A.1

(a) Tensile test specimens RH 3

(b) Tensile test specimens UV1

Figure A.2

(a) Tensile test specimens UV2

(b) Tensile test specimens UV3

Figure A.3

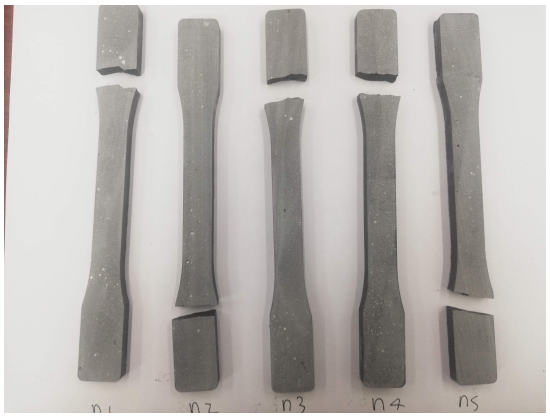

(a) Tensile test specimens TC1

(b) Tensile test specimens TC2

Figure A.4

(a) Tensile test specimens TC3

(b) Tensile test specimens WS1

Figure A.5

(a) Tensile test specimens WS2

(b) Tensile test specimens WS3

Figure A.6

A.2.2. Lap-shear specimens

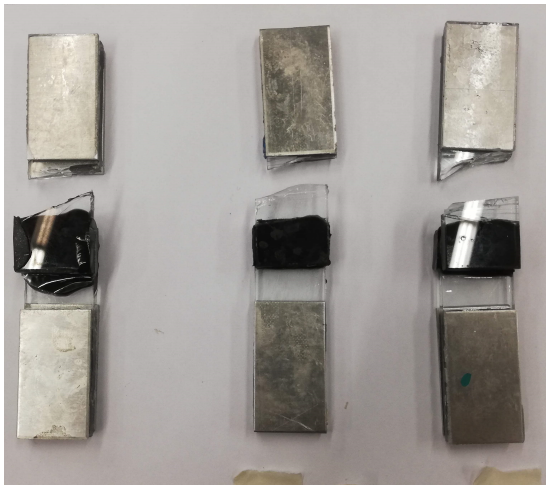

(a) Lap-shear test specimens RH 1

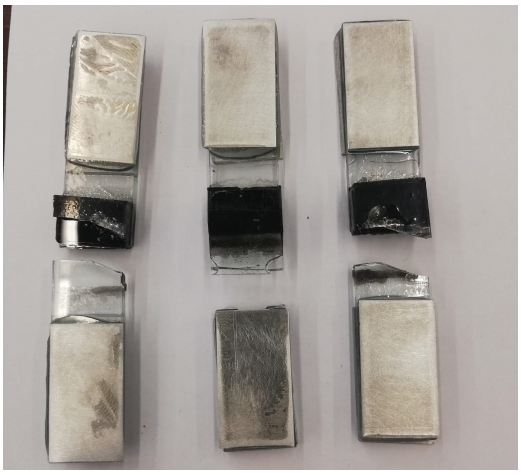

(b) Lap-shear test specimens RH 2

Figure A.7

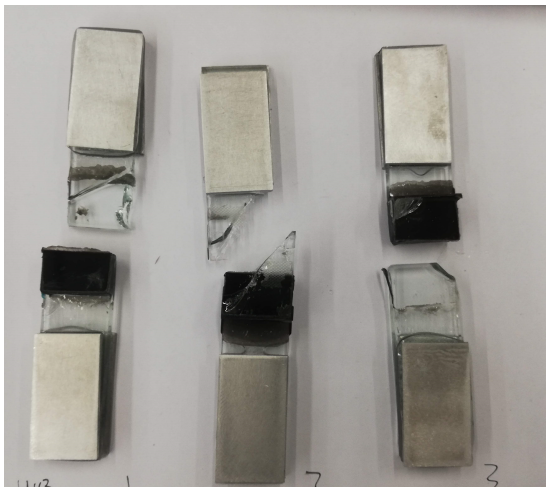

(a) Lap-shear test specimens RH 3

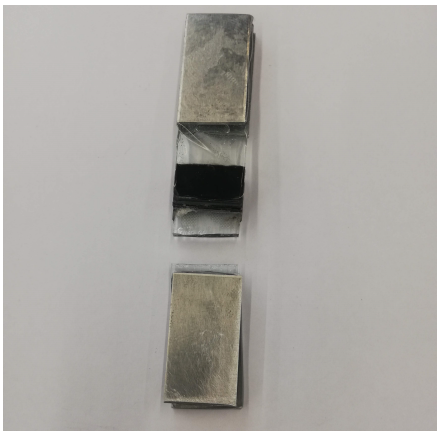

(b) Lap-shear test specimens UV1

Figure A.8

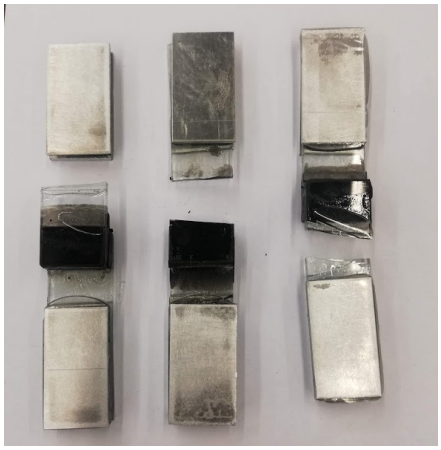

(a) Lap-shear test specimens UV2

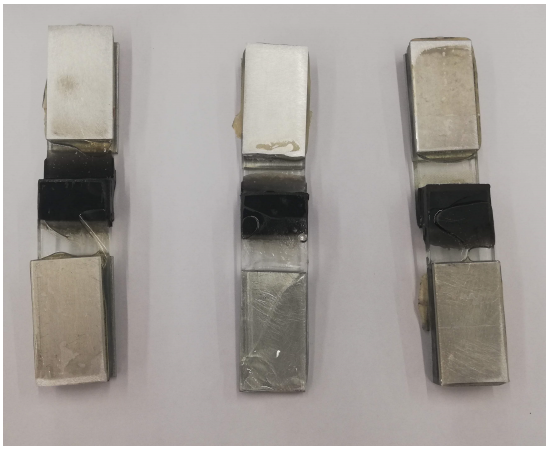

(b) Lap-shear test specimens UV3

Figure A.9

(a) Lap-shear test specimens TC1

(b) Lap-shear test specimens TC2

Figure A.10

(a) Lap-shear test specimens WS1

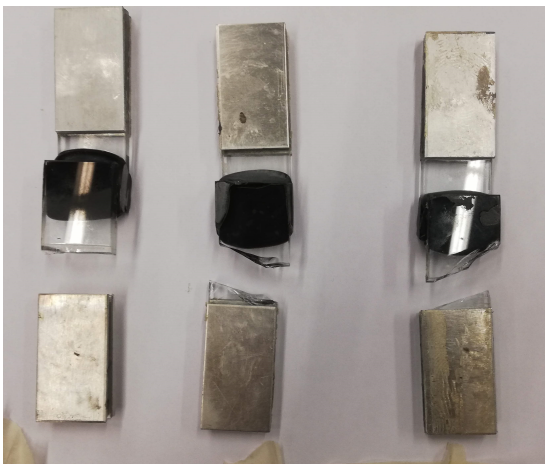

(b) Lap-shear test specimens WS2

Figure A.11

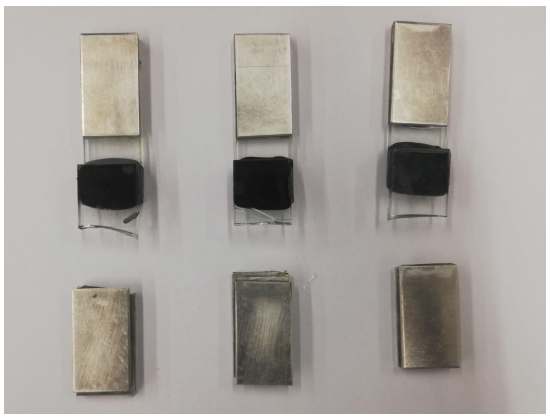

(a) Lap-shear test specimens WS3

Figure A.12

A.2.3. Compression specimens

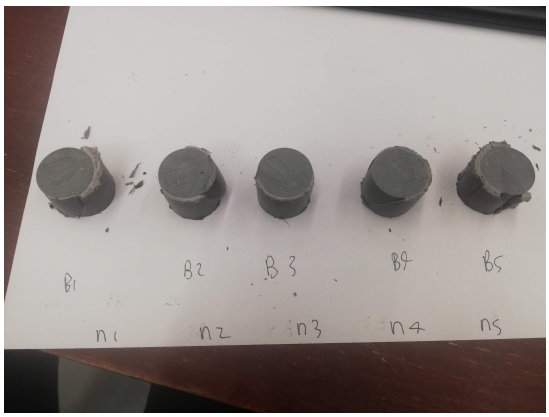

(a) Compression test specimens RH 2

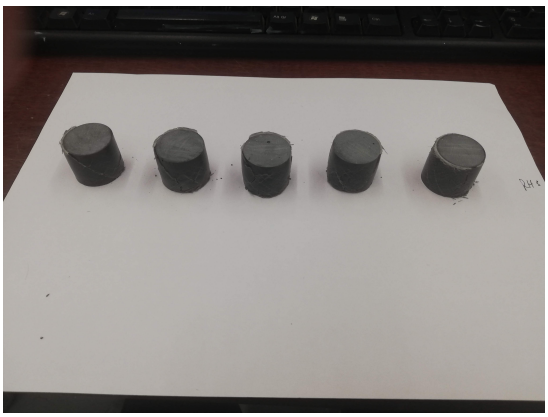

(b) Compression test specimens RH 3

Figure A.13

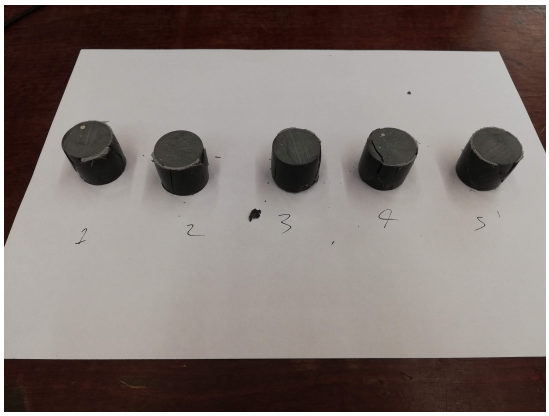

(a) Compression test specimens UV1

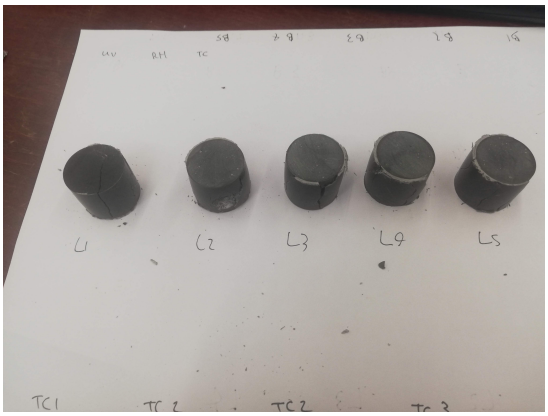

(b) Compression test specimens UV2

Figure A.14

(a) Compression test specimens TC1

(b) Compression test specimens UV 3, RH 3 TC 2

Figure A.15

(a) Compression test specimens TC3

(b) Compression test specimens WS1

Figure A.16

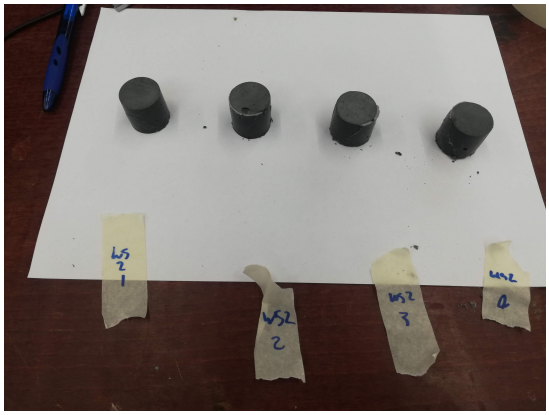

(a) Compression test specimens WS2

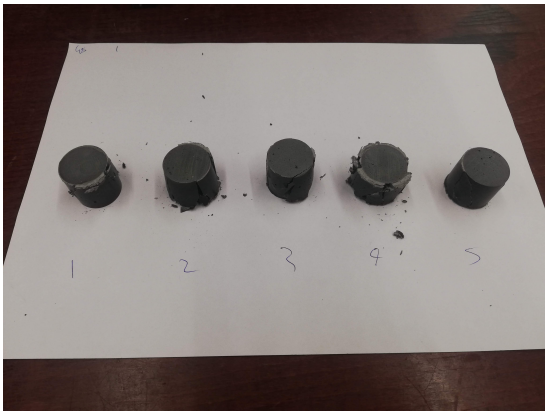

(b) Compression test specimens WS3

Figure A.17

B

Weight change

B.1. Weight change reproduced samples

Table B.1: Reproduced specimens weight change measurements over time

Sample type	Cylindrical			Dogbone		
Exposure time	Weight at t=0 [g]	Weight after ageing [g]	% change	Weight at t=0 [g]	Weight after ageing [g]	% change
350 hours	20.78	20.8	0.096%	32.19	32.19	0
	20.94	20.96	0.096%	31.11	31.12	0.032%
	20.9	20.91	0.048%	31.49	31.49	0
	20.85	20.86	0.048%	32.2	32.21	0.031%
	20.9	20.92	0.096%	31.5	31.51	0.032%
700 hours	20.9	20.9	0	31.85	31.9	0.156%
	20.78	20.77	0.048%	31.76	31.8	0.126%
	21.03	21.02	0.048%	31.44	31.49	0.159%
	20.97	20.96	0.048%	32.09	32.12	0.093%
	20.57	20.56	0.049%	32.3	32.32	0.062%
1050 hours	20.93	20.91	-0.095%	32.06	32.13	0.218%
	20.79	20.8	0.048%	31.84	31.89	0.157%
	20.81	20.83	0.096%	31.65	31.68	0.095%
	20.64	20.66	0.098%	31.95	32	0.156%
	20.95	20.97	0.095%	31.45	31.48	0.095%

B.2. Weight change LMC sample

Table B.2: LMC weight change measurements over time, with un-treated sample, dried sample, moisture cycle and followed by dry cycle

Hours	LMC weight [g]	% change	RP weight [g]	% change
Non-dried sample				
0	0.6666	0.11%	0.844	0.00%
Moisture cycle				
0	0.6659	0.00%	0.844	0.00%
18	0.6674	0.23%	0.8437	-0.04%
90	0.6687	0.42%	0.8448	0.09%
138	0.6693	0.51%	0.845	0.12%
186	0.6704	0.68%	0.8459	0.23%
Dry cycle				
24	0.6678	0.29%	0.844	0.00%
48	0.67	0.62%	0.8439	-0.01%
72	0.6662	0.05%	0.8439	-0.01%

C

FTIR Spectra

C.1. Aged reproduced samples

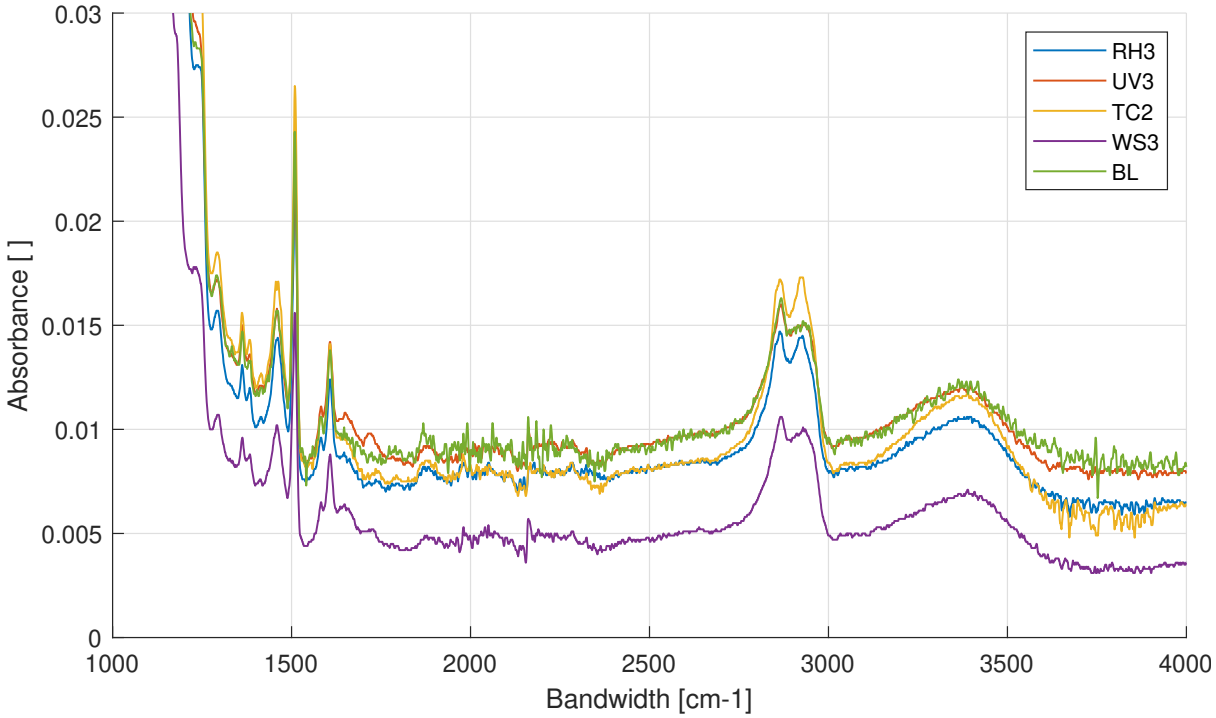

Figure C.1: FTIR ALL

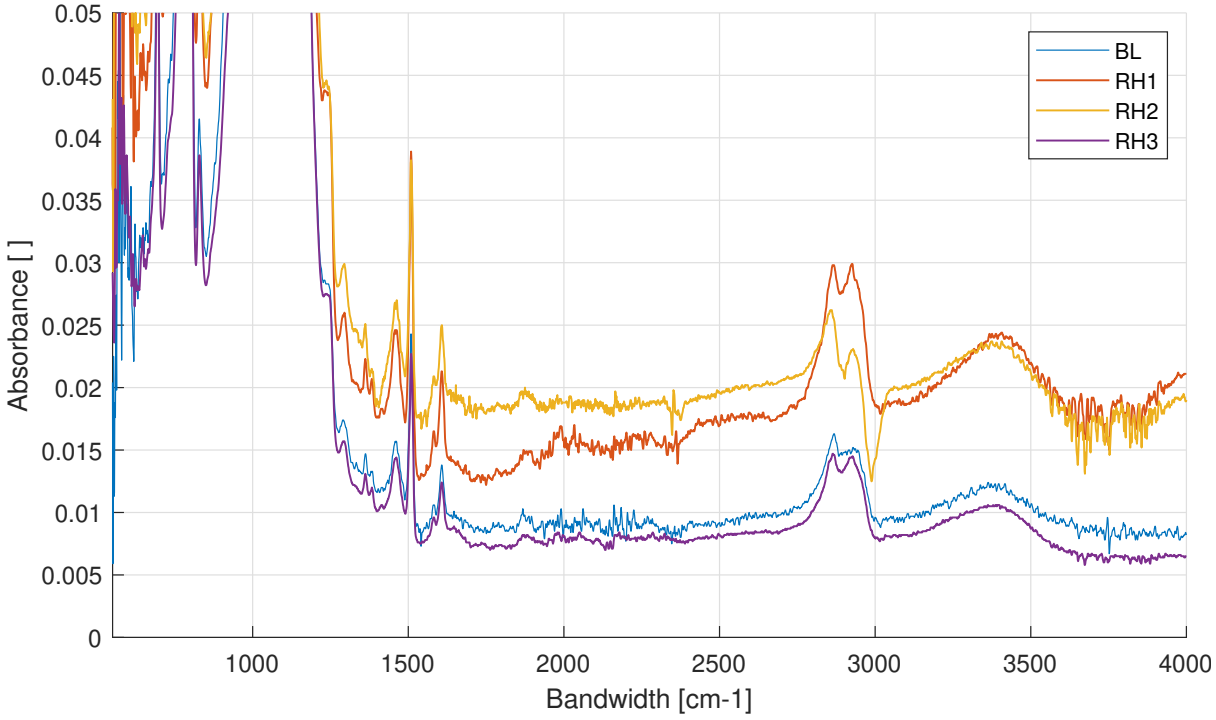

Figure C.2: FTIR graph RH after ageing

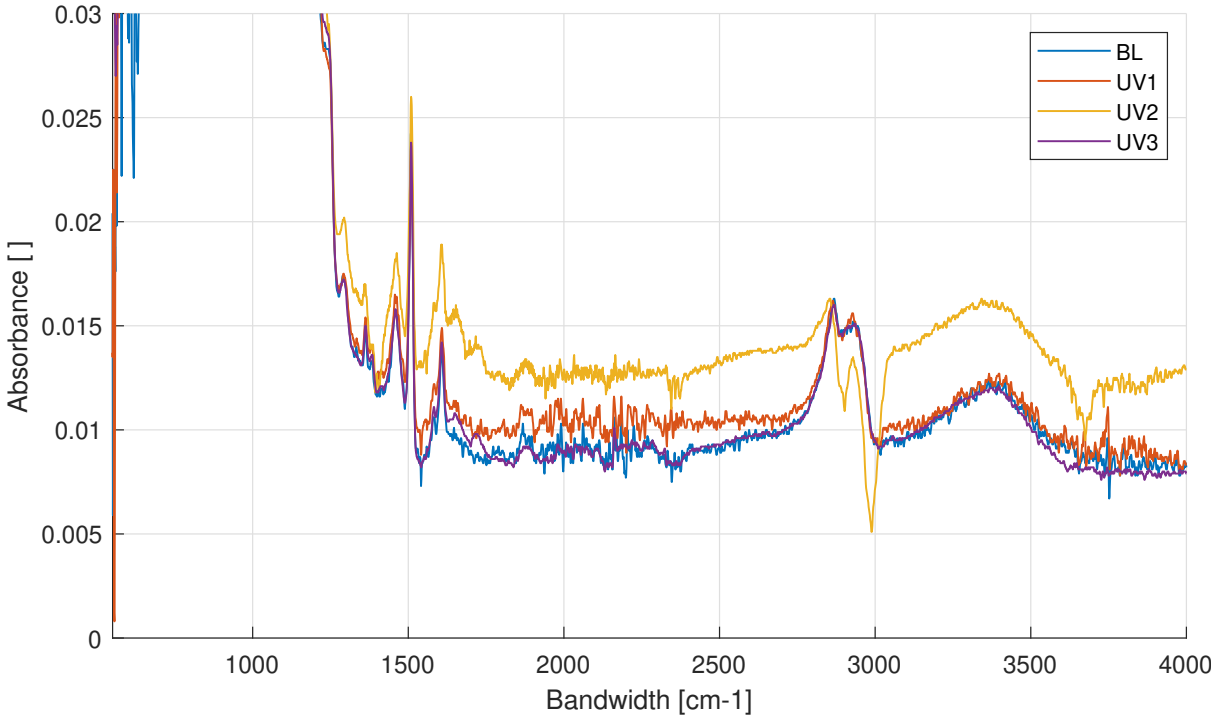

Figure C.3: FTIR graph UV after ageing

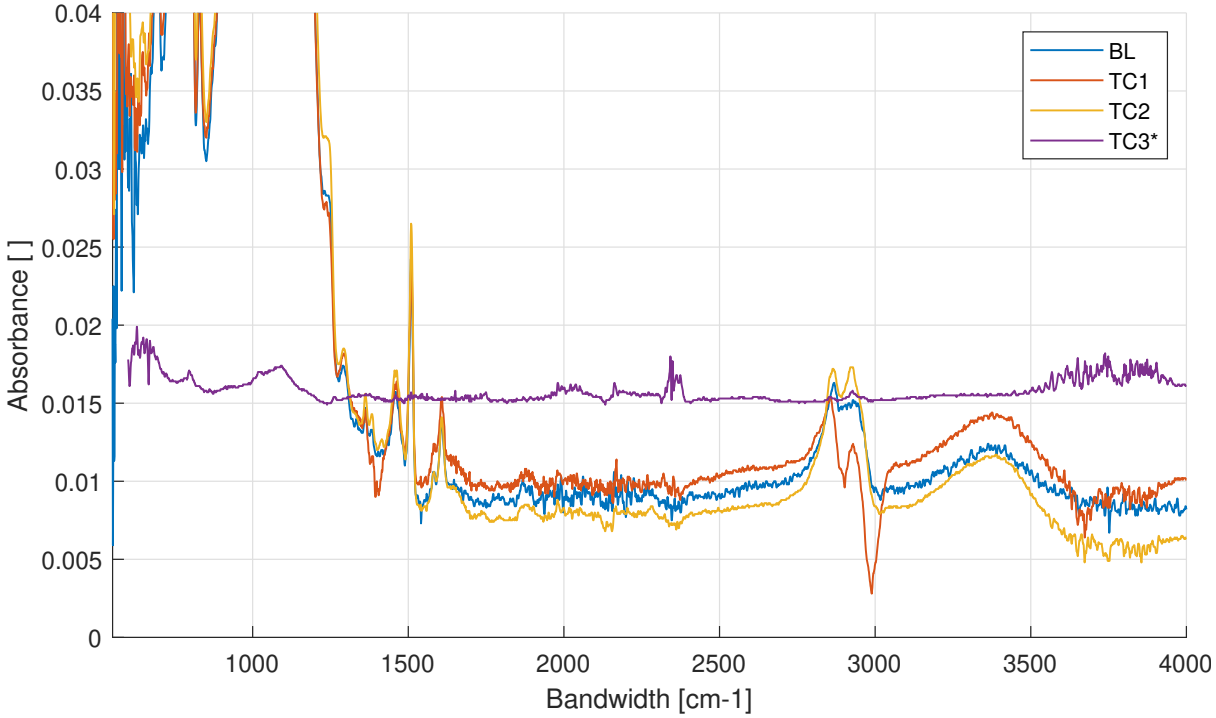

Figure C.4: FTIR graph TC after ageing

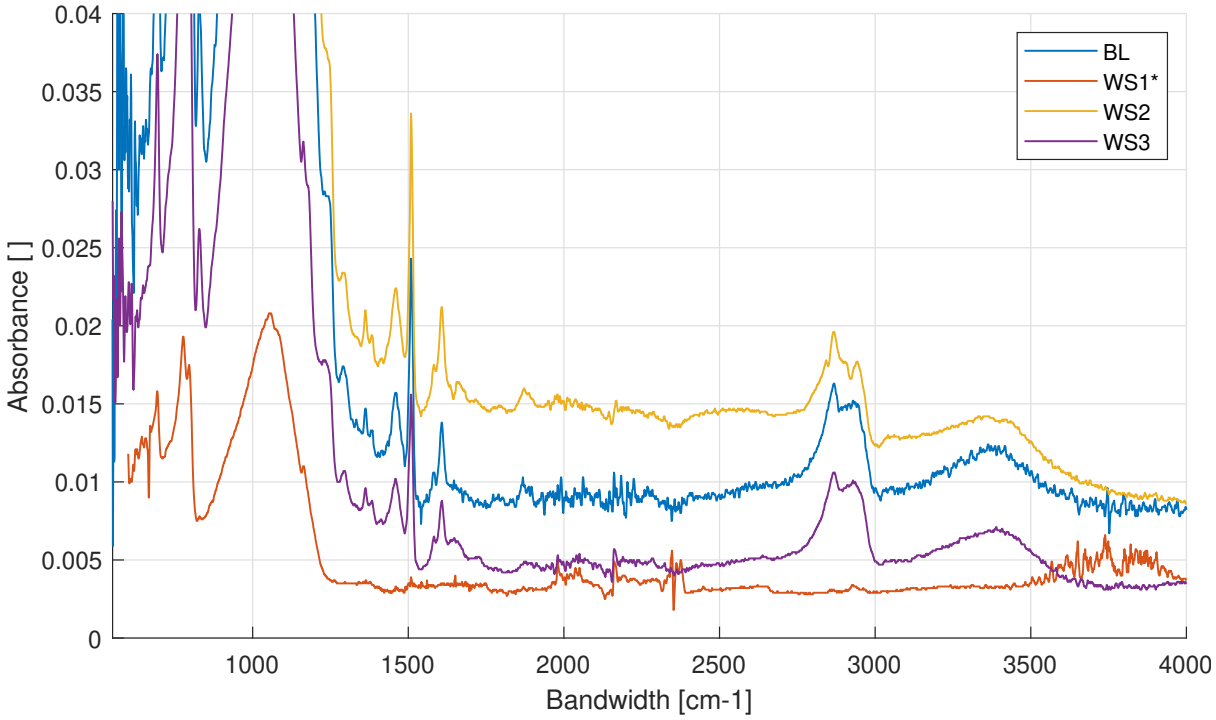

Figure C.5: FTIR graph WS after ageing

C.2. Aged LMC samples

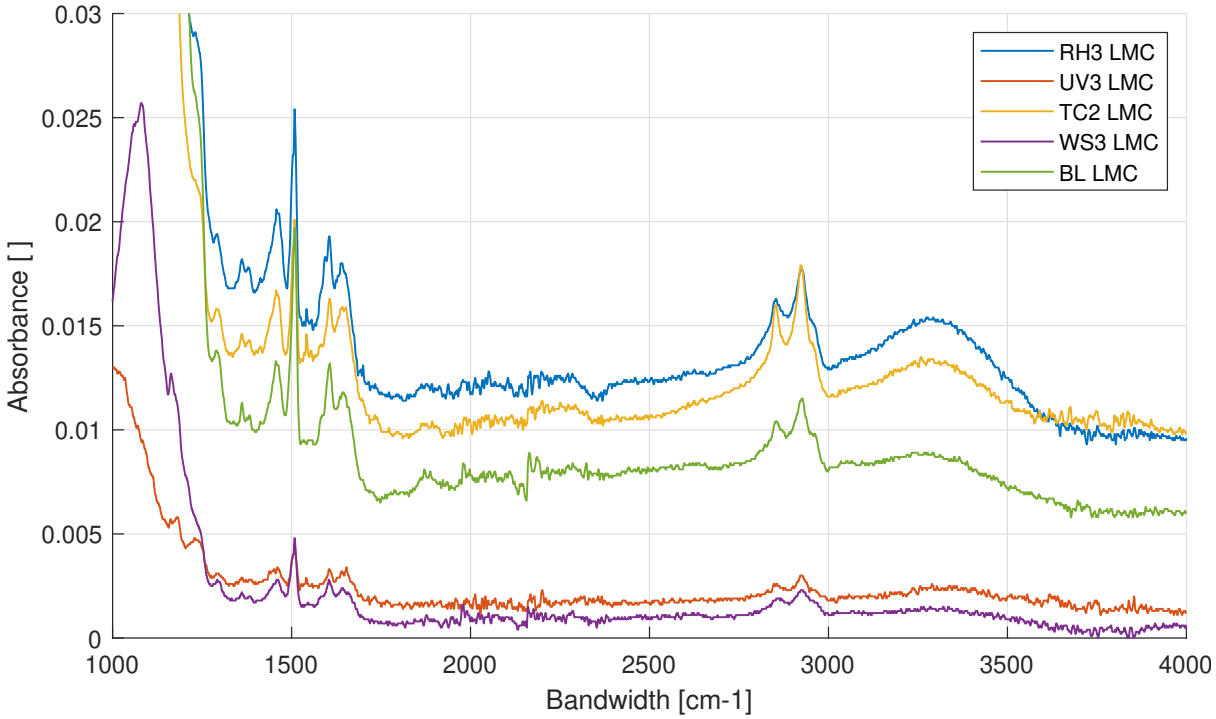

Figure C.6: FTIR ALL LMC

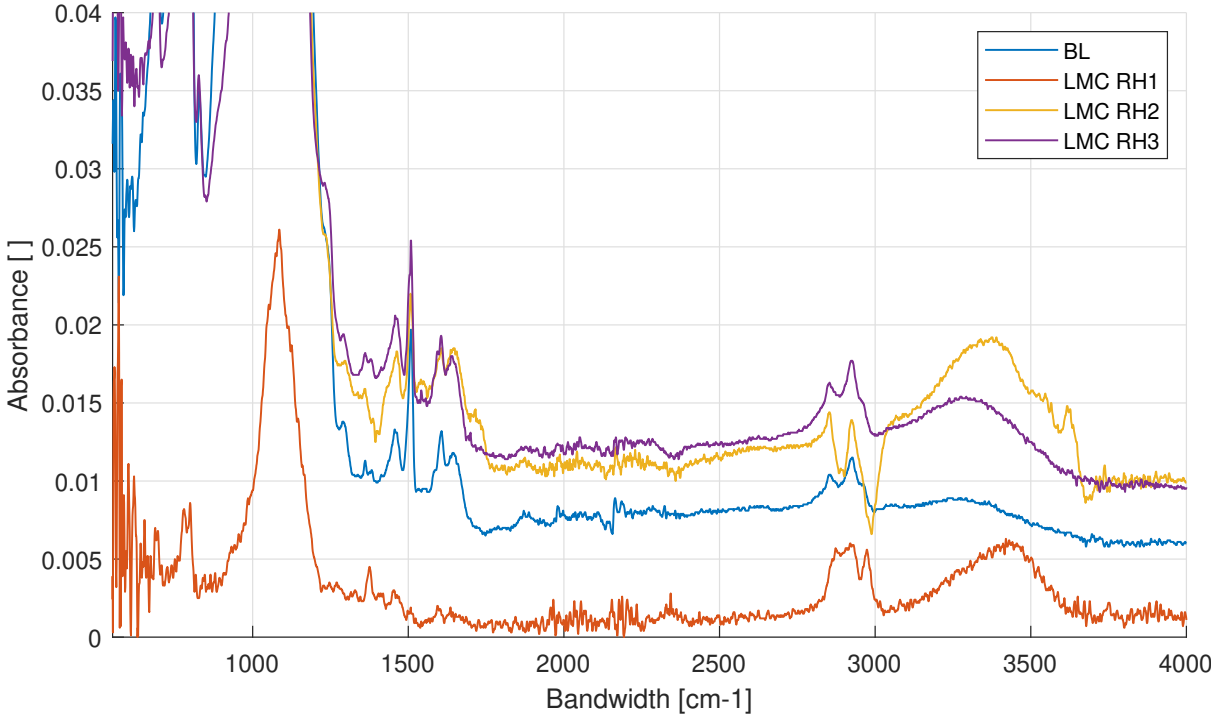

Figure C.7: FTIR graph RH after ageing

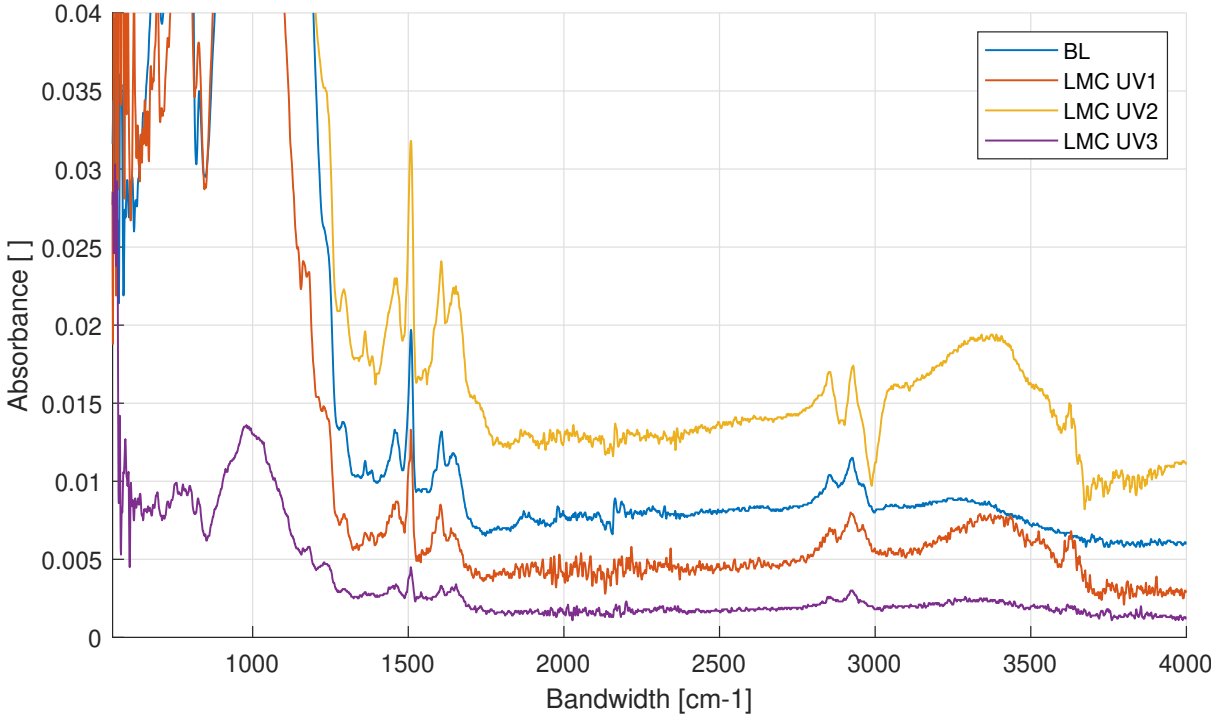

Figure C.8: FTIR graph UV after ageing

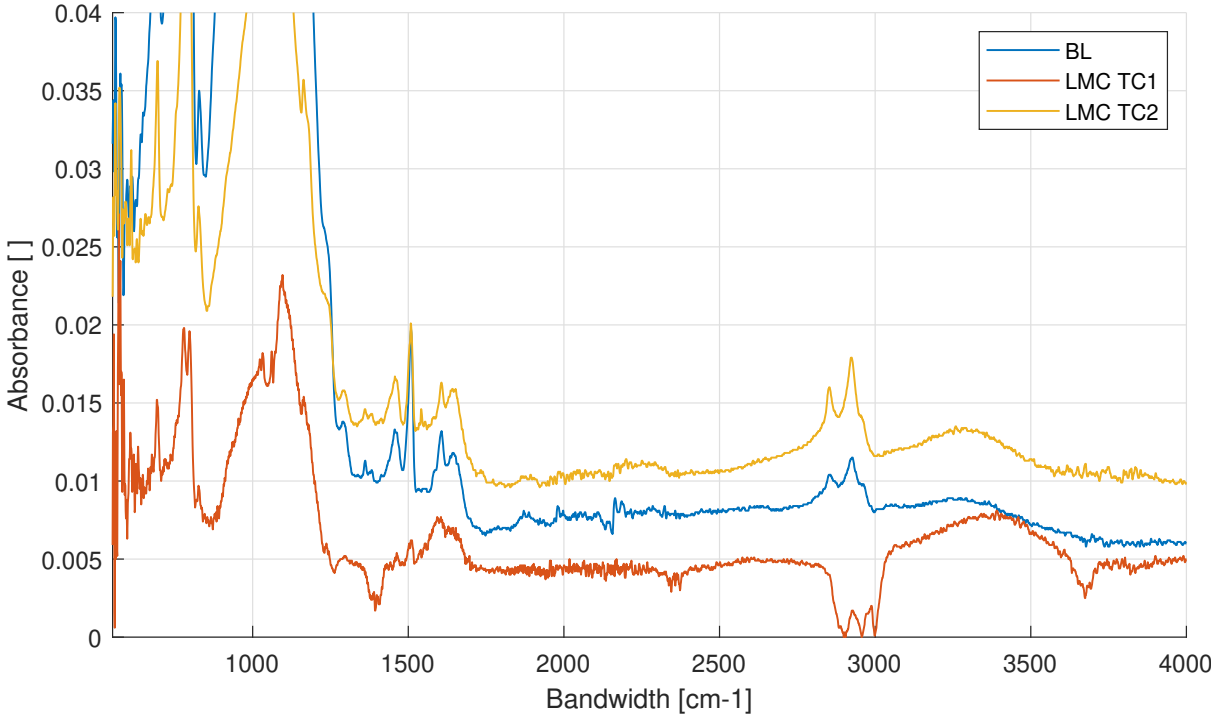

Figure C.9: FTIR graph TC after ageing

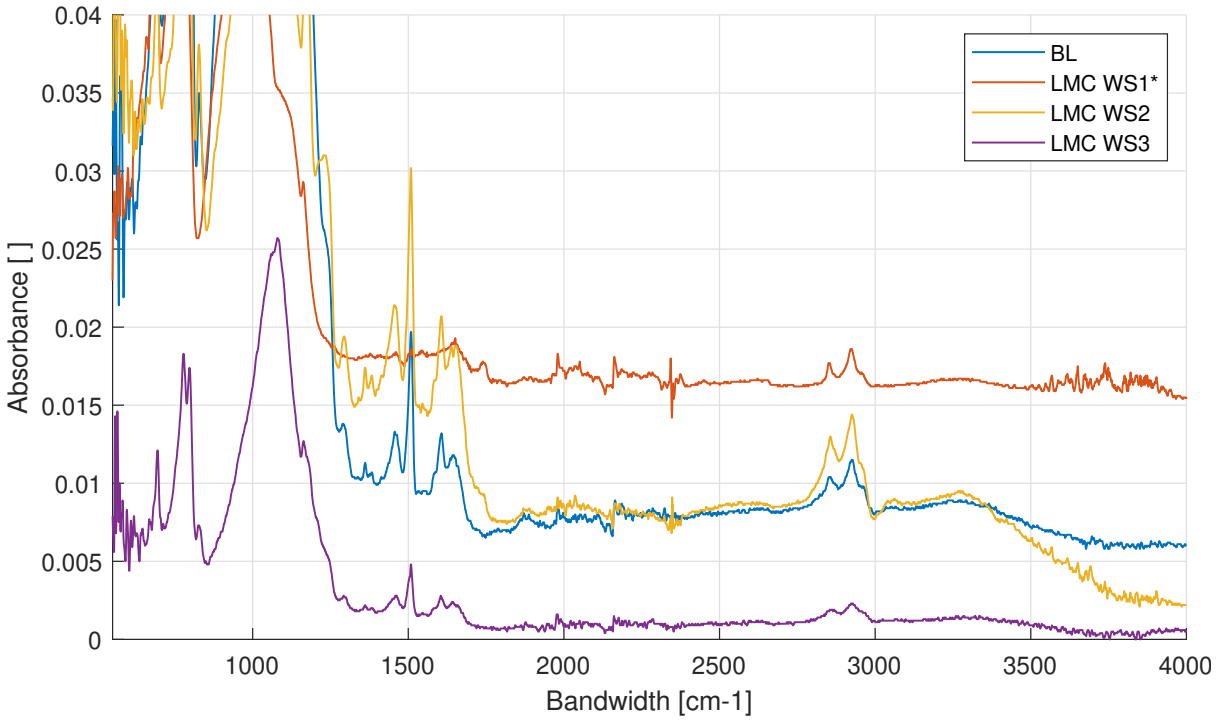

Figure C.10: FTIR graph WS after ageing

D

DSC results

D.1. Aged reproduced samples

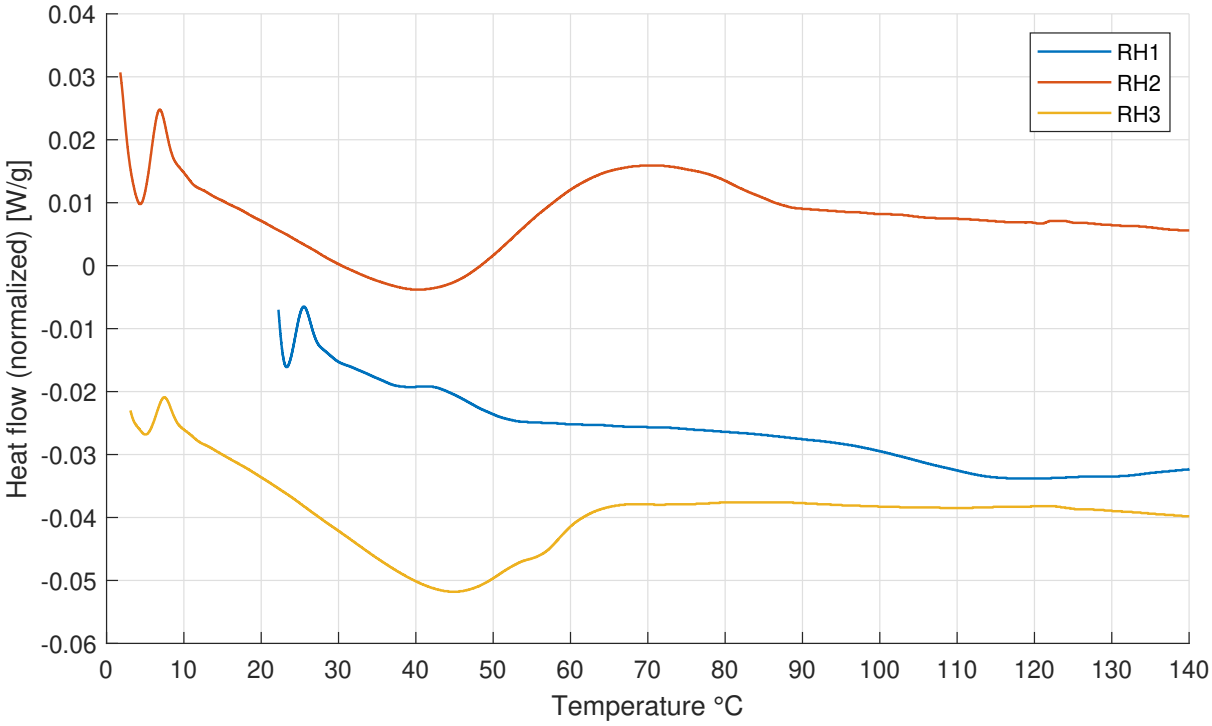

Figure D.1: DSC graph of reproduced RH ageing

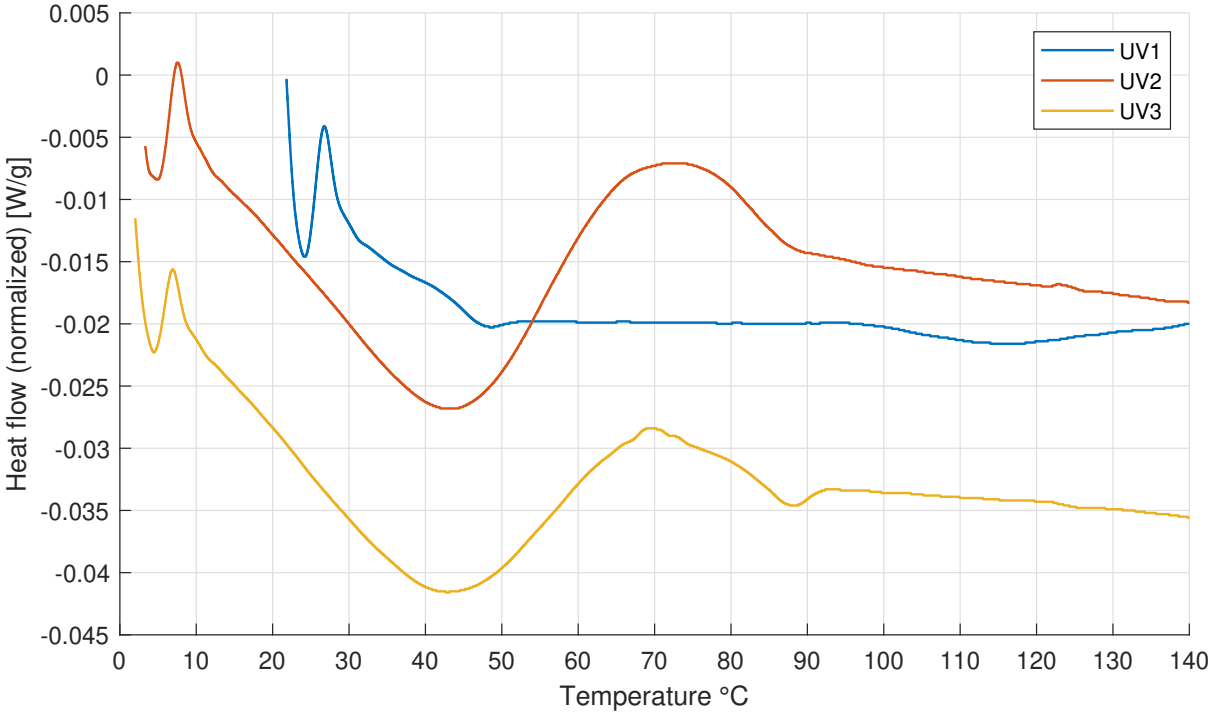

Figure D.2: DSC graph of reproduced UV ageing

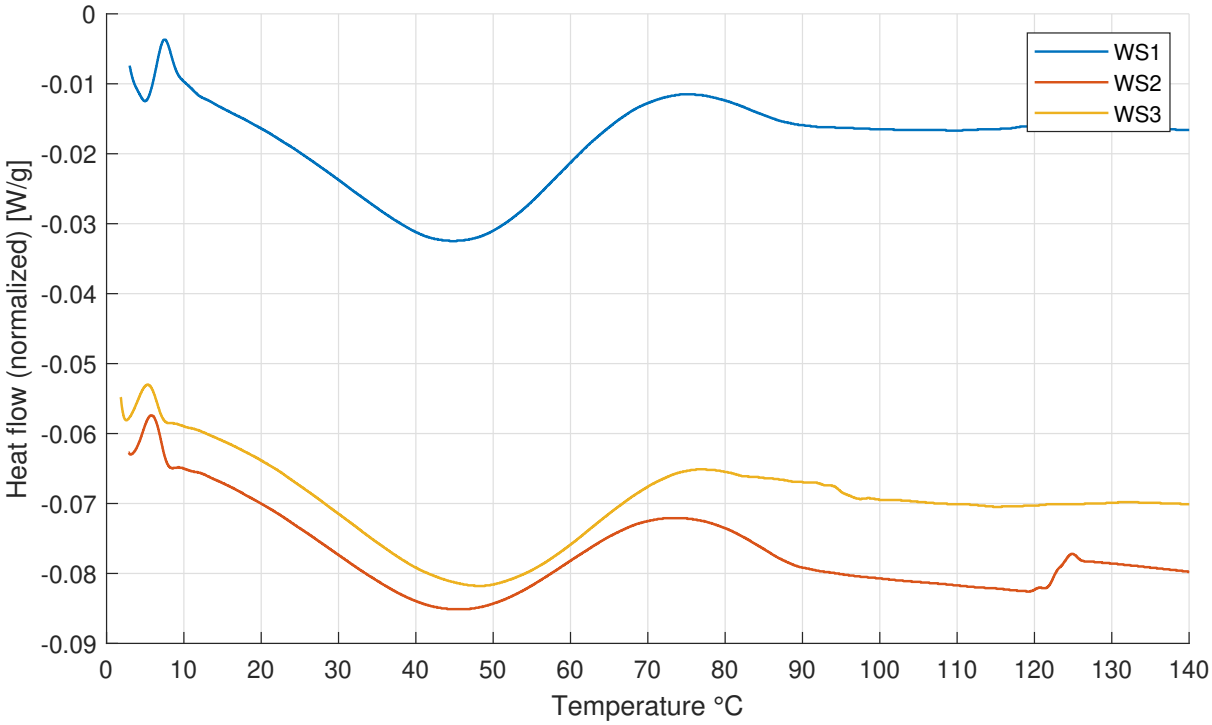

Figure D.3: DSC graph of reproduced TC ageing

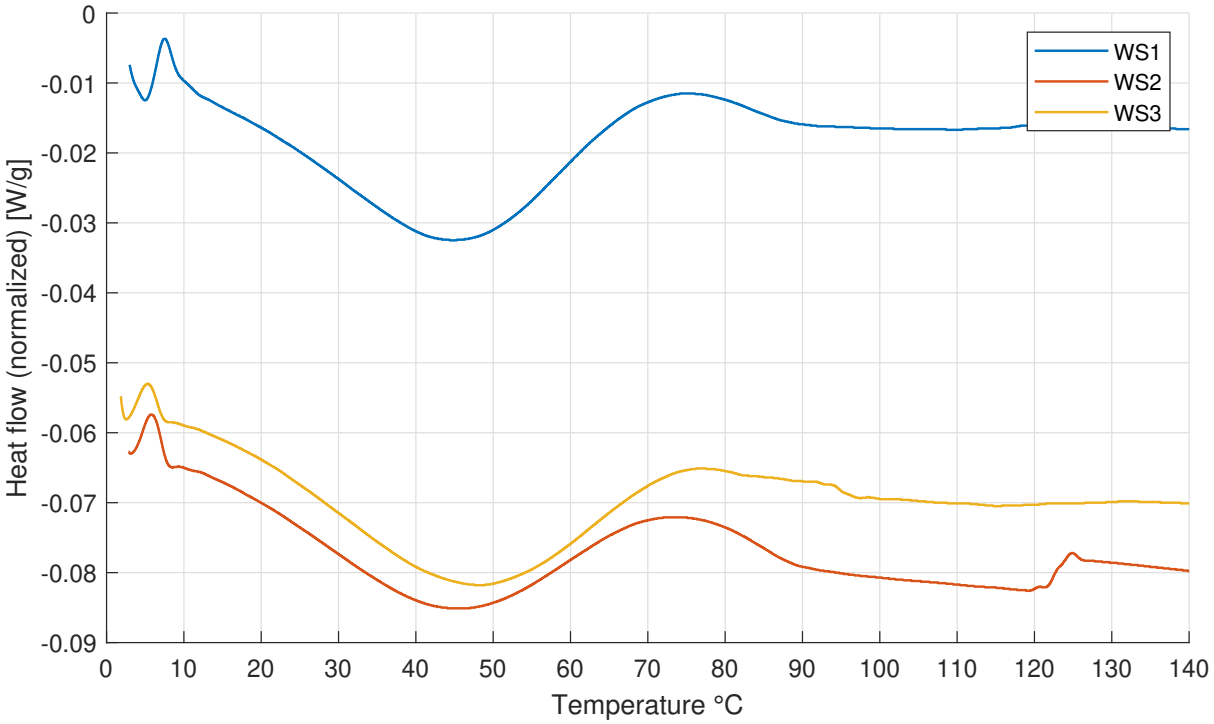

Figure D.4: DSC graph of reproduced WS ageing

D.2. Aged LMC samples

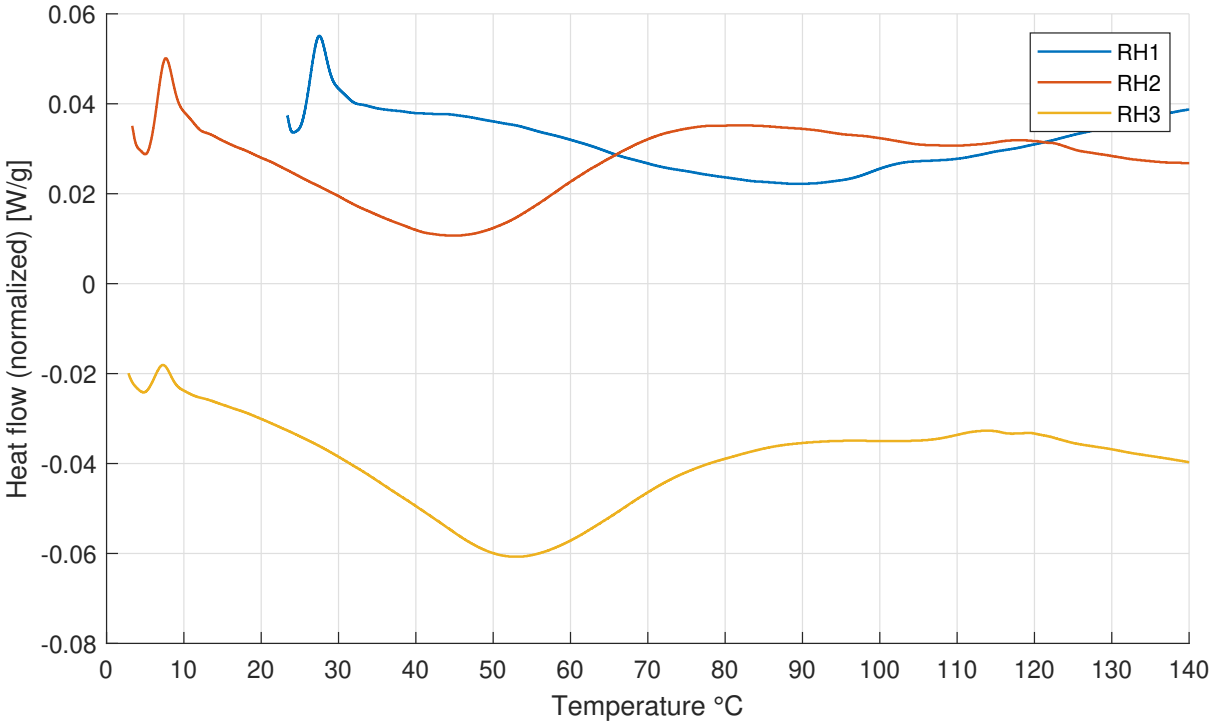

Figure D.5: DSC graph of LMC RH ageing

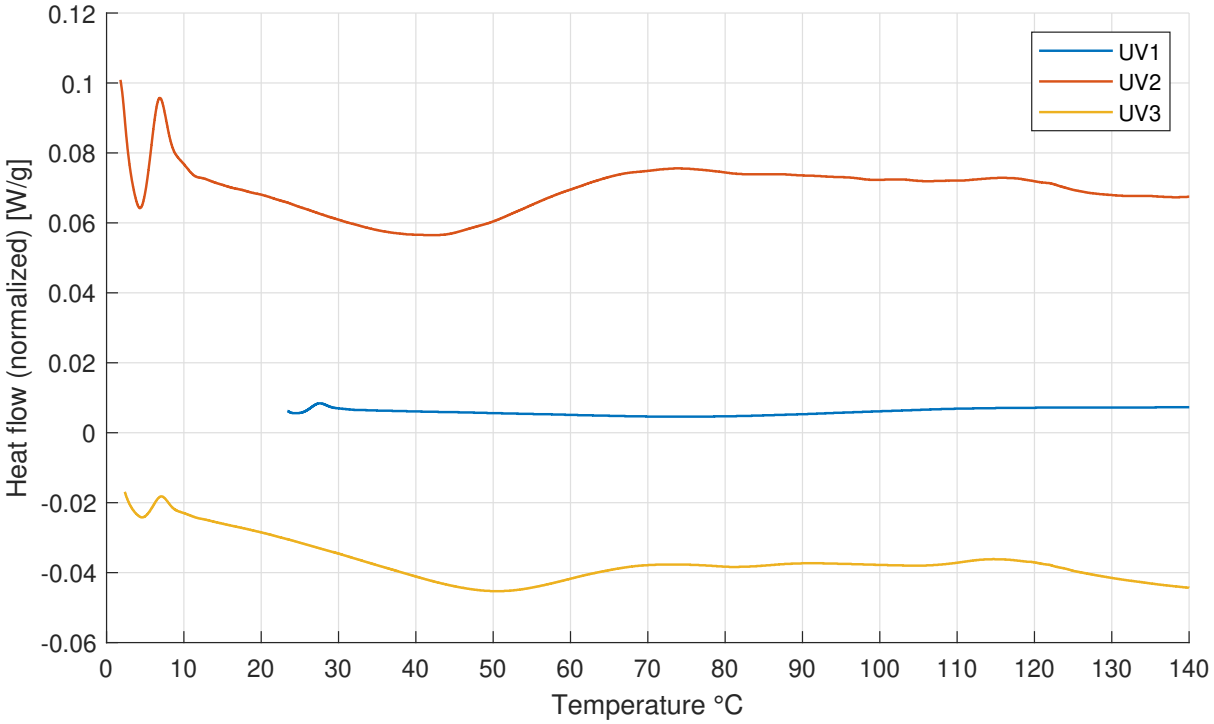

Figure D.6: DSC graph of LMC UV ageing

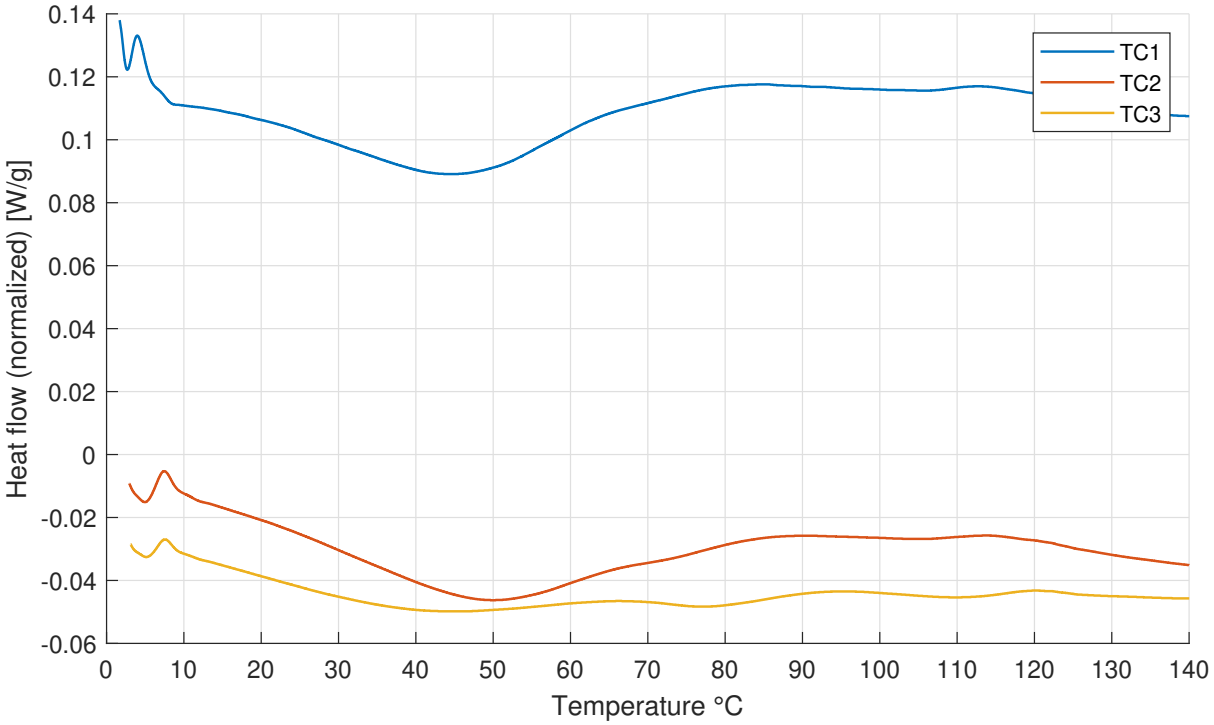

Figure D.7: DSC graph of LMC TC ageing

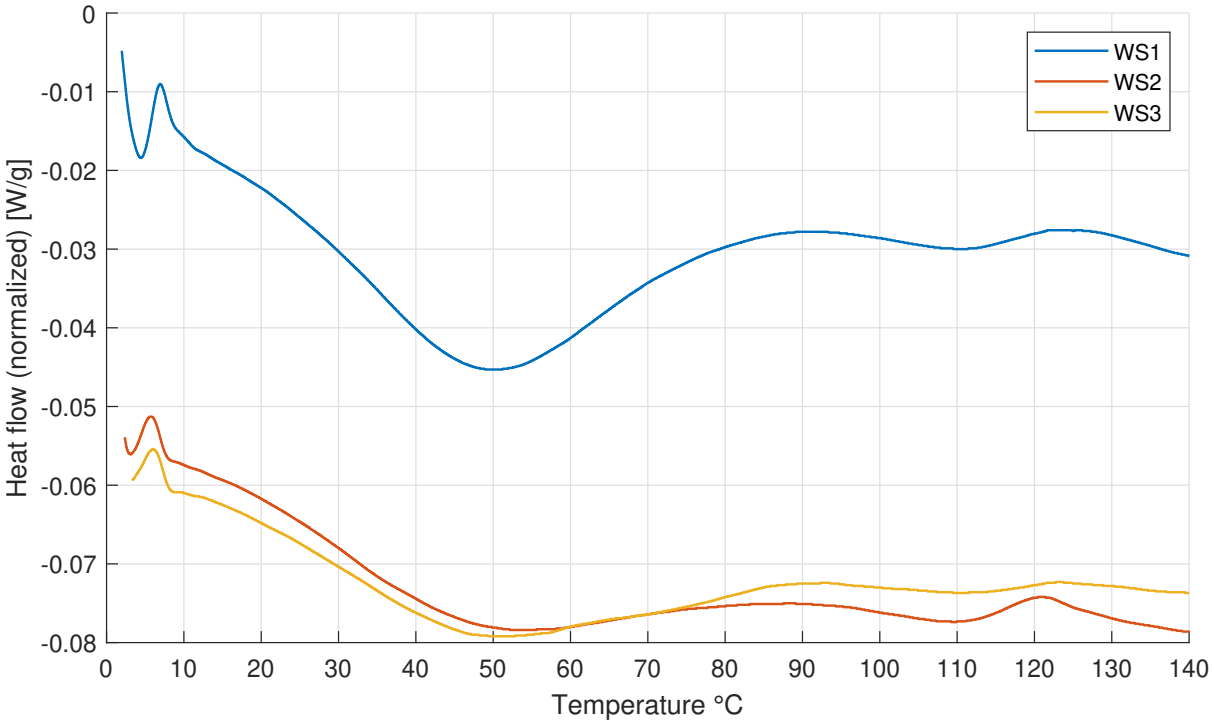

Figure D.8: DSC graph of LMC WS ageing

E

XPS results

E.1. Aged reproduced samples

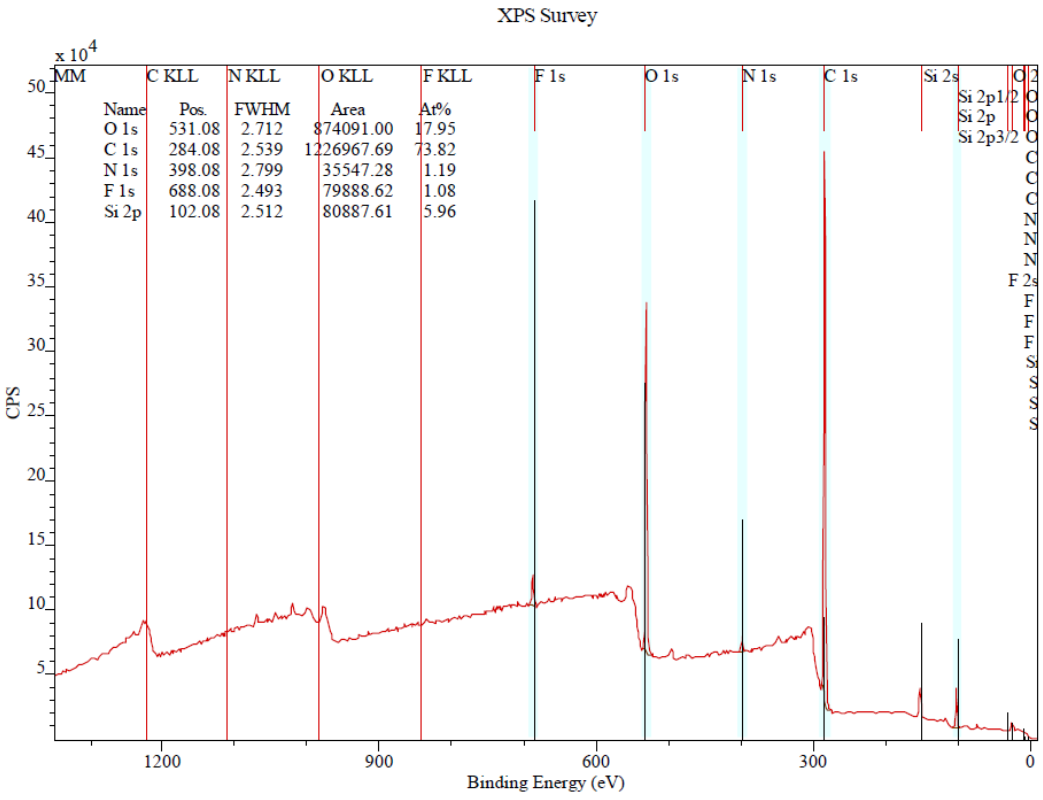

Figure E.1: XPS survey scan baseline reproduced sample

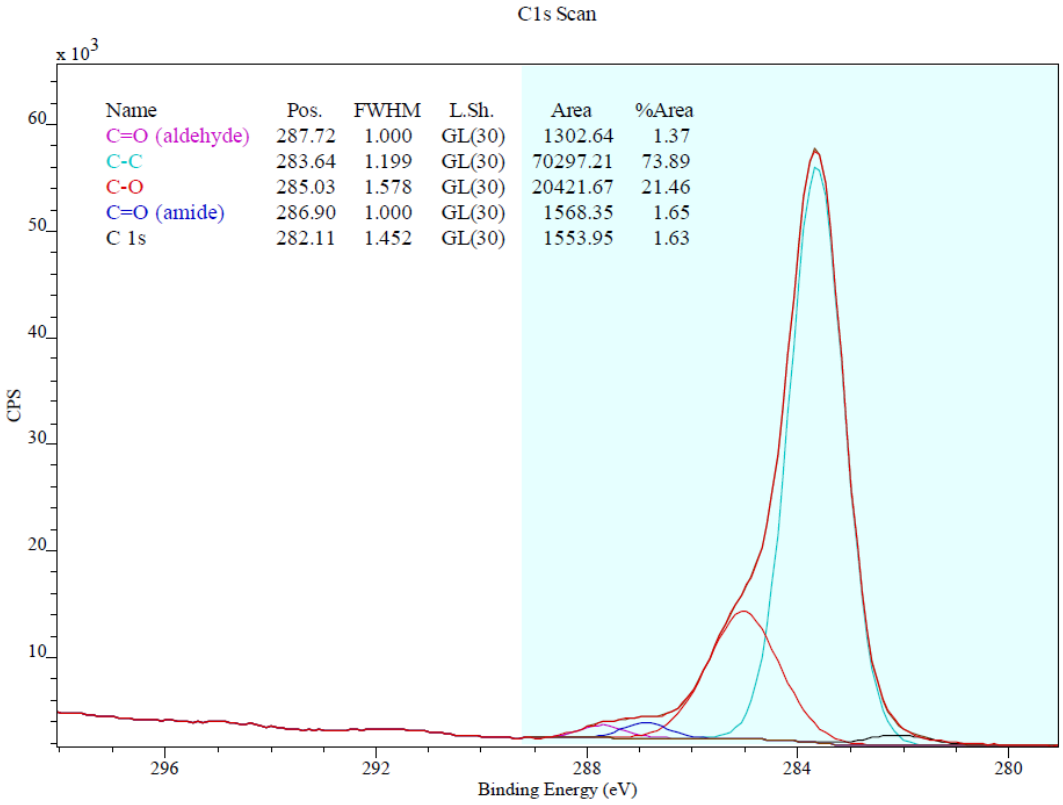

Figure E.2: XPS detailed scan carbon peak baseline reproduced sample

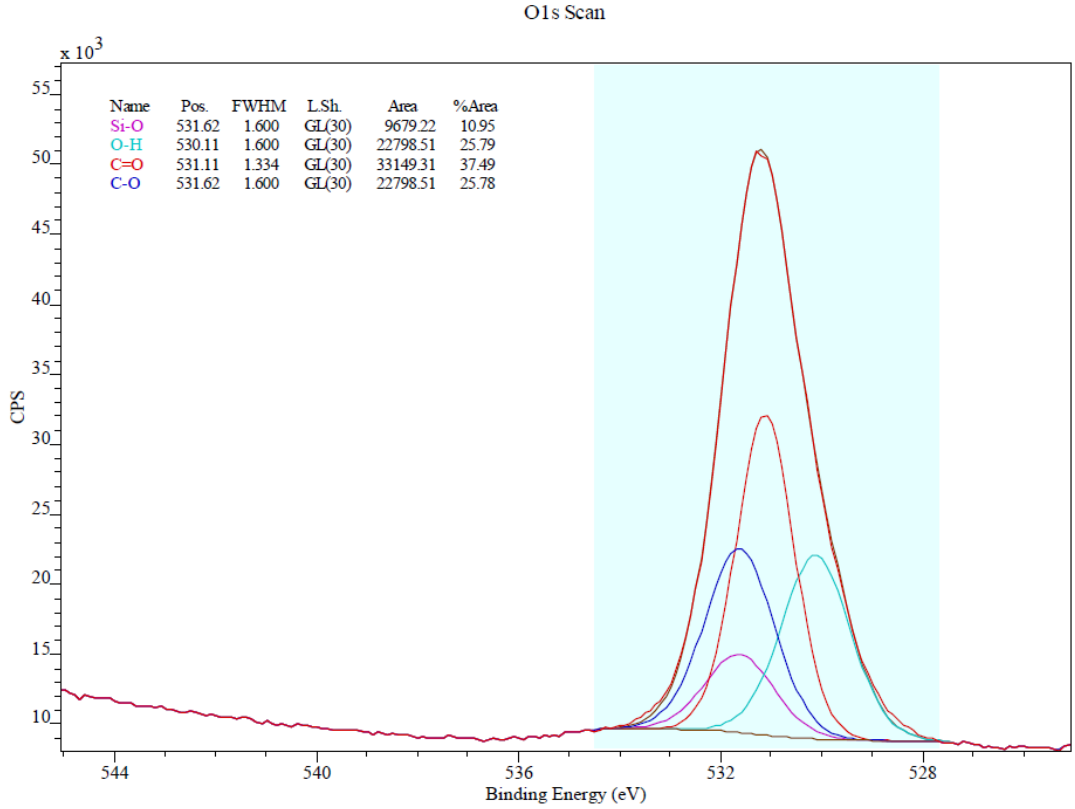

Figure E.3: XPS detailed scan oxygen peak baseline reproduced sample

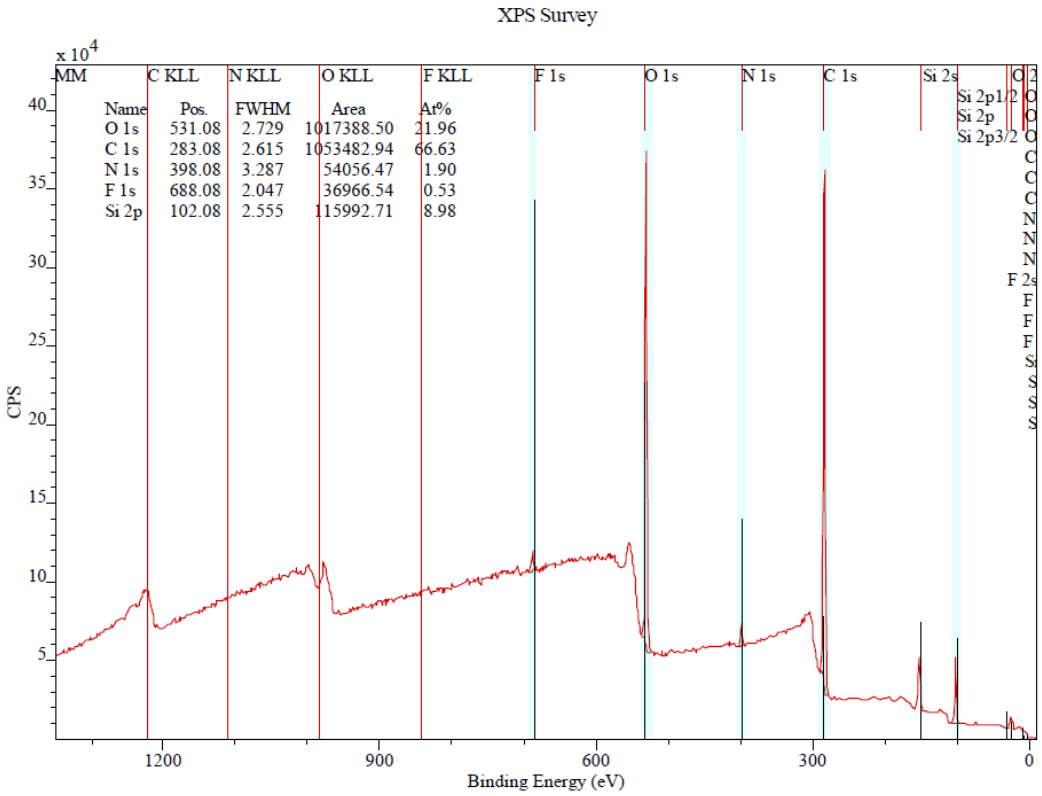

Figure E.4: XPS survey scan UV reproduced sample

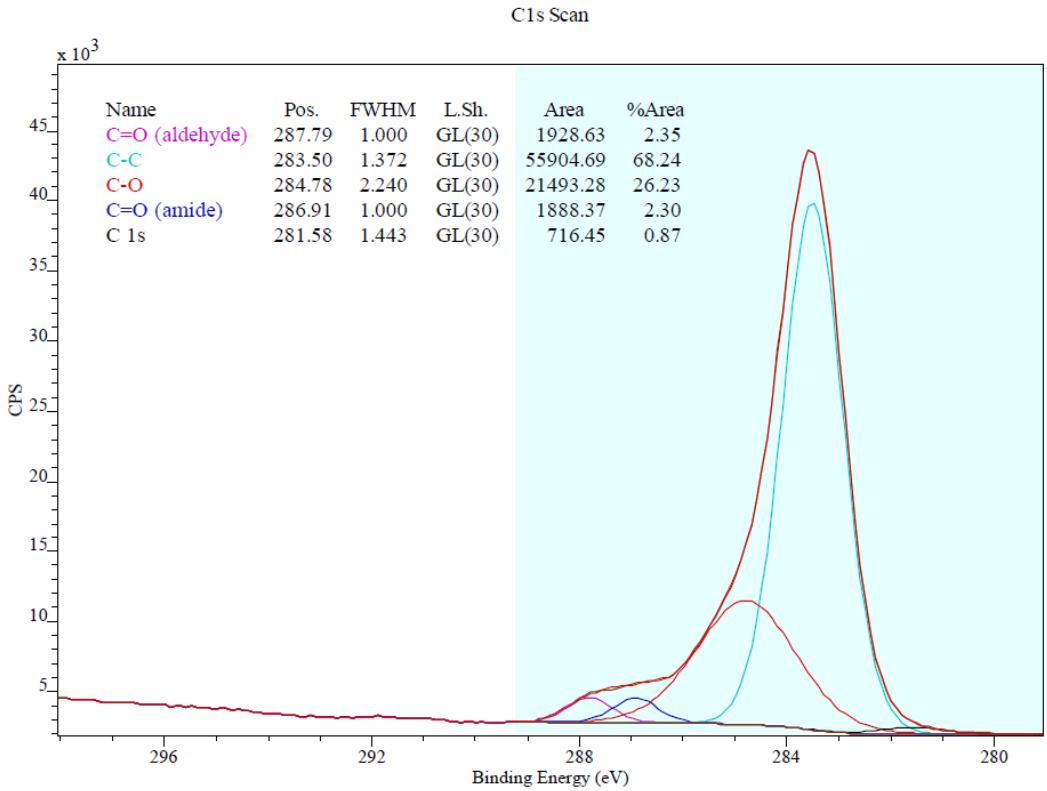

Figure E.5: XPS detailed scan carbon peak UV reproduced sample

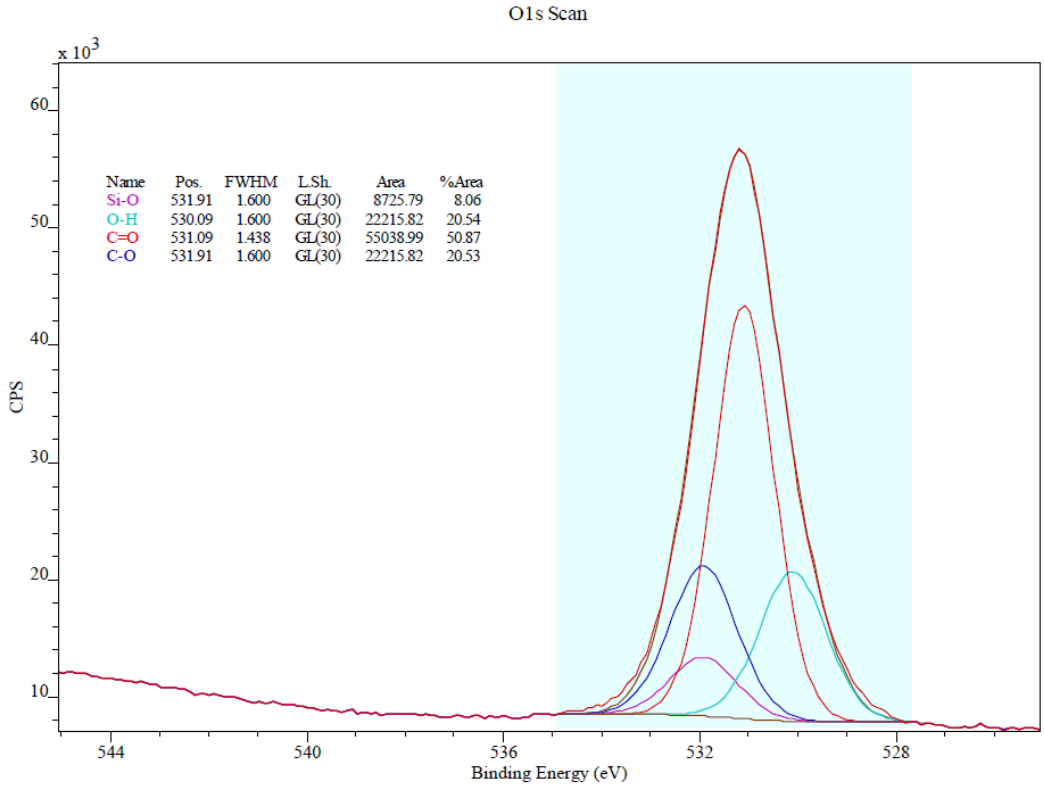

Figure E.6: XPS detailed scan oxygen peak baseline UV sample

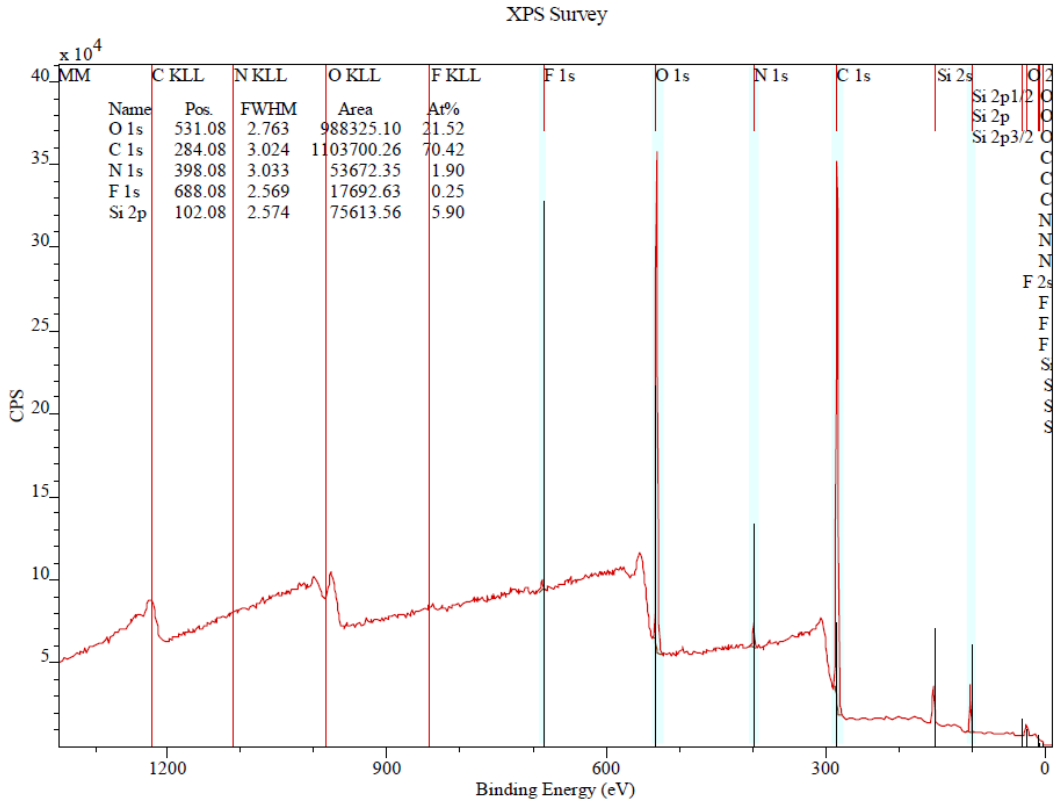

Figure E.7: XPS survey scan RH reproduced sample

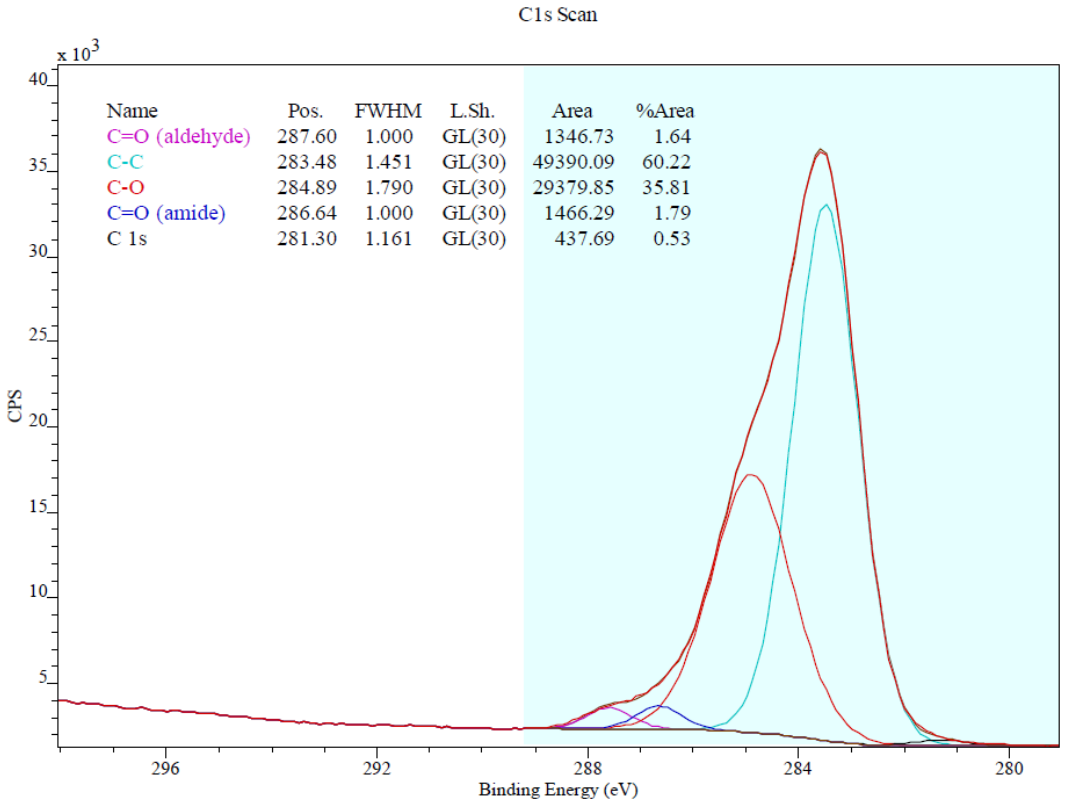

Figure E.8: XPS detailed scan carbon peak RH reproduced sample

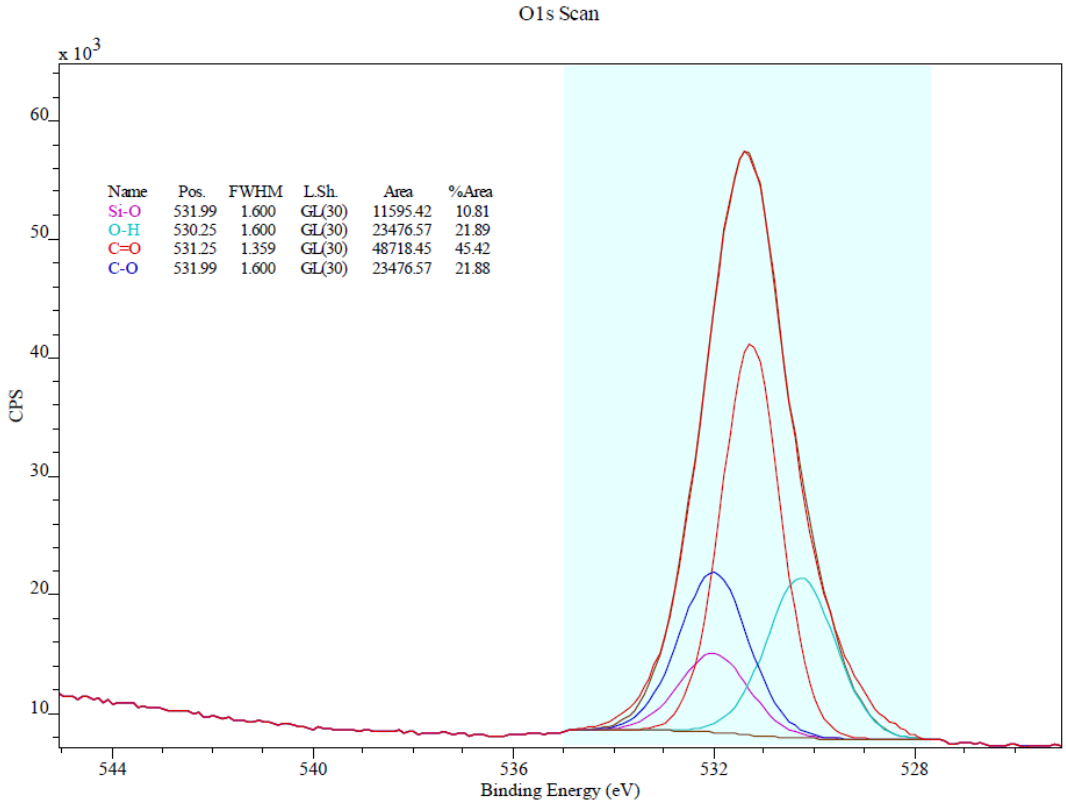

Figure E.9: XPS detailed scan oxygen peak baseline RH sample

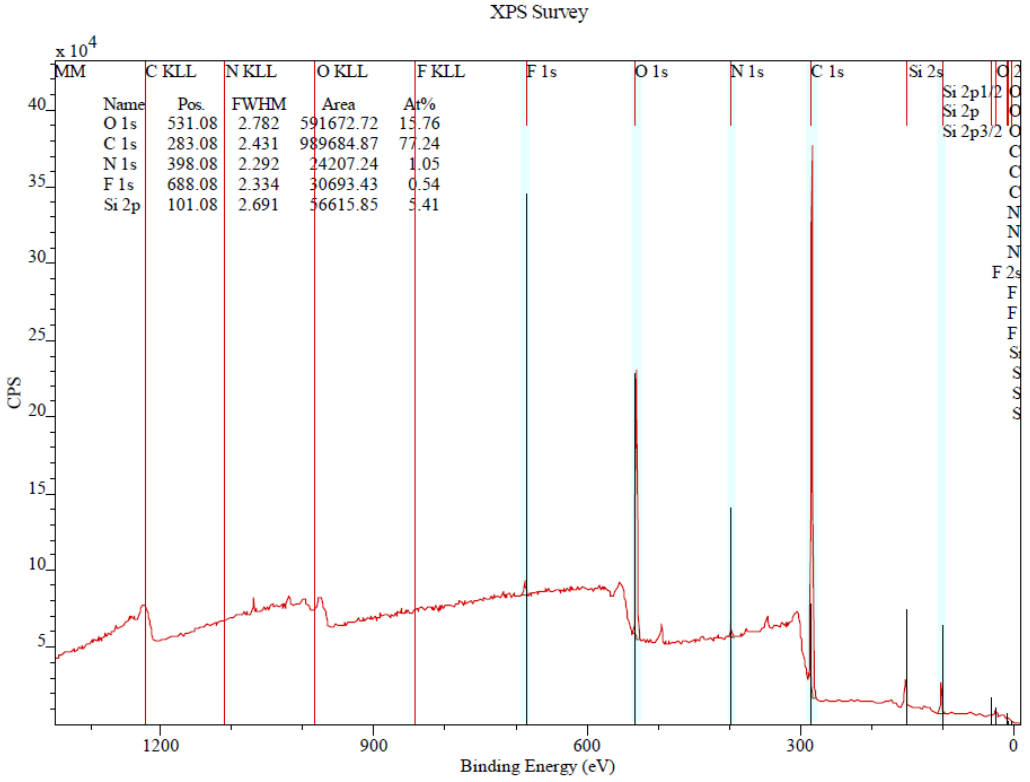

Figure E.10: XPS survey scan TC reproduced sample

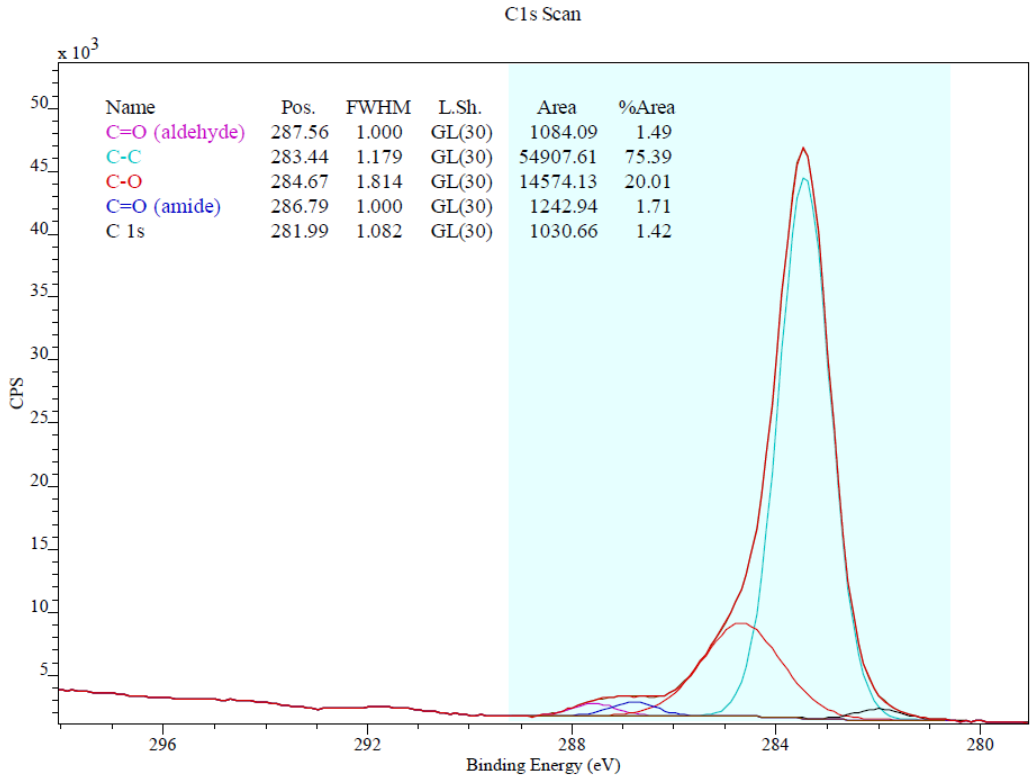

Figure E.11: XPS detailed scan carbon peak TC reproduced sample

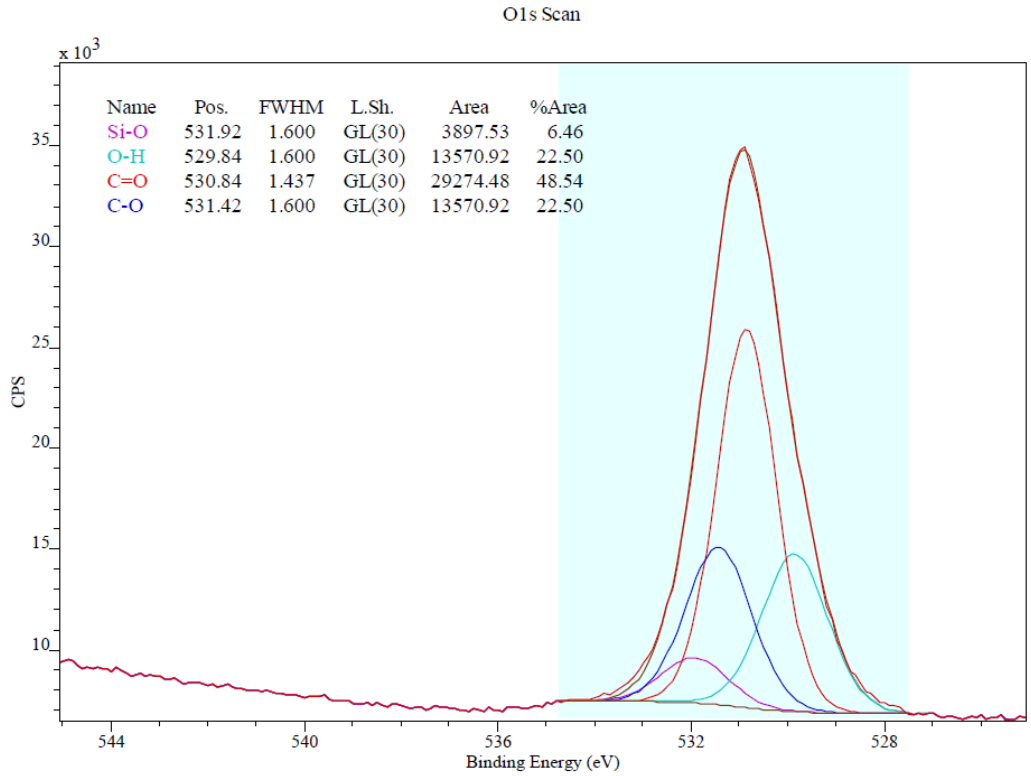

Figure E.12: XPS detailed scan oxygen peak baseline TC sample

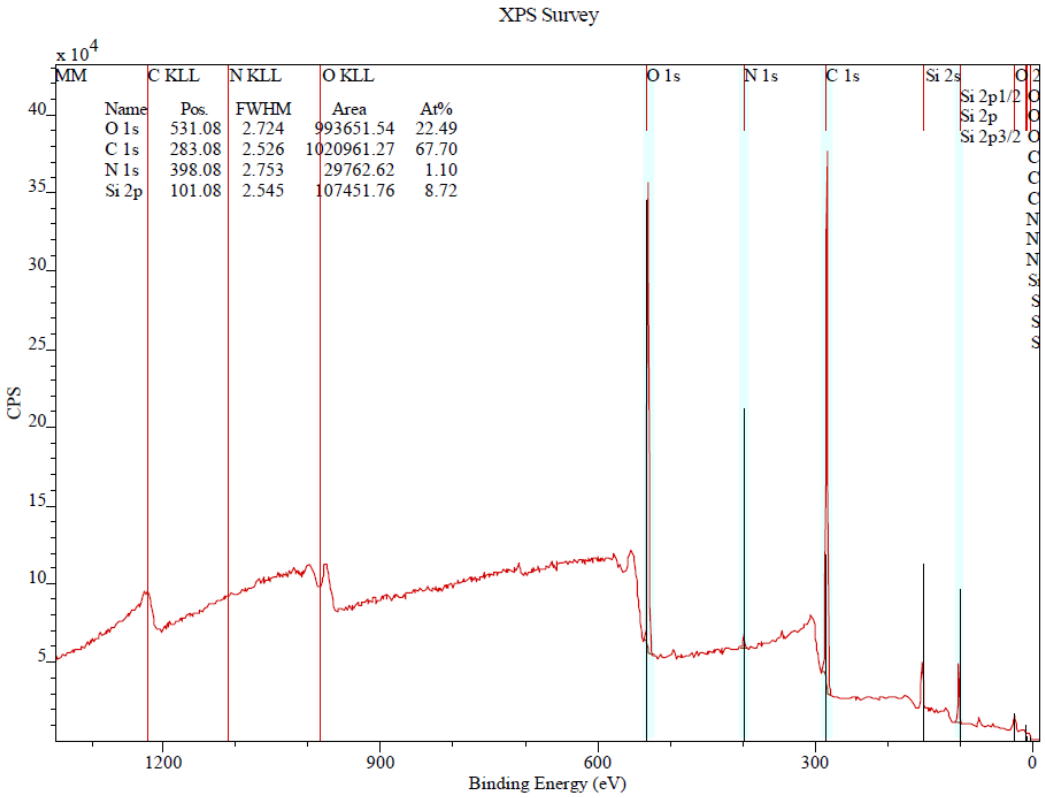

Figure E.13: XPS survey scan WS reproduced sample

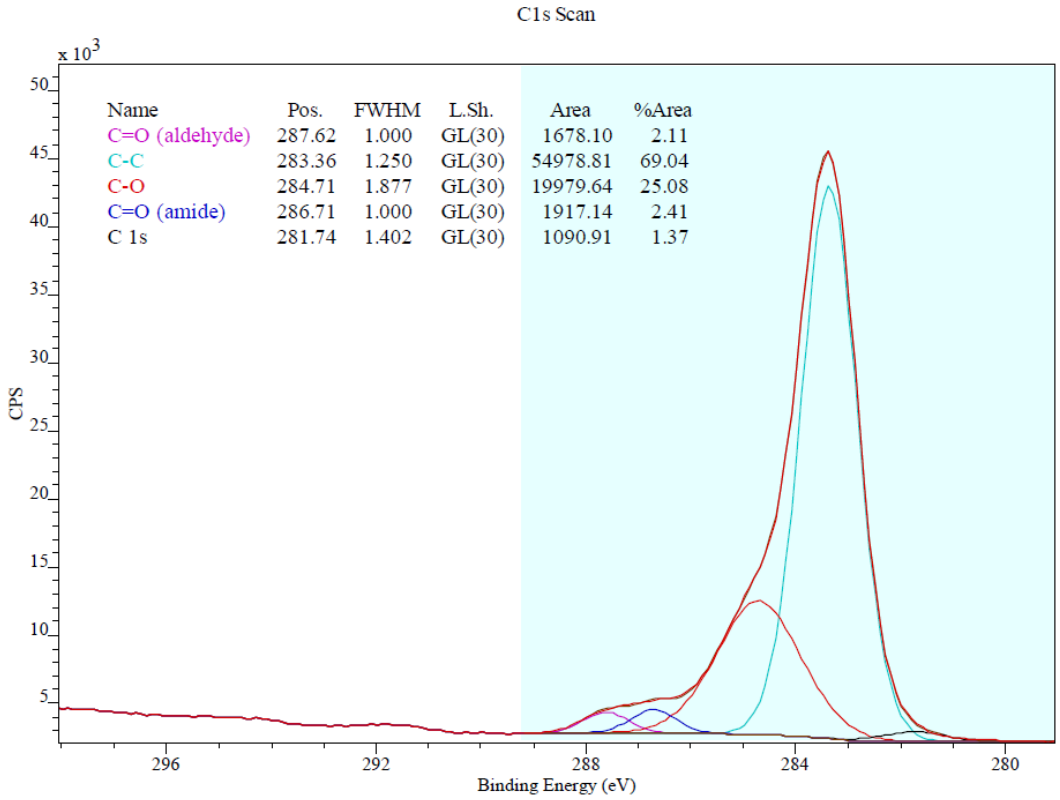

Figure E.14: XPS detailed scan carbon peak WS reproduced sample

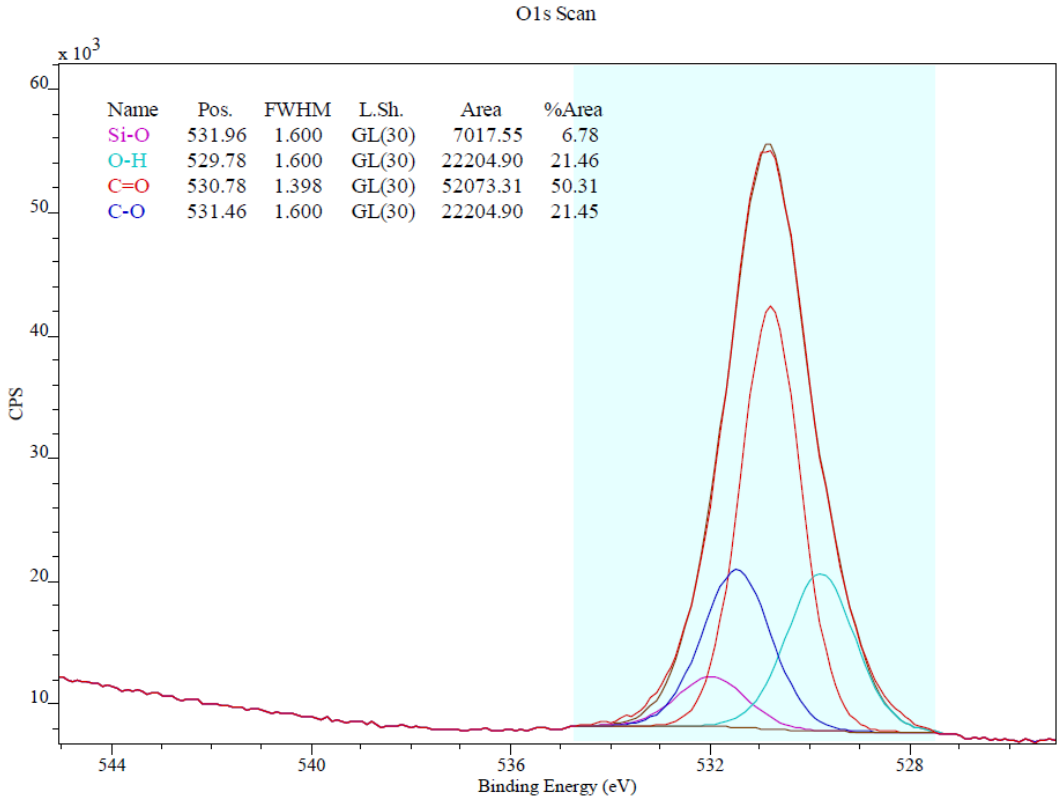

Figure E.15: XPS detailed scan oxygen peak WS reproduced sample

E.2. Aged LMC samples

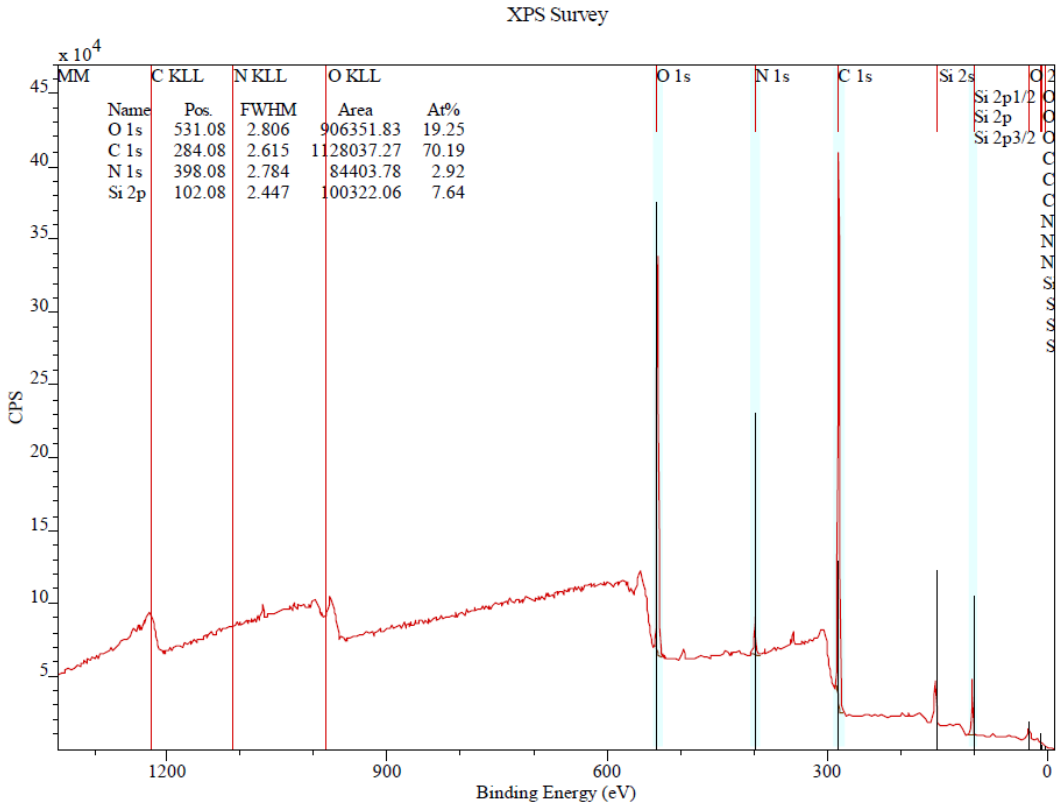

Figure E.16: XPS survey scan LMC reproduced sample

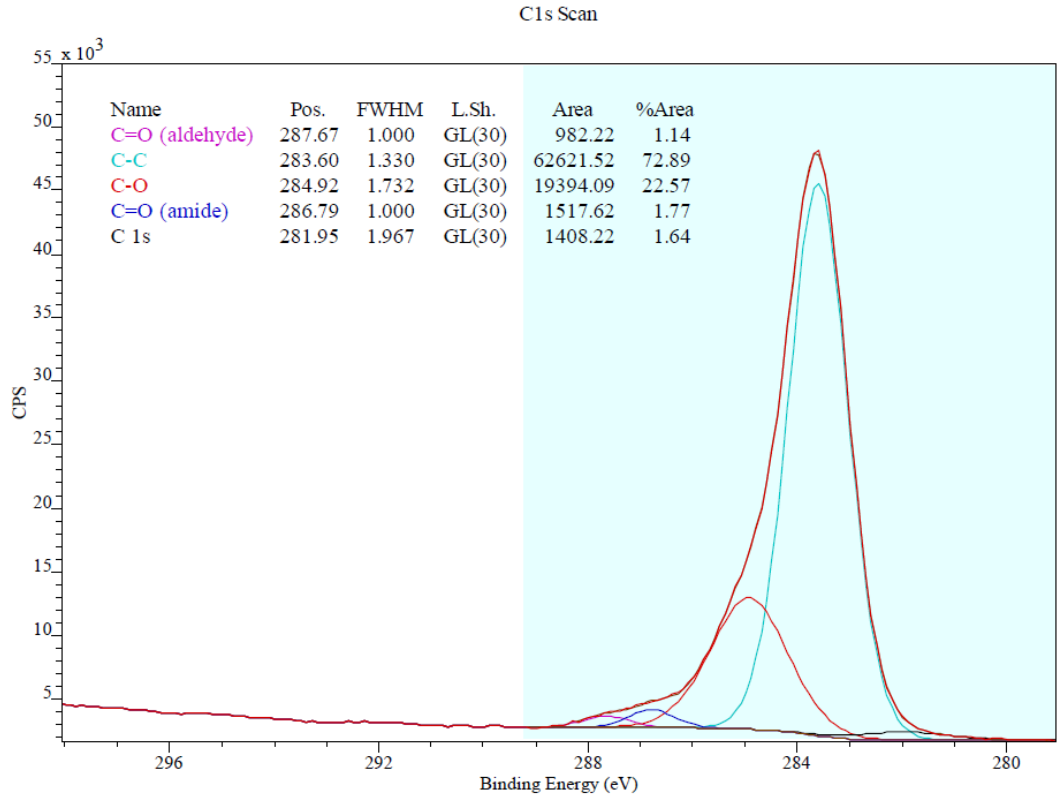

Figure E.17: XPS detailed scan carbon peak baseline LMC sample

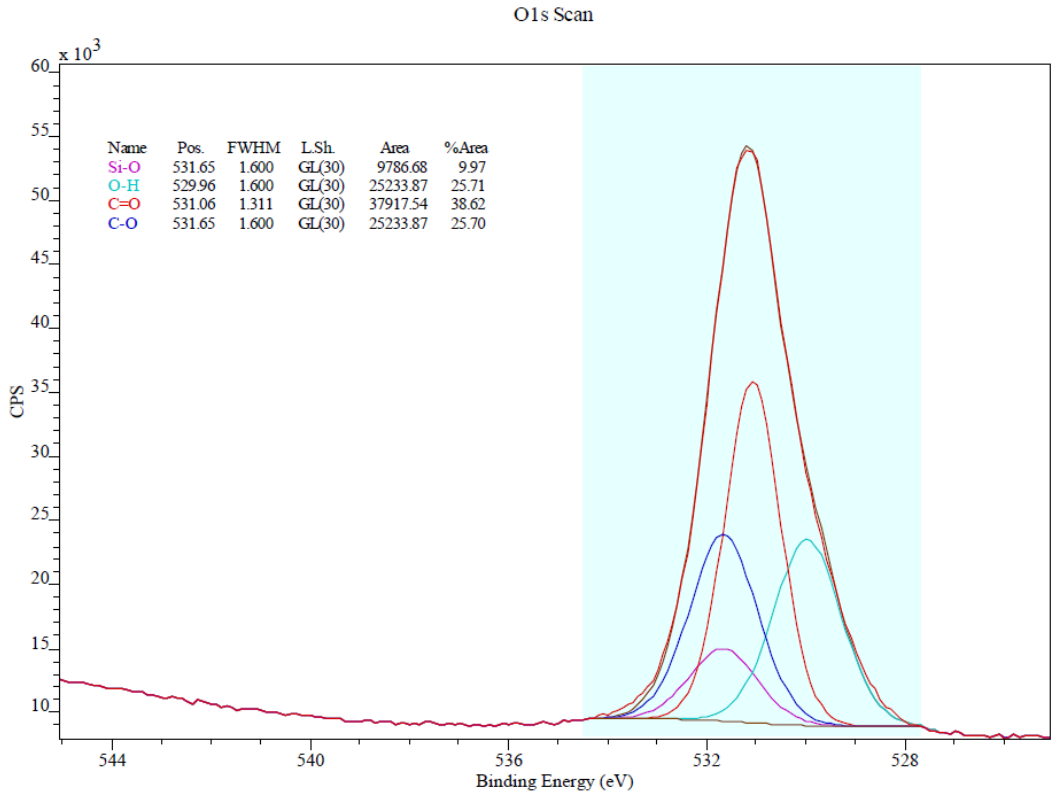

Figure E.18: XPS detailed scan oxygen peak baseline LMC sample

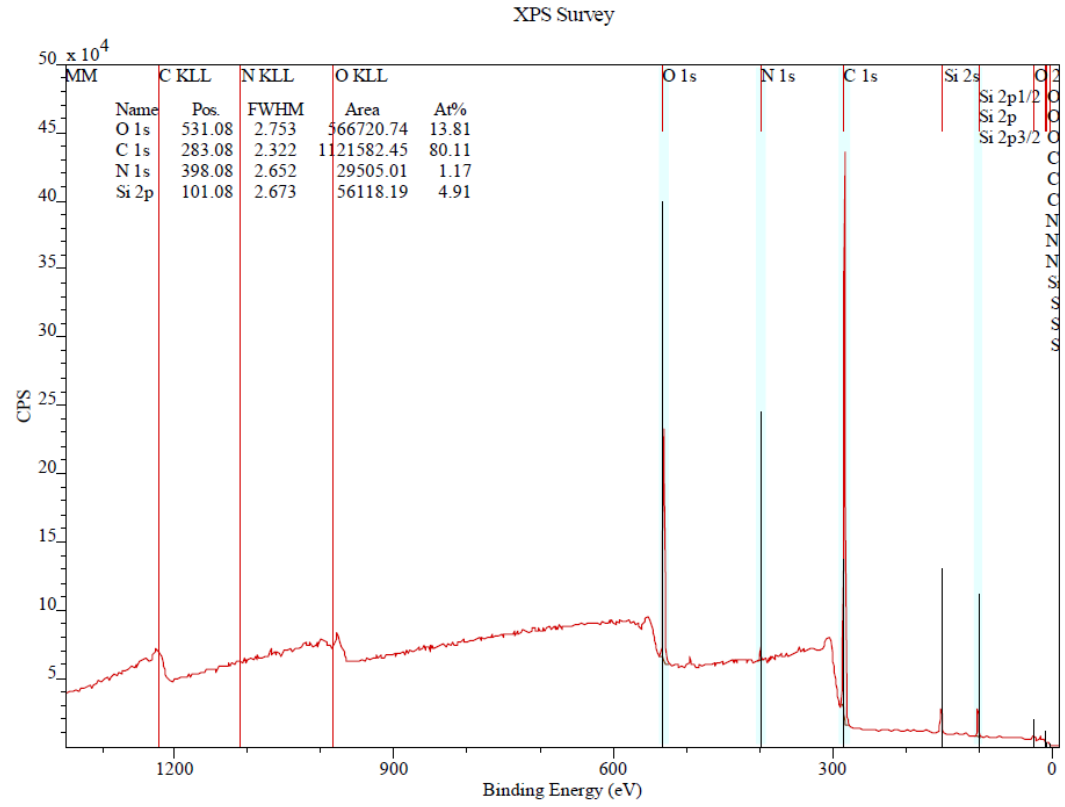

Figure E.19: XPS survey scan UV LMC sample

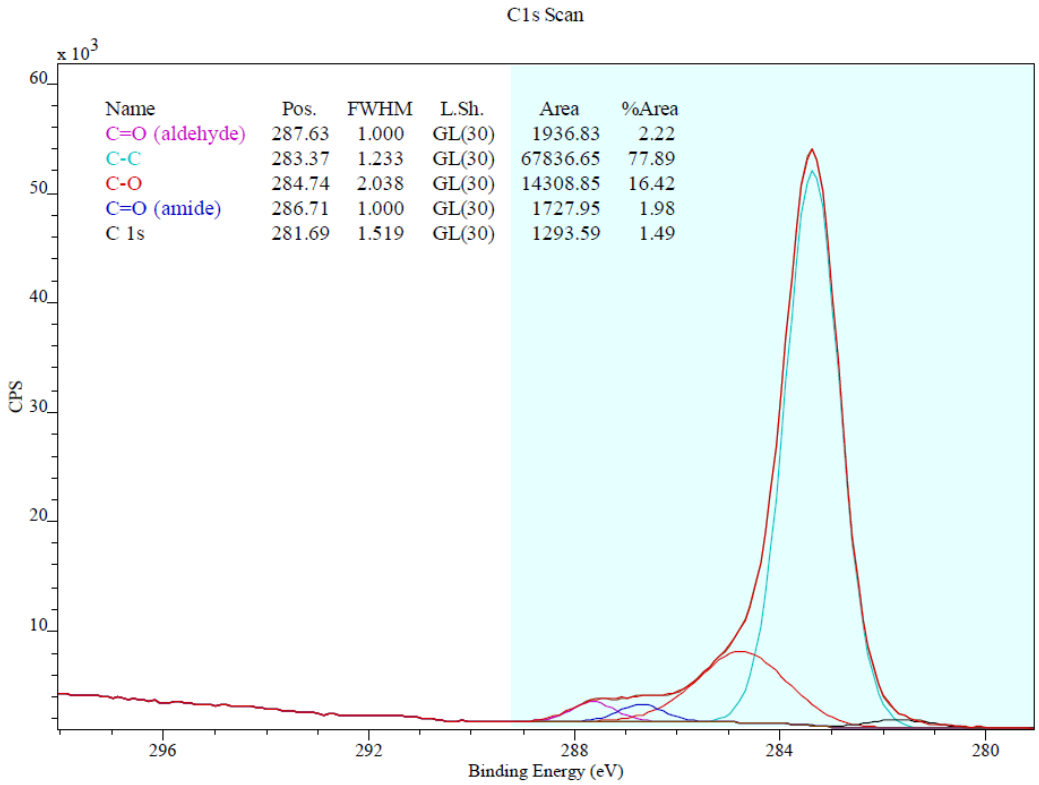

Figure E.20: XPS detailed scan carbon peak UV LMC sample

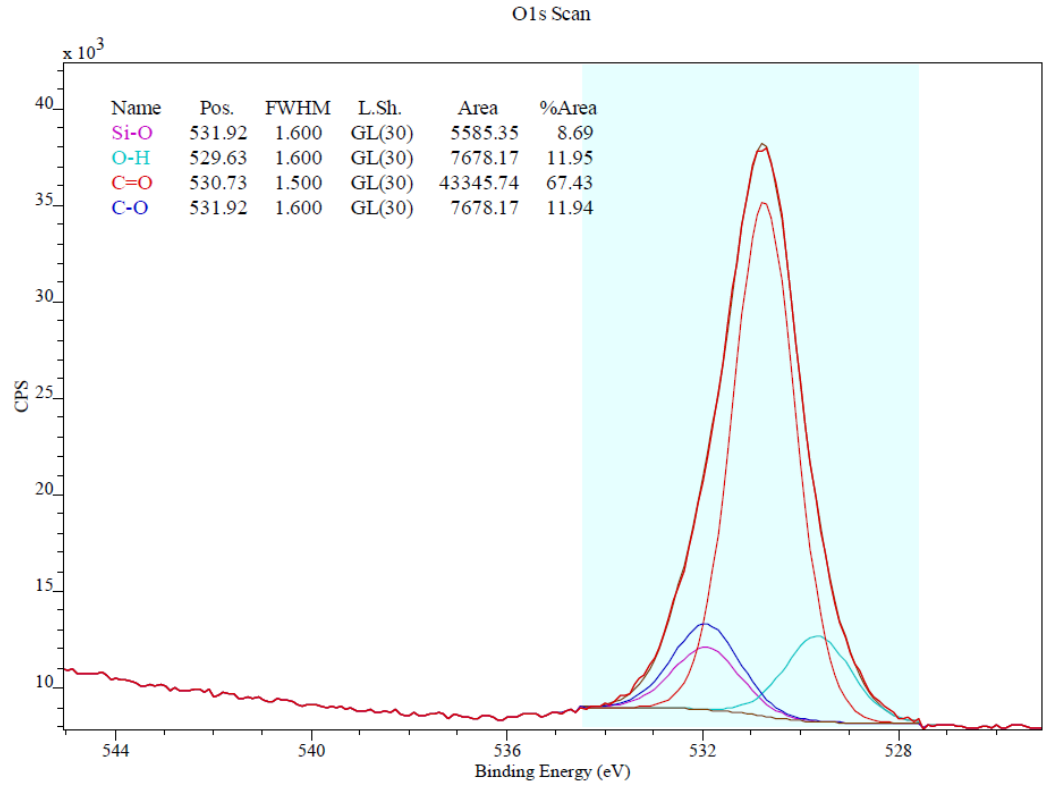

Figure E.21: XPS detailed scan oxygen peak baseline UV sample

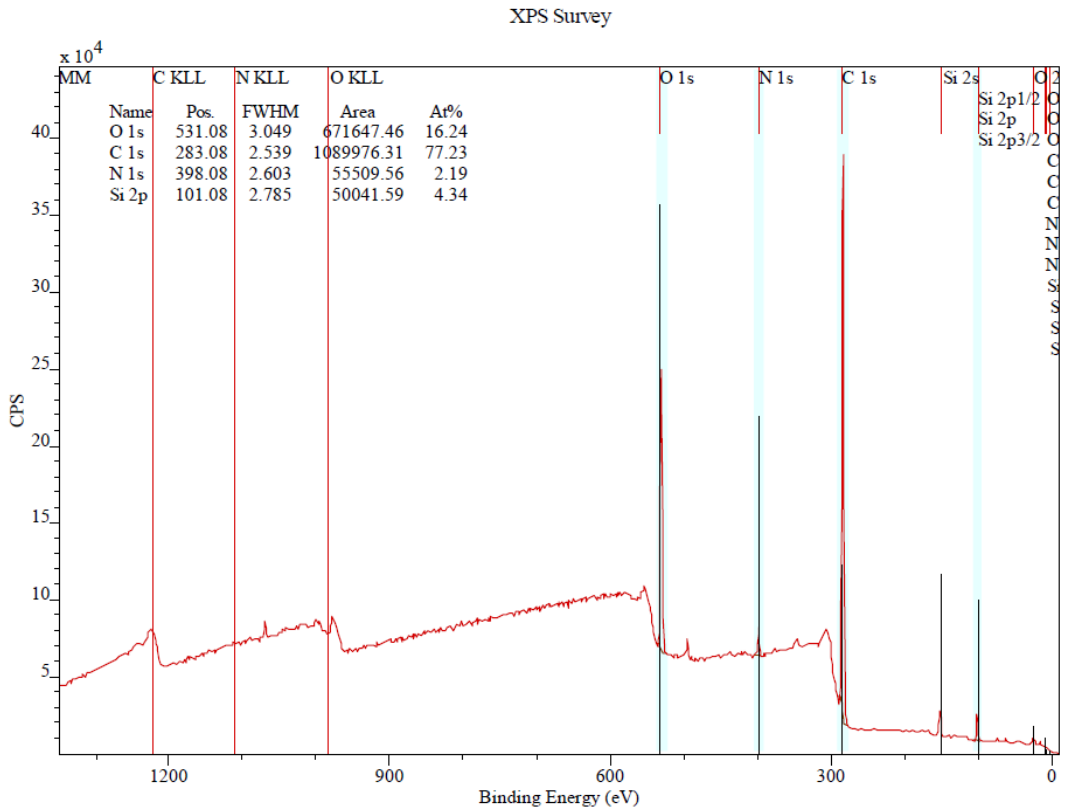

Figure E.22: XPS survey scan RH LMC sample

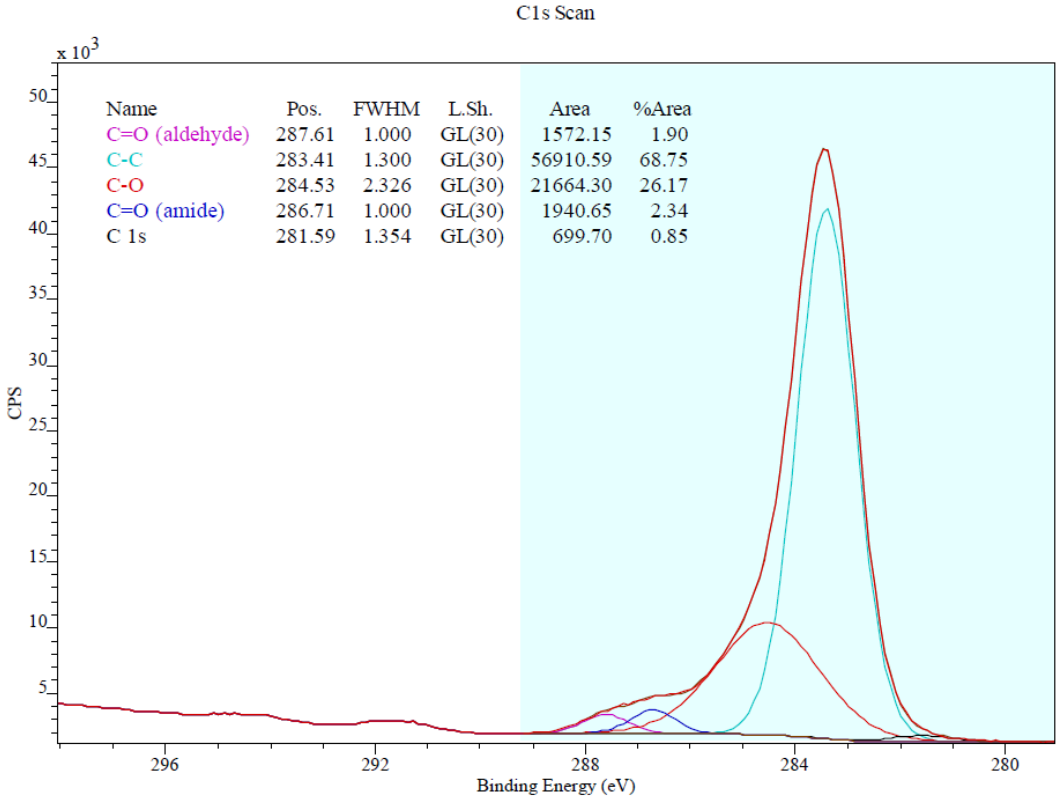

Figure E.23: XPS detailed scan carbon peak RH LMC sample

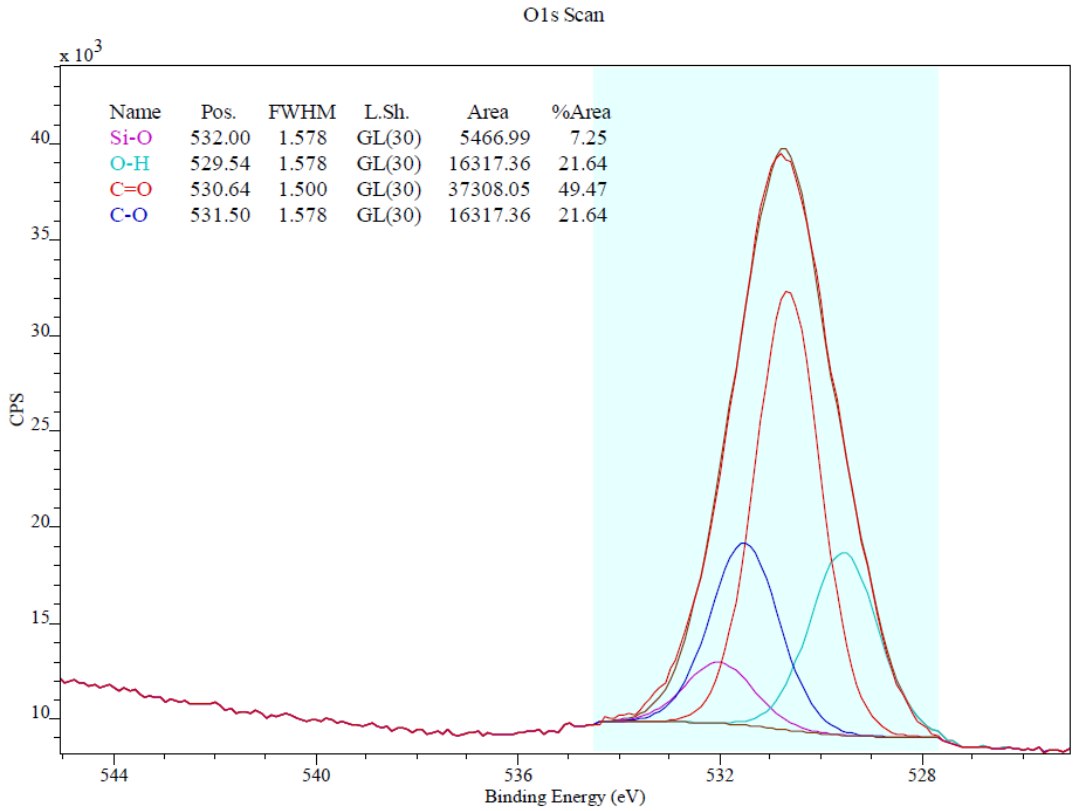

Figure E.24: XPS detailed scan oxygen peak baseline RH sample

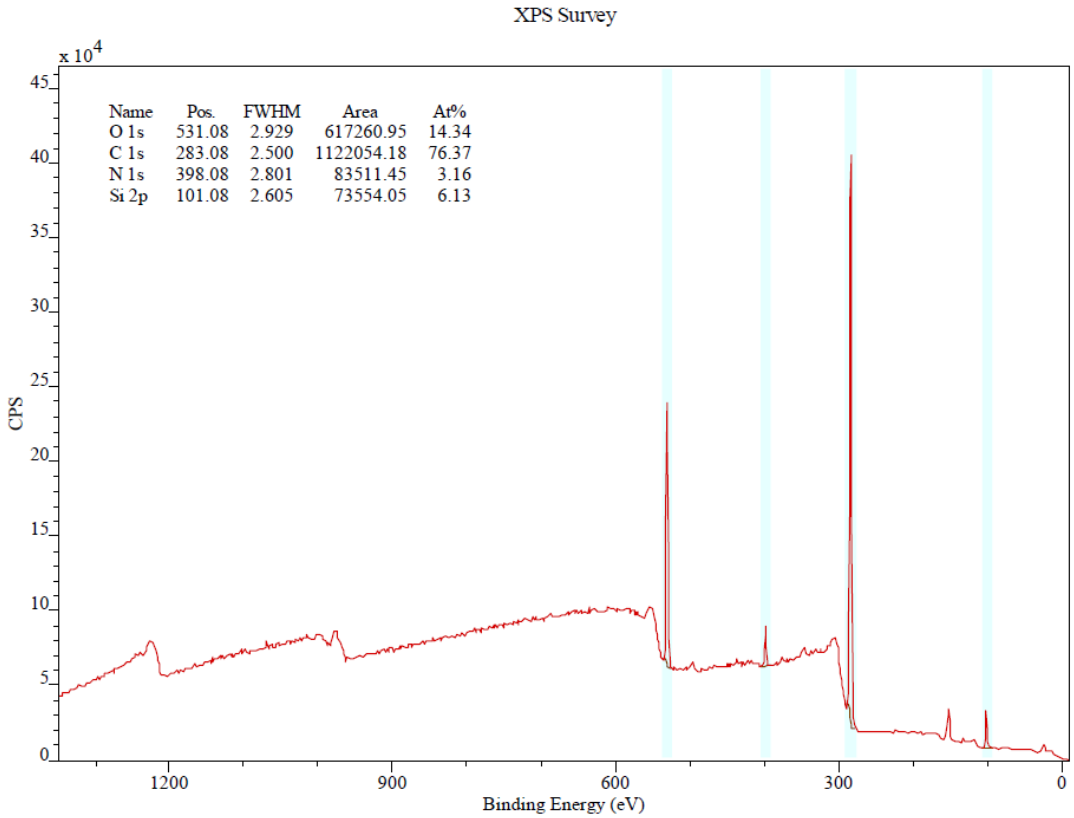

Figure E.25: XPS survey scan TC LMC sample

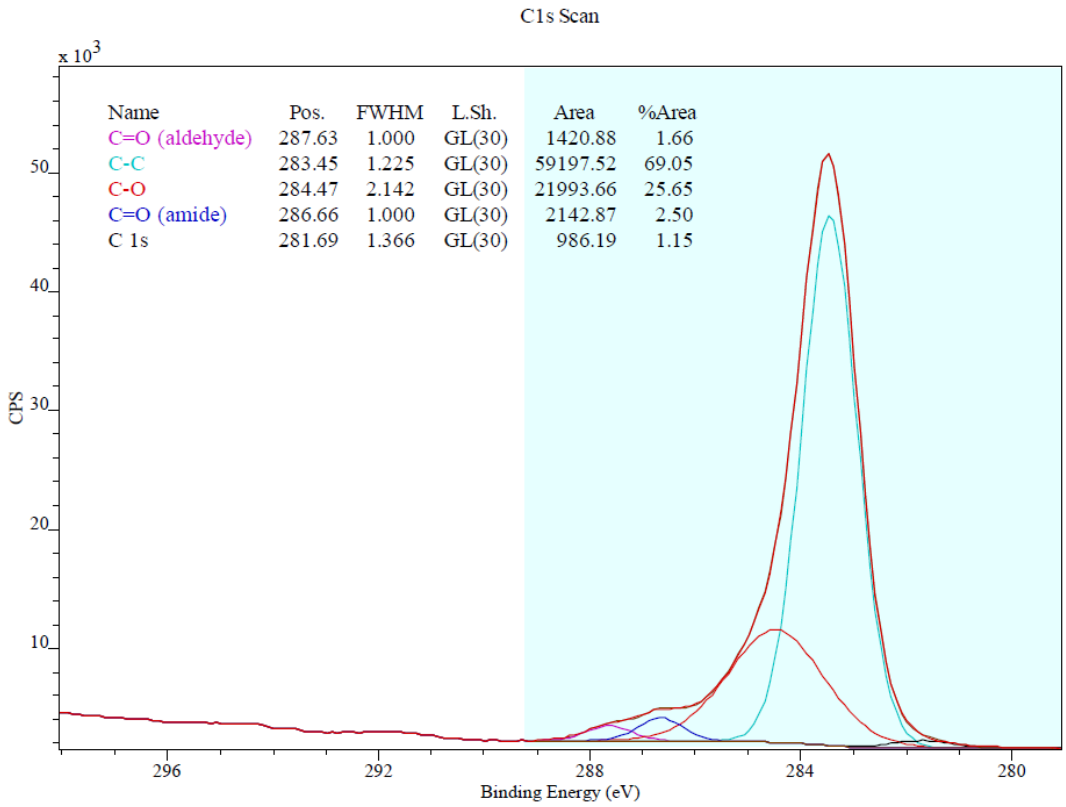

Figure E.26: XPS detailed scan carbon peak TC LMC sample

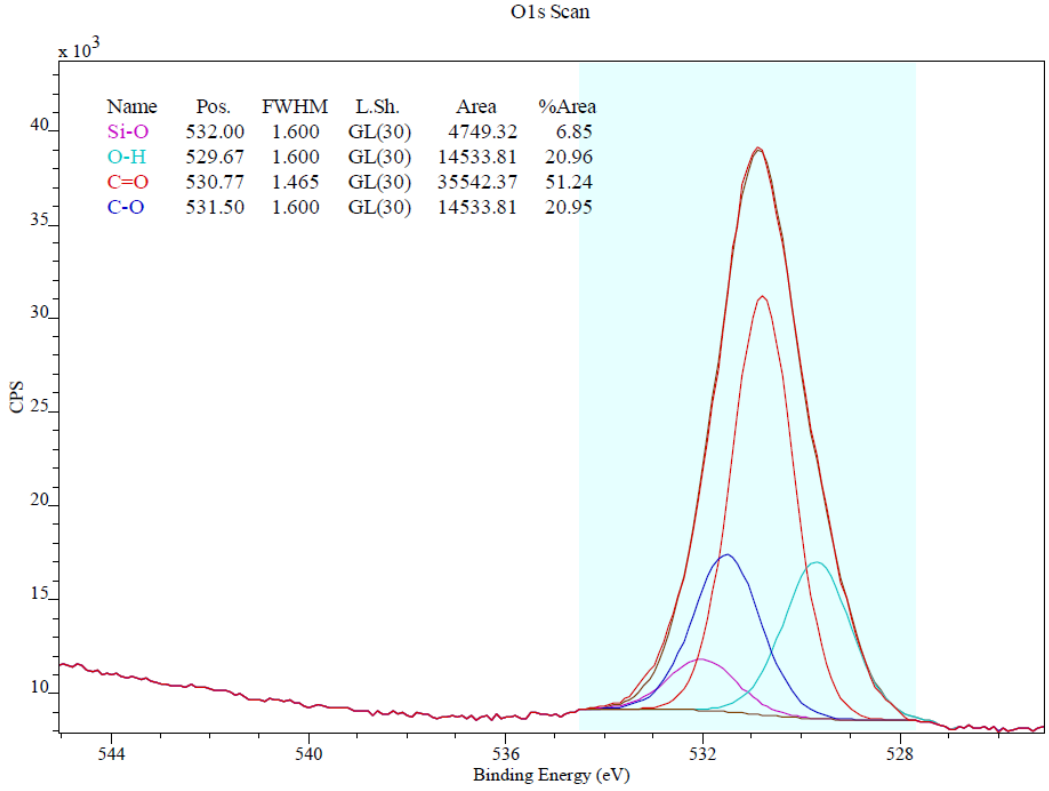

Figure E.27: XPS detailed scan oxygen peak baseline TC sample

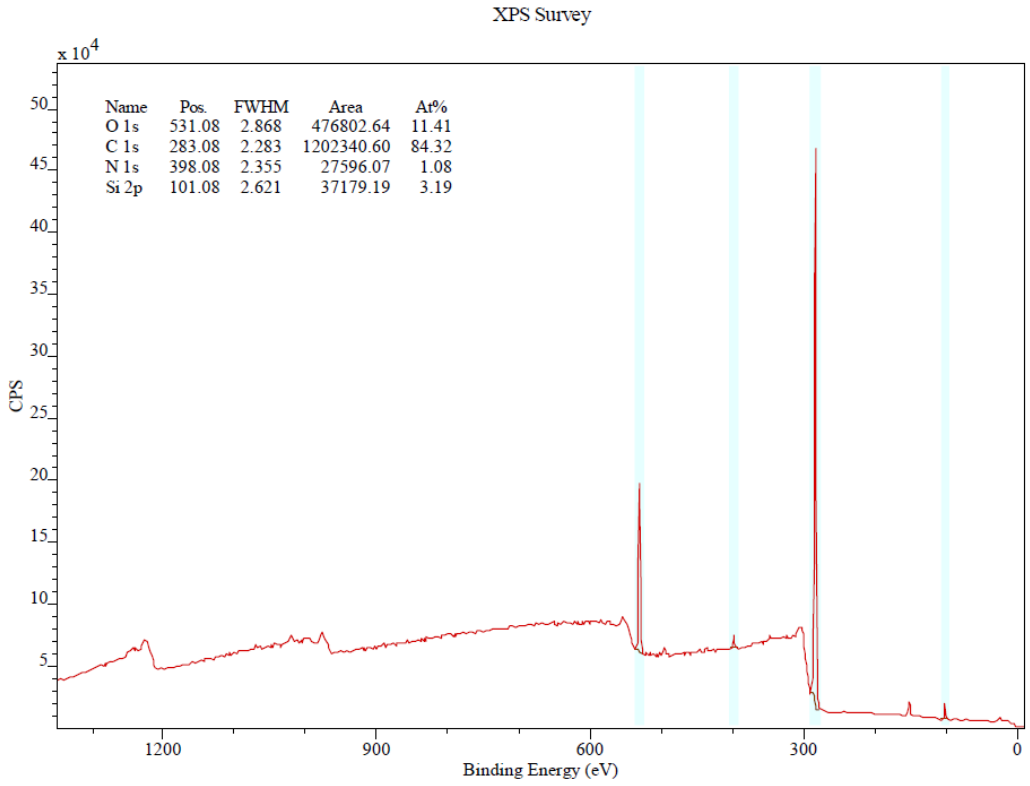

Figure E.28: XPS survey scan WS LMC sample

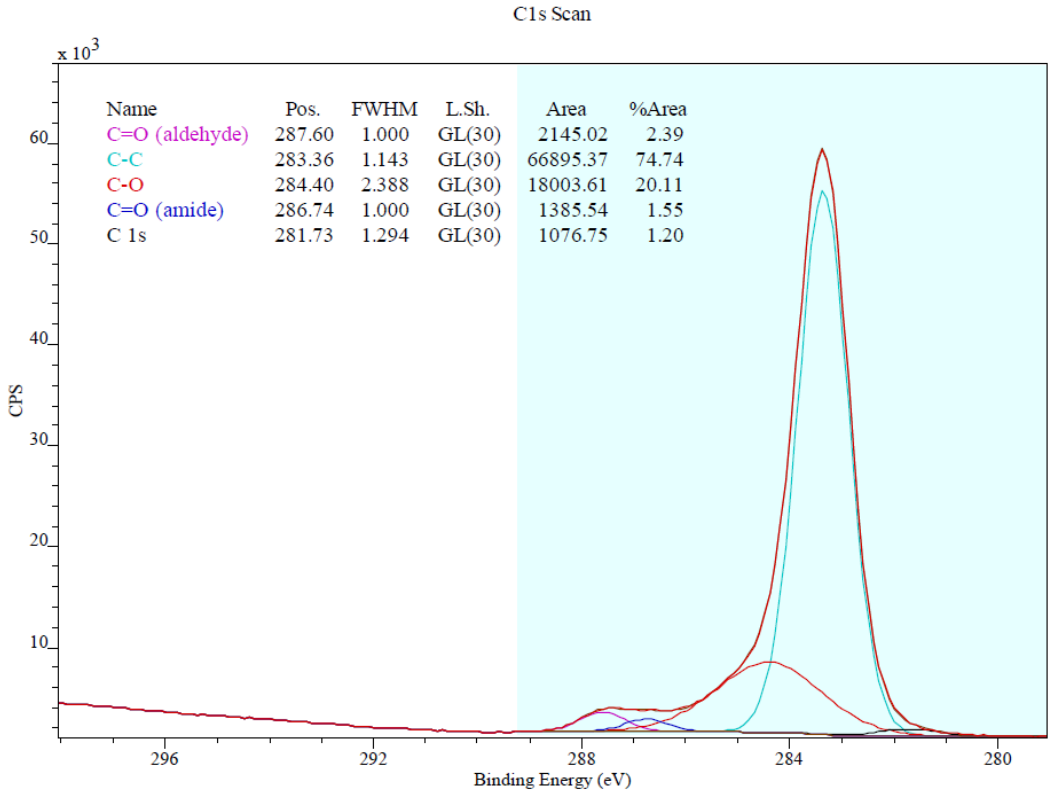

Figure E.29: XPS detailed scan carbon peak WS LMC sample

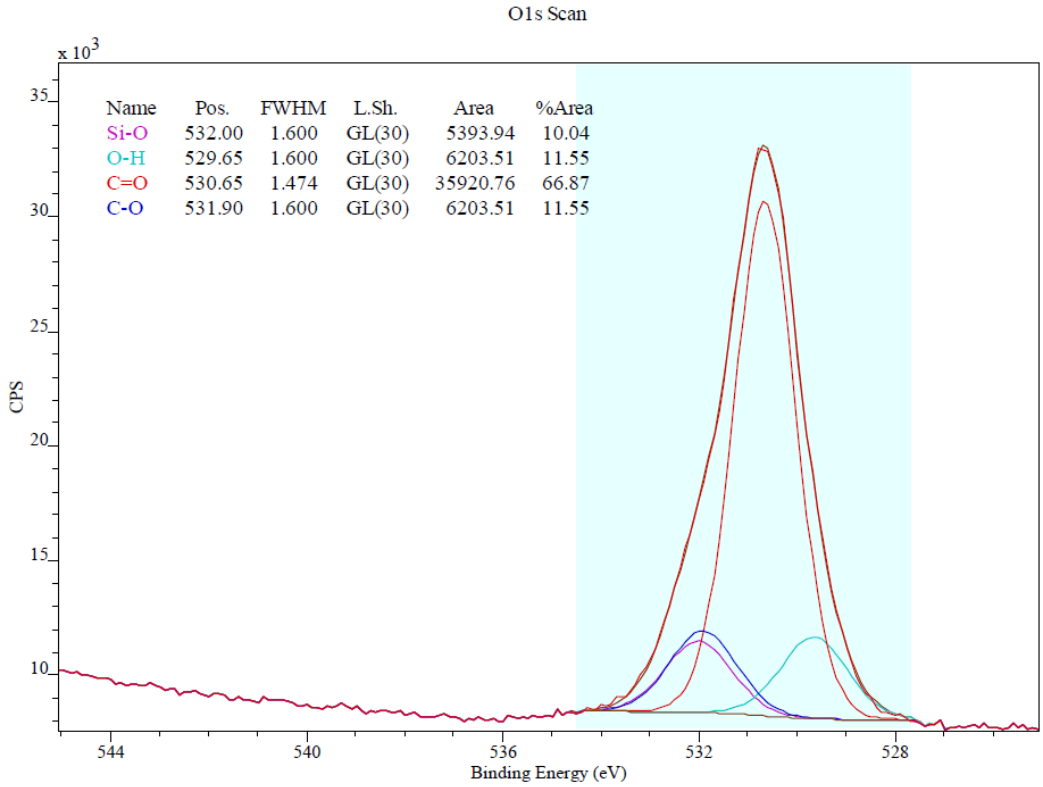

Figure E.30: XPS detailed scan oxygen peak WS LMC sample